



**Calhoun: The NPS Institutional Archive**  
**DSpace Repository**

---

Theses and Dissertations

1. Thesis and Dissertation Collection, all items

---

1989

# A coning motion apparatus for hydrodynamic model testing in a non-planar cross-flow.

Johnson, David Craig

Massachusetts Institute of Technology

---

<http://hdl.handle.net/10945/25780>

---

*Downloaded from NPS Archive: Calhoun*



Calhoun is the Naval Postgraduate School's public access digital repository for research materials and institutional publications created by the NPS community. Calhoun is named for Professor of Mathematics Guy K. Calhoun, NPS's first appointed -- and published -- scholarly author.

**Dudley Knox Library / Naval Postgraduate School**  
**411 Dyer Road / 1 University Circle**  
**Monterey, California USA 93943**

<http://www.nps.edu/library>



WILLIAM KNOX  
NAVAL POSTGRADUATE SCHOOL  
MONTEREY, CALIFORNIA 93943-6002







742910  
55746  
**A CONING MOTION APPARATUS FOR HYDRODYNAMIC MODEL  
TESTING IN A NON-PLANAR CROSS-FLOW**

by

**DAVID CRAIG JOHNSON**

B.S., Aerospace Engineering  
United States Naval Academy  
(1982)

Submitted to the Departments of Ocean Engineering  
and Mechanical Engineering in Partial Fulfillment of the  
Requirements for the Degrees of

**NAVAL ENGINEER**

and

**MASTER OF SCIENCE IN MECHANICAL ENGINEERING**

at the

**MASSACHUSETTS INSTITUTE OF TECHNOLOGY**

June 1989

© Massachusetts Institute of Technology 1989



---

# *A CONING MOTION APPARATUS FOR HYDRODYNAMIC MODEL TESTING IN A NON-PLANAR CROSS-FLOW*

---

LT David C. Johnson  
Department of Ocean Engineering, MIT

Submitted to the Departments of Ocean Engineering and Mechanical Engineering  
on 12 May 1989 in partial fulfillment of the requirements for the  
Degrees of Naval Engineer and Master of Science in Mechanical Engineering

## **Abstract**

As part of continuing research into the flow about slender bodies of revolution, a coning motion apparatus for hydrodynamic model testing was built and demonstrated. This is the first known use of a rotary balance apparatus for external flow hydrodynamic applications. The rotary rig allows for captive model testing with simultaneous roll and yaw components, and with non-planar cross-flow effects. Coning characterizes the non-planar nature of a general motion that cannot be constructed from contributions due to any planar motions.

Demonstration tests were conducted with a length/diameter = 9.5, body of revolution. Force and moment measurements were taken via an internally mounted, 6-component balance, capable of capturing all six force and moment components acting on the model. The tests covered coning angles to  $20^\circ$ , spin rates to 200 rpm, and free stream velocities to 30 ft/s. Reynolds number based on model length ranged from  $4.04 \times 10^6$  to  $6.06 \times 10^6$ . Cross-flow Reynolds number based on body diameter extended from  $1.5 \times 10^5$  to  $3.0 \times 10^5$ , covering flow regimes near the transition from laminar to turbulent separation. The non-dimensional forces and moments generally show a non-linear variation with spin rate for coning angles greater than  $14^\circ$ . The measured out-of-plane force was significant, reaching a magnitude of 30% of the in-plane force. Experiment data correlated fairly well with numerical predictions (using laminar separation criteria).

Thesis Supervisor: Dr. J. E. Kerwin, Professor of Ocean Engineering

Thesis Reader: Dr. H. K. Kytömaa, Assistant Professor of Mechanical Engineering





## Acknowledgements

The successful completion of this project would never have been possible without the considerable effort of several individuals. From the start, the experiment required team participation from all the players: General Dynamics, Electric Boat Division and Convair Division, Stevens Institute of Technology, Davidson Laboratories, MIT and Nielsen Engineering and Research. I would like to give special thanks to the following individuals:

- Dr. Chuck Henry and Gerry Fridsma of Electric Boat, for their sponsorship of the study, their technical guidance and encouragement, and their origination of the coning motion concept for external flow, slender body of revolution experiments.
- Dr. Peter Brown, Dr. Glenn Mckee, Dick Krukowski, and the model shop personnel of Davidson Laboratories for their great effort in not only building the model and apparatus, but assisting in getting it to work.
- Phil Mole and the calibration team at Convair for their excellent work in preparing the balance for use.
- Mike Mendenhall and Stanley Perkins of NEAR for their SUBFLO numeric studies that were invaluable for data comparison.
- Dr. Jake Kerwin and Dr. Harri Kytömaa of MIT for their active involvement with the study and their help.
- LT Norbert Doerry, a fellow MIT 13A, for his assistance in many aspects of the project.
- A very special thanks to S. Dean Lewis of the MIT variable pressure water tunnel, who designed all of the mechanical components for the tunnel modifications and assisted with their installation. His help was invaluable!
- Ronnie St. Jean and the Nuclear Engineering Machine shop for their instant service in building and modifying the many components for the test.
- Finally, a very special thanks to my wife, Carol, who patiently stood by through all the trials of getting a new experiment up and running, and provided the moral encouragement to complete this project.



# Table of Contents

Chapter 1 Introduction .....	10
1.1 Coning Motion .....	11
1.2 Model Testing .....	13
1.2.1 Non-Planar Cross-Flow Effects .....	13
1.2.2 Roll Component Effects .....	16
1.3 Hydrodynamic Math Model .....	17
Chapter 2 Description of Test Apparatus .....	20
2.1 Model .....	20
2.2 Balance and Sting Assembly .....	21
2.3 Tunnel Installation .....	22
2.3.1 Calculations .....	23
2.3.1.1 Required Torque .....	24
2.3.1.2 Speed Regulation .....	25
2.3.1.3 System Torsional Resonance .....	26
2.3.2 Modifications .....	28
2.3.3 System Characteristics .....	29
2.3.4 Test Section Installation .....	30
2.4 Data Acquisition and Reduction System .....	31
2.4.1 Instrument Group .....	32
2.4.2 Amplifier/Filter Group .....	33
2.4.3 Computer Group .....	33
2.4.4 Slip Rings .....	34
Chapter 3 Test Procedure and Tare Measurements .....	35
3.1 Balance Calibration and Check-out .....	35
3.1.1 Data Reduction Model .....	36
3.1.2 Balance Operation .....	37
3.1.2.1 Weight Calibration and Axis Convention .....	38
3.1.2.2 Model Weight and CG .....	39
3.1.2.3 Temperature Effects .....	40
3.2 Test Procedure .....	41
3.2.1 Test Logic .....	41
3.2.2 Code Development .....	43
3.2.2.1 Timing .....	43
3.2.2.2 Desired Results .....	45
3.3 Tare Measurements .....	47
3.3.1 Static .....	48
3.3.2 Rotational .....	48
3.4 Test Matrix .....	53
Chapter 4 Test Results .....	54
Chapter 5 Data Analysis .....	64
5.1 Comparison with Numerical Results .....	64
5.2 Frequency Analysis .....	68



Chapter 6 Conclusions and Recommendations .....	77
6.1 Conclusions .....	77
6.2 Recommendations .....	78
REFERENCES .....	80
Appendix A Taylor Series Expansion .....	82
Appendix B Inertia, Gravity and Buoyancy Forces .....	90
Appendix C Test Data .....	96
Appendix D FORTRAN Routines .....	111





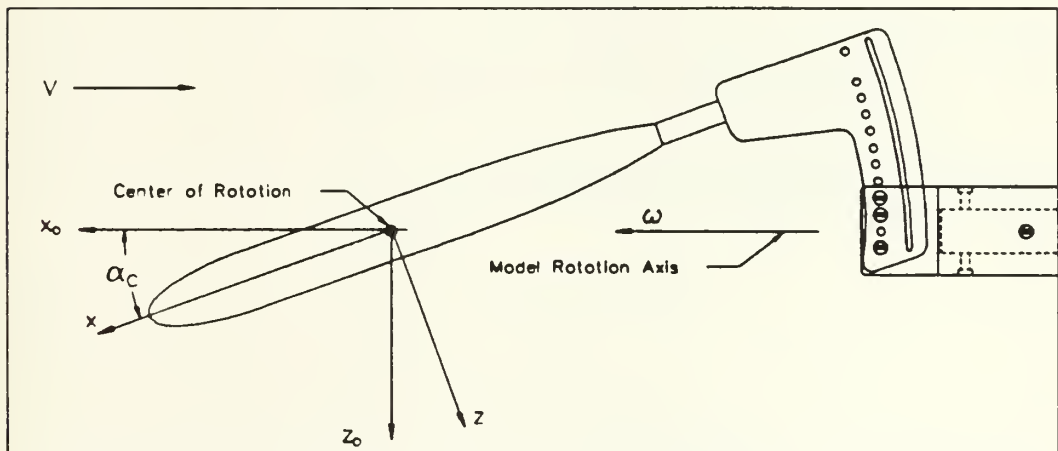
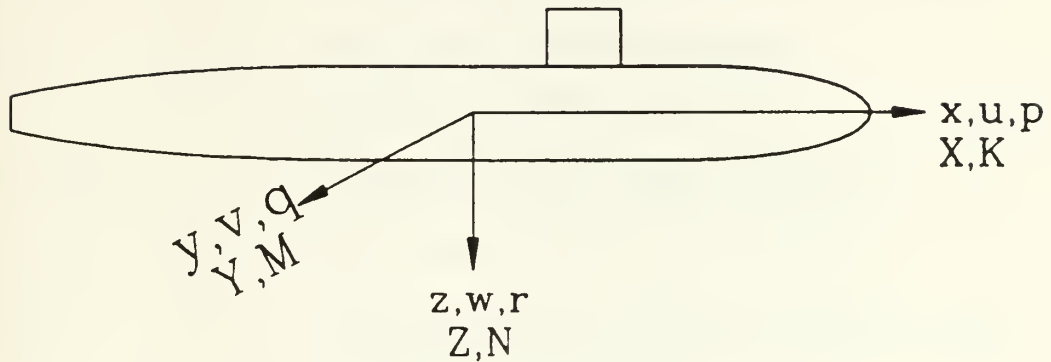
## Table of Figures

Coning Motion .....	11
Flow types and force regimes for increasing angle of attack .....	14
Unappended body of revolution cross-flow .....	15
L/D=9.5 hull in coning motion .....	16
Mathematical model process .....	18
Coning motion model .....	20
Coning motion model and balance assembly .....	21
Coning motion apparatus .....	23
Torsional vibration model .....	27
Forces measured by balance for constant rotation rate .....	30
Coning motion apparatus in tunnel test section .....	31
Data acquisition and reduction system .....	32
Phase shift in raw count data .....	45
Phase shift vs frequency .....	46
Amplitude ratio vs frequency .....	47
X and Z Inertia Forces, 20° .....	50
M Inertial Moment, 20° .....	50
X and Z Inertia Forces, 14° .....	51
M Inertial Moment, 14° .....	51
Y' and Z' non-dimensional forces, 20° .....	55
M' and N' non-dimensional moments, 20° .....	56
Y' and Z' non-dimensional forces, 14° .....	57
M' and N' non-dimensional moments, 14° .....	58
Y' and Z' non-dimensional forces, 8° .....	59
M' and N' non-dimensional moments, 8° .....	60
Y' vs coning angle .....	61
N' vs coning angle .....	62
Predicted and experiment non-dimensional forces .....	67
Predicted and experiment non-dimensional moments .....	68
Summed raw counts output, 20°, 30 ft/s .....	69
FFT of N1 & N2 raw counts, 200 rpm .....	71
FFT of N1 & N2 raw counts, inertia run .....	72
FFT of Y1 & Y2 raw counts, 200 rpm .....	73
200 RPM, Inertia and full-up run FFT results .....	74
25 RPM, Inertia and full-up run FFT results .....	75



## LIST OF NOMENCLATURE

### Body Fixed Axis System



### AXES

Body Fixed:

- $x$  the longitudinal axis, directed from the after to the forward end of the model
- $y$  the transverse axis, directed to starboard
- $z$  the normal axis, directed from top to bottom



## **Tunnel Fixed:**

- $x_o$  the fixed longitudinal axis, colinear with the tunnel longitudinal centerline.
- $y_o$  the fixed transverse axis, perpendicular to  $x_o$  in a horizontal plane, directed to starboard
- $z_o$  the vertical axis, directed downwards

## **COORDINATES AND DISTANCES**

- $x_B, y_B, z_B$  coordinates of the CB relative to body axes
- $x_G, y_G, z_G$  coordinates of the CG relative to body axes
- $\alpha_c$  coning angle, measured from the  $x_o$  axis to the  $x$  axis

## **FORCES AND MOMENTS**

- $X, Y, Z$  force components relative to body axes, referred to as longitudinal, side, and normal forces respectively
- $K, M, N$  moment components relative to body axes, referred to as rolling, pitching, and yawing moments, respectively, referenced to the COR
- $W$  weight of the model;  $W = mg$
- $B$  model buoyancy force

## **INERTIA CHARACTERISTICS**

- $I_x, I_y, I_z$  moments of inertia of the model about the  $x$ ,  $y$ , and  $z$  axes, respectively
- $m$  mass of model

## **SPECIFIC POINTS ON BODY**

- CB center of buoyancy of model
- CG center of mass of the model





- COR Center of rotation, the reference point for all measured and calculated forces and moments, located 11.31 inches aft of the model bow, on the longitudinal axis
- BMC Balance moment center, .895 inches aft of the COR, on the model longitudinal axis

### VELOCITIES

- $u, v, w$  components along body axes of velocity of origin of body axes relative to fluid
- $p, q, r$  angular velocity components relative to body axes  $x, y, z$ ; angular velocities of roll, pitch, and yaw
- $\overline{\omega}$  model rotation vector in tunnel fixed axes;  $\overline{\omega} = \omega \hat{u}_{x_0}$

### MISCELLANEOUS

- $A$  model maximum cross sectional area; area projected onto  $y$ - $z$  plane
- $\rho$  density of fresh water = 1.9348 slugs/ft<sup>3</sup> ( $t=77^\circ\text{F}$ )



***A CONING MOTION APPARATUS FOR HYDRODYNAMIC MODEL TESTING  
IN A NON-PLANAR CROSS-FLOW***

## **Chapter 1 Introduction**

For many years, the primary goal of researchers in the motion dynamics field has been to develop the ability to accurately predict the full-scale motions of vehicles. Even today, with the powerful computational tools available, reliable motion predictions of vehicles in all portions of the maneuvering envelope are not possible. Murray Tobak and Lewis B. Shiff pointed out that the difficult problem is to correctly describe the relationship between the aerodynamic reactions and the motion variables in the inertial equations of motion of an aircraft [1]. This same difficulty applies to the motion of hydrodynamic vehicles as well. For slender body shapes with fin appendages, the problem is compounded by the complex wake structure formed by the maneuvering vehicle. The vorticity shed by the hull and appendages creates a wake field that interacts with the velocity distribution over the vehicle's surface. This in turn effects the surface pressure distribution and thus, when integrated over the body's surface, the total force on the hull/appendage combination. It is this interaction that prevents a closed-form analytic solution to the problem.

To further the understanding of the basic flow field about a slender body, the MIT Marine Hydrodynamics Laboratory has been conducting experimental studies on slender body of revolution configurations, both with and without fin appendages. Previous research by Coney[2], Kaplan[3], Reed[4], and Shields[5], has focused on experimentally determining the nature and strength of the vortical wakes shed from a body of revolution, both with and without a single attached fin. Their test program included both force block measurements of



fin force and moment as well as laser-doppler velocimeter (LDV) measurements for producing cross-flow velocity maps at different stations along the body and for determining vortex strengths.

As both a continuation of the above past research and a step in a new direction, the goal of this study is to construct and demonstrate a coning motion apparatus for hydrodynamic model testing. The primary purpose of this research is to determine the forces and moments on the model as a function of the coning rate. The need for the coning motion captive model test will be developed from both flow field and mathematical model considerations.

## 1.1 Coning Motion

Coning motion can be described as the continuous rolling motion of the vehicle longitudinal axis about the free-stream velocity vector. To generate such a motion in the water tunnel, the model is fixed to some type of support system that can be rotated at constant rotation speed about an axis that is parallel to

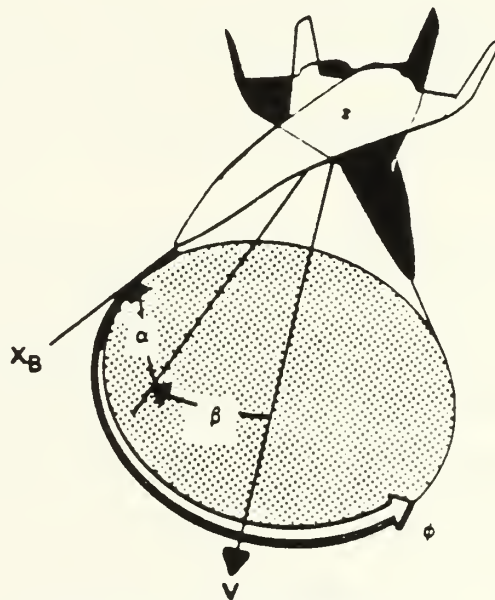


Figure 1. Coning Motion

the free stream velocity vector of the tunnel. In accomplishing this, the model sees a constant attitude with respect to the free stream throughout a rotation cycle. This is a steady coning motion as shown in figure 1. The motion allows for combinations of roll ( $p'$ ) and yaw ( $r'$ ) velocities simultaneously:  $p' = (\cos \alpha_c)\omega'$ ,  $r' = (\sin \alpha_c)\omega'$ .





In a coning motion study, the experimenter has control over six variables:

- $V$ : free-stream velocity
- $\omega$ : body rotation rate
- $\alpha_c$ : coning angle
- $\beta$ : sideslip angle
- $\phi$ : body roll angle
- $d$ : perpendicular distance of the body reference point from the rotation axis

For this study, only three of the available variables were used;  $V$ ,  $\omega$ , and  $\alpha_c$ . The sideslip angle,  $\beta$ , and the body roll angle,  $\phi$ , were set = 0. No sideslip simplified the experiment apparatus and simplified the motion for this test. The roll angle is only significant for bodies with attached appendages. The reference point chosen for the experiment is the center of rotation, therefore  $d = 0$ .

The choice of the parameter  $d$  has a significant impact on the actual inflow velocity to the model. The reference point and the perpendicular distance from the rotation axis for this experiment were chosen to minimize inertial force effects, as shown later in section 2.3.4 and Appendix B. To be completely standard, the reference point should be a function of the body geometry (for comparison with other body shapes). The geometric reference point is the body center of volume, located on the body longitudinal axis, .8 inches forward of the center of rotation.

The coning motion apparatus has been in use by aeronautic researchers since 1926. For their purposes, the coning motion apparatus provided test data on aircraft maneuverability at high angles of incidence and on aircraft steady state spin motion and spin recovery. Later on, the mathematical model developed by Tobak and Schiff indicated that



coning motion is one of the fundamental characteristic motions required for prediction of conventional, nonspinning maneuvers. A good historical account of the development of the coning motion apparatus and its employment at a number of test facilities around the world is given in Reference [6].

## 1.2 Model Testing

Current hydrodynamic captive model testing comprises planar motion simulations, mostly because of the facility limitations. Conventional captive model test types include:

- Straight tow tank or circulating water tunnel at a fixed angle of attack
- Straight tow tank or circulating water tunnel with an oscillator attached to the model (i.e., planar motion mechanism)
- Rotating arm

All of these tests suffer two major deficiencies:

- Cross-flow velocity vectors along the body length lie in a plane
- No roll component of angular velocity ( $p$ )

The significance of these shortcomings can be seen by first looking at the non-planar cross-flow effects and then the roll component effects.

### 1.2.1 Non-Planar Cross-Flow Effects

A body of revolution with no attached appendages in a **planar** cross-flow will exhibit four basic flow types, depending on the angle of attack and Reynolds number. Shown in figure 2 are the four flows along with the normal and side force experienced by an ogive-cylinder at varying angles of attack [7].



The cylinder sheds symmetric vortices with no resultant side force for angles of attack up to the onset angle of attack where the flow transitions to steady asymmetric vortex flow with substantial side force, and then to wake-like flow with minimal side force.

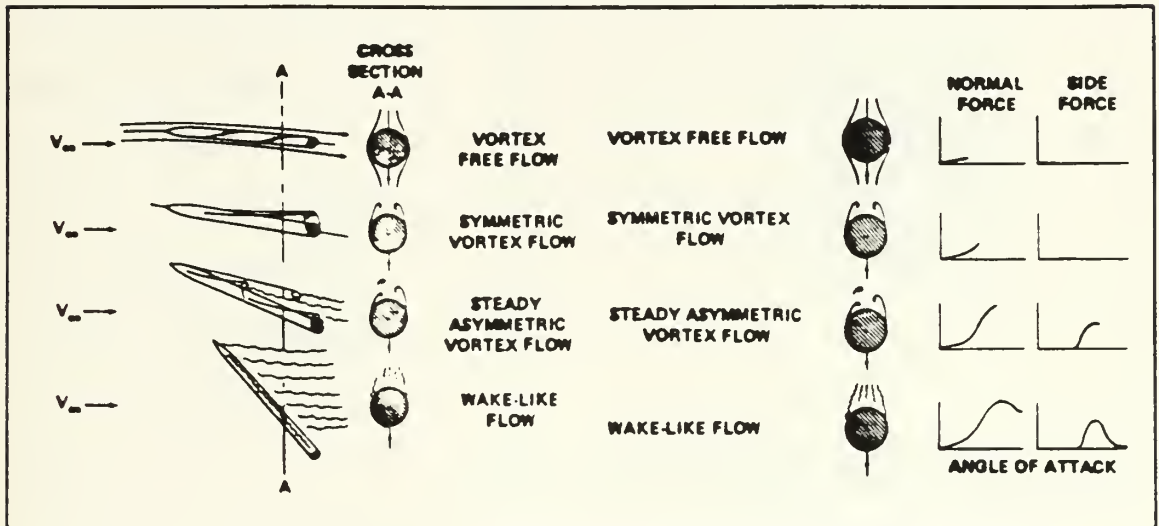


Figure 2. Flow types and force regimes for increasing angle of attack on ogive-cylinder.

Experiments conducted at MIT by Shields[5] on a submerged body of revolution at a Reynolds number of approximately  $6 \times 10^6$  based on model length and at moderate angles of attack (up to  $14^\circ$ ) demonstrated that the body shed symmetric vortices for all angles of attack. The plot of perturbation velocities for  $\alpha = 14^\circ$  shown in figure 3 clearly depicts the two symmetric body vortices. The symmetry here is a direct result of the planar cross-flow that the model is exposed to.





Some work has been accomplished on captive models subjected to non-planar cross-flows. Visual studies done by Tobak, Schiff, and Peterson [8] on a body of revolution in coning motion clearly portrayed the asymmetric vortex field shed by the body in the non-planar cross-flow.

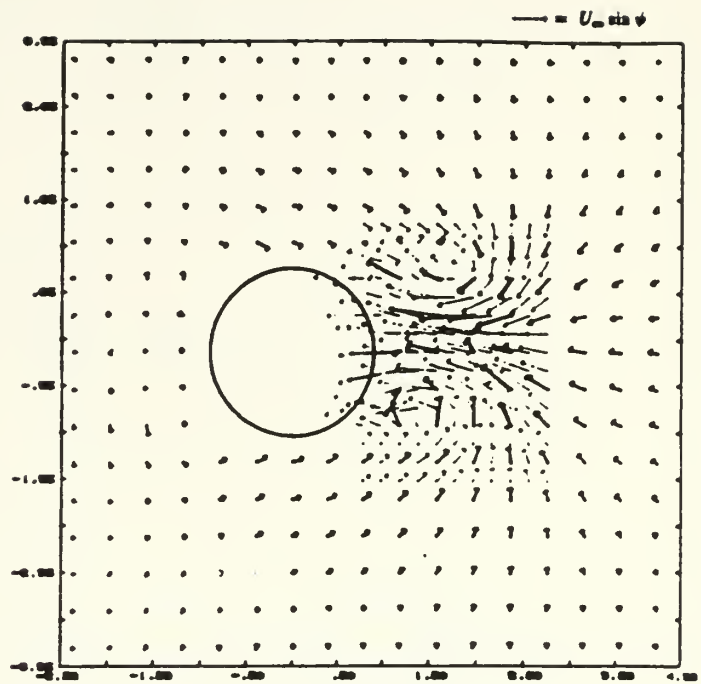


Figure 3. Unappended body of revolution,  $\alpha = 14^\circ$ .

More recently, Nielsen Engineering and Research (NEAR) has run a coning motion case with their SUBFLO, vortex cloud computer code and predicted similar results [9]. The preliminary results are shown in figure 4 for a length/diameter = 9.5 body of revolution in coning motion with  $\alpha=20^\circ$ . The predicted out-of-plane force (i.e., side or Y force) was 50% of the normal (Z) force value.



Current model test techniques cannot capture this effect because of their planar flow limitations. Since actual submersibles rarely operate in a planar cross-flow, the coning motion test provides a more realistic test condition for obtaining coefficient data. Coning characterizes the non-planar nature of a general motion that cannot be constructed from contributions due to any planar motions. The presence of the non-planar motion is a prerequisite for the existence of the coupling terms that are so important in accurately describing the general motion of a six degree of freedom body (e.g., yaw-pitch coupling).

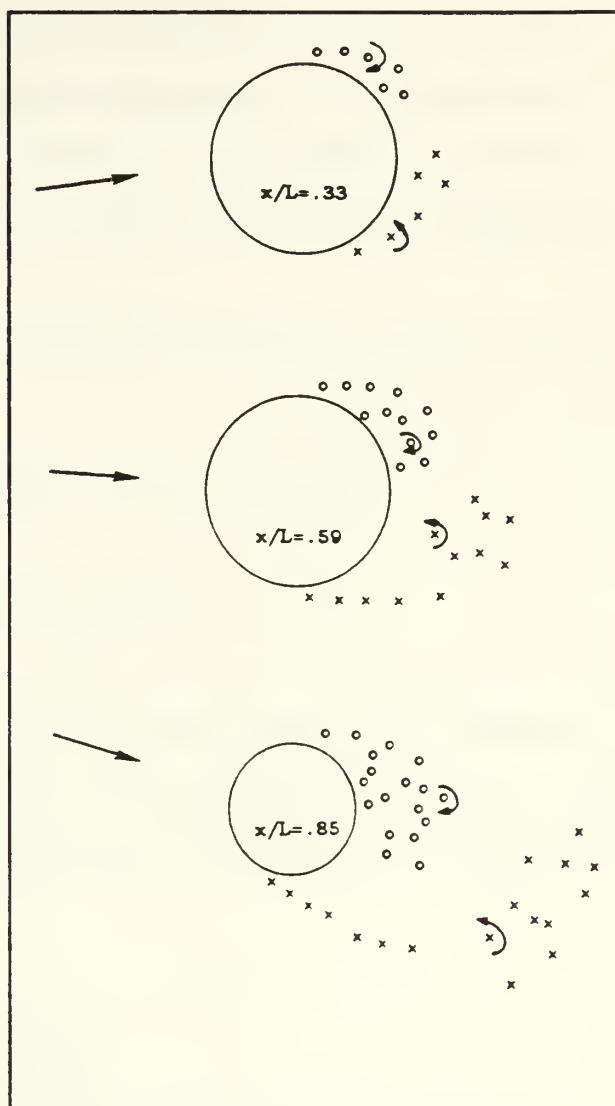


Figure 4.  $L/D = 9.5$  hull in coning motion;

$$\alpha = 20^\circ, p' = .82, r' = .30.$$

## 1.2.2 Roll Component Effects

The Taylor Series expansion approach that is described in section 1.3 produces many coefficients with a roll component,  $p'$ . In the past, these hydrodynamic derivatives have been ignored, mostly because of the inability to obtain model test data for



these derivatives. Three pertinent examples are the linear derivatives,  $Y'_p$ ,  $K'_p$ , and  $N'_p$ , for which there is little or no experimental results available [10].  $K'_p$ , the linear roll damping, is believed to be important on the basis of theory, and has been shown in model tests of missiles to be an even function of angle of attack and to vary considerably for angles of attack above  $5^\circ$  [10].

There are two classes of higher order hydrodynamic derivatives involving roll that are of importance:

- Nonlinear variations of roll damping rate with angle of attack:

- $K'_{\dot{\alpha}p}$ ,  $K'_{r\dot{p}}$ ,  $K'_{qqp}$

- Nonlinearities associated with cross-flow drag:

- $Y'_{ppp}$ ,  $Z'_{ppp}$ ,  $K'_{ppp}$ ,  $M'_{ppp}$ ,  $N'_{ppp}$

The nonlinear roll damping terms will have a much greater influence on an axisymmetric body with an attached fin than the body used in this experiment. The cross flow drag terms are associated with the nonlinear variation of the cross force with the model angle of attack.

## 1.3 Hydrodynamic Math Model

The forces and moments acting on a submerged vehicle are generally non-linear functions of the linear and angular displacements, velocities, and accelerations of the vehicle and the motion of the control surfaces relative to the fluid [11]. Ideally, the functional relationship between the forces and moments and the motion and control parameters would be known and used directly in forming the equations of motion. Unfortunately, the functional relationship is generally unknown. Without this relationship, the function is expressed as a Taylor Series expansion with respect to the rectilinear and angular velocity



components about a chosen condition. For this study, the chosen condition is straight and level operation at the instantaneous surge velocity,  $u(t)$ . Appendix A details a 3<sup>rd</sup> order Taylor Series expansion and simplification for representative forces and moments.

For any mathematical representation of a physical process, the validity of the mathematical model depends on whether the assumed form of the equations of motion adequately represent the physical hydrodynamics and whether the resulting coefficients are realistic. It is not the purpose to this study to validate the use of a Taylor Series expansion as a mathematical modeling tool for this case, but rather to present the framework for the use of the force and moment data obtained from experiment. The interrelation of the mathematical model, theoretical work, and model test data is best described by figure 5. The experimenter's purpose is to provide the experimental results (e.g., non-dimensional forces and moments) and the understanding of the dynamics involved to validate the theoretical work, thereby improving the comprehension of the actual physical processes at work.

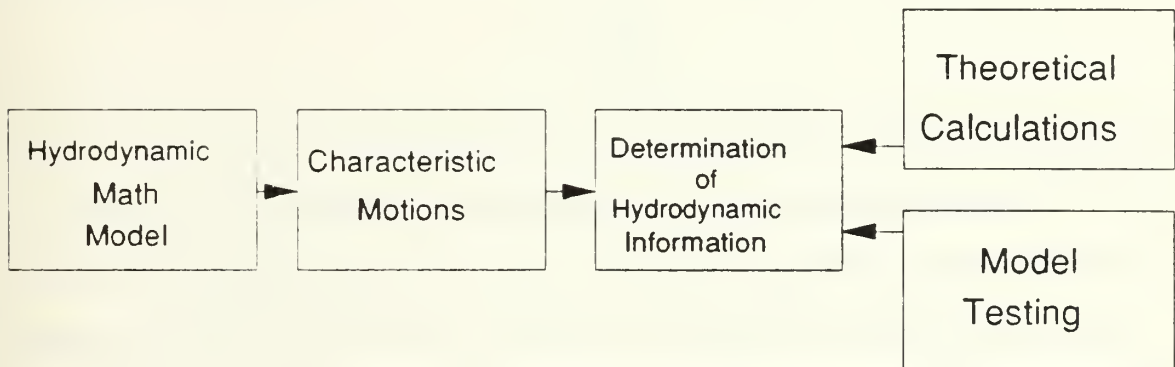


Figure 5. Mathematical model process.

The Taylor series expansion is advantageous from the standpoint that it is numerically efficient and provides a convenient structure for correlating data. However, it has





the disadvantage in that truncation of the series to a certain order limits the range of applicability from the expansion point. Current motion simulators require expansions up to 4<sup>th</sup> order to adequately model yaw-pitch coupling and 5<sup>th</sup> order for slender body lift. In addition to the algebraic burden of the high-order expansion, for the formulation to be useful, the coefficients must be accurately determined.

A simplified expansion for the X force equation, retaining only linear terms is as shown:

$$X' = X'_o + (X'_v v' + X'_w w' + X'_p p' + X'_q q' + X'_r r') + \dots$$

The typical coefficient of a linear term in the expansion takes the form of a partial derivative of a force or moment component with respect to a variable evaluated at the original condition; for example,

$$X_v = \left( \frac{\partial X}{\partial v} \right)_o$$

The form of the hydrodynamic formulation is determined by the coefficients resulting from the expansion. The coefficients determine the characteristic motions that must be evaluated, either analytically or experimentally. Because of the inability to analytically determine the coefficients, model testing, and more recently, full scale ship trials have been used for determining not only the magnitude of the coefficients, but also which coefficients are of primary importance.



## Chapter 2 Description of Test Apparatus

All testing reported in this paper was performed in the MIT Marine Hydrodynamic Laboratory's variable pressure water tunnel.

### 2.1 Model

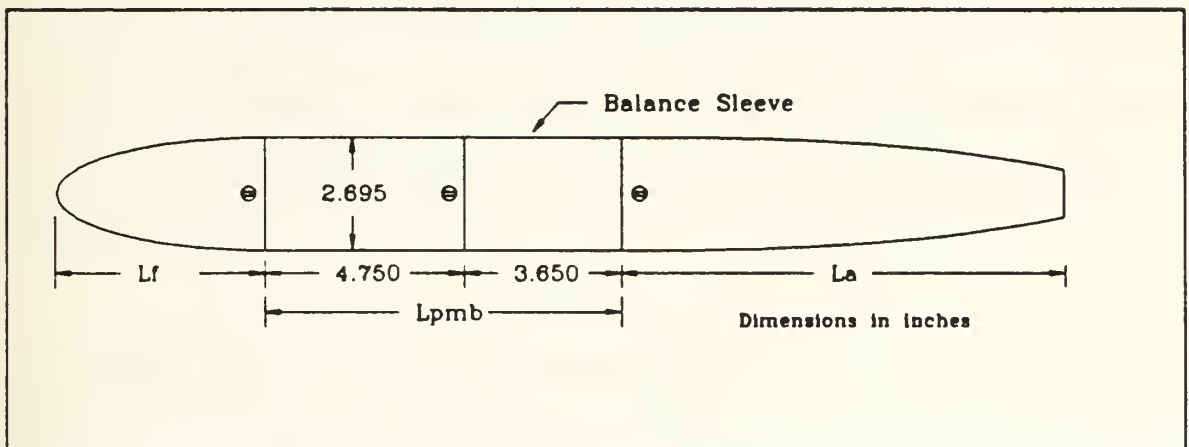


Figure 6. Coning Motion Model

The model used for the experiment has the following characteristics:

- Length/Diameter 9.5
- Length 23.50 inches
- Diameter 2.695 inches
- Weight 10.45 lbs
- Buoyancy 3.23 lbs
- % Parallel Midbody 39.6%
- Length Forward 4.85 inches
- Length Aft 10.25 inches



The model shape shown in figure 6 is the standard  $L/D = 9.5$ , body of revolution used for previous studies carried out at MIT (Ref. [3], [4], & [5]), Stevens Institute of Technology, Davidson Laboratory, and Nielsen Engineering and Research (Ref. [9]). The shell of the model consists of three anodized aluminum pieces which mate to the stainless steel sleeve. The sleeve is mounted to the shell of the balance itself. This sleeve is the only support for the model shell and allows the balance to sense the forces and moments experienced by the model. Void spaces in the assembly were filled with grease to prevent water leakage into the model. At the aft end of the model, some clearance from the sting was allowed to provide for model deflections. This prevented "shorting out" the balance, but also allowed some water to enter the rear cavity. The inertial force contribution from this water was calculated as negligible. The next section describes the balance itself and its waterproofing.

## 2.2 Balance and Sting Assembly

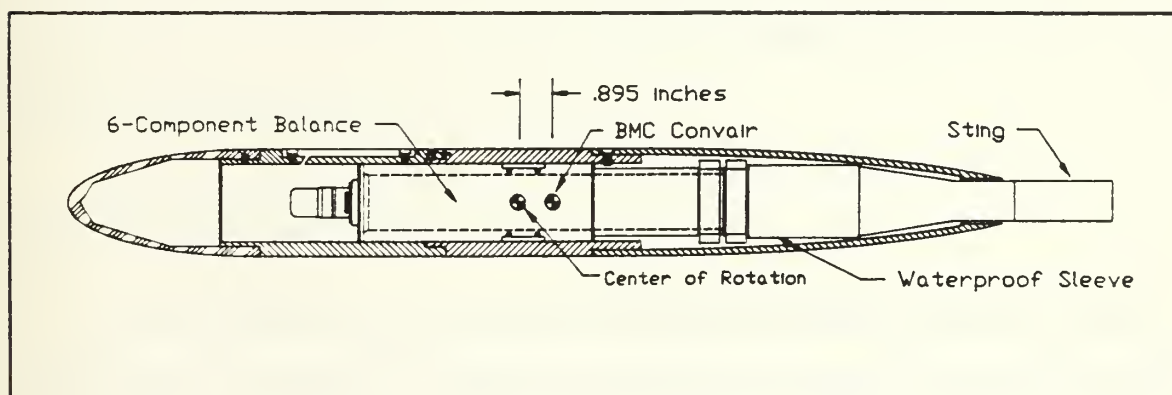


Figure 7. Coning Motion Model and Balance Assembly

Unlike past models, the present body of revolution is equipped with an internally mounted, 6-component balance for measuring hydrodynamic loads (figure 7). The balance



provided by General Dynamics, Convair Division is a 1000 pound rated balance, calibrated to 150 lbs, and adapted for water testing. The balance was fit inside a waterproof sleeve, with the strain gage bridge wires routed out the back through a watertight seal. The balance is hollow and allows for wires from the future fairwater force block to pass through the balance and out with the balance wires. Great care was taken to ensure that the fine wires coming from the balance were adequately waterproofed. Tygon tubing covered the wires from the balance to their exit out the water tunnel.

The balance consists of nine strain gage bridges:

- 2 Normal force bridges
- 2 Side force bridges
- 2 Roll bridges
- 3 Axial bridges

Only six of the bridges are used at one time for producing force and moment readings.

The preferred set of bridges was determined during the calibration done by Convair. Calibration of the balance is discussed in Chapter 3.

## 2.3 Tunnel Installation

A considerable portion of this project was spent on the design, selection, building and installation of components. During the design phase, emphasis was placed on simplicity, reliability, and cost. The resulting system is shown in figure 8.





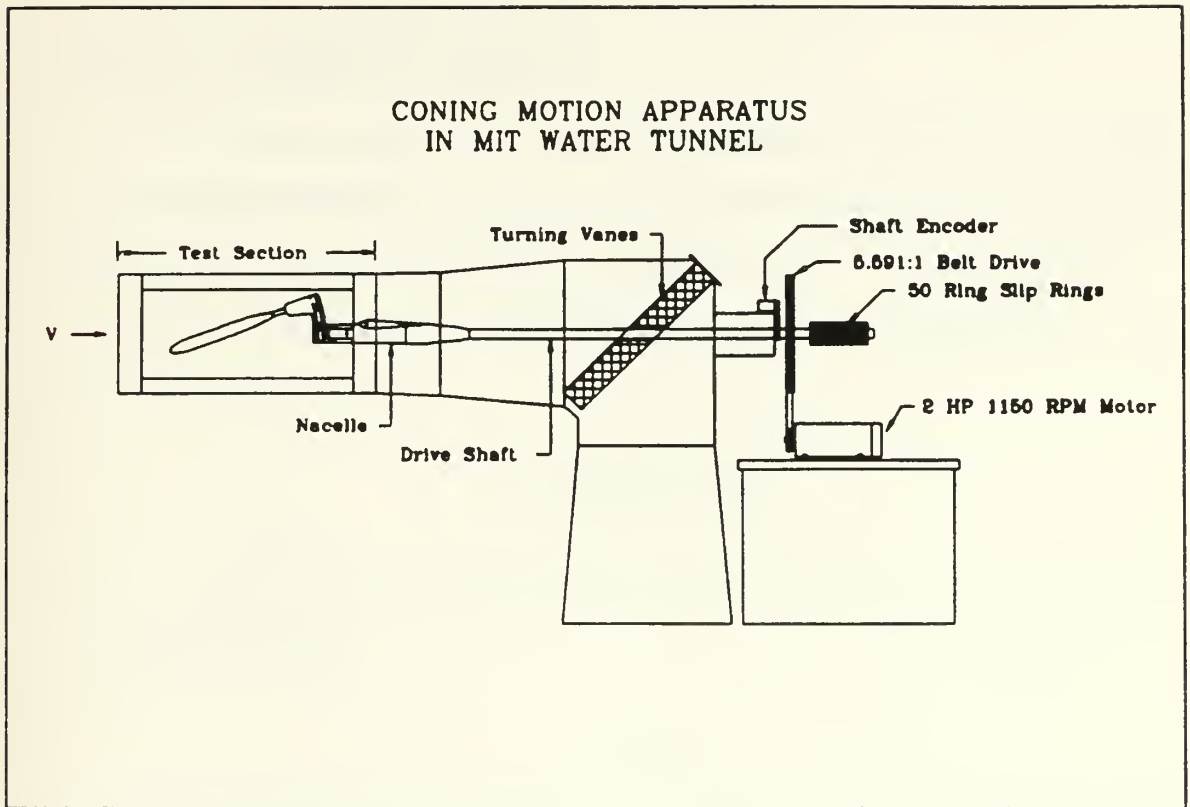


Figure 8. Coning Motion Apparatus

### 2.3.1 Calculations

Because of the first time nature of this type of test in the hydrodynamics field, calculations of the various loads on the system had to be carried out. The calculations were integral to the component selection and design process. These estimates included:

- Model drag and torque at maximum tunnel velocity and rotational speed
- Model and shaft drive system speed variation at different rotational speeds for a "free" system
- Shaft loads and system resonances
- Bearing loads and wear allowances



### 2.3.1.1 Required Torque

The model assembly drag and torque were calculated by modelling the body as a cylinder and the sector as a flat plate. A 2-D strip theory approach was taken, where the model and sector were divided into small strips, and the drag calculated for a cross-flow velocity equal to  $\omega r_i$  for each strip with a drag coefficient based on Reynolds number:

$$D_i = C_D \left( \frac{1}{2} \rho (\omega r_i)^2 \right) A_i$$

$A_i$  is the area of each strip. Torque was then found from summing up the drag contributions from each strip:

$$\tau_h = \sum_{i=1}^n r_i D_i$$

Because of the off-center weight effect that the model and sector produced, the weight torque had to be added to the hydrodynamic torque. Weight torque was calculated using the same sectioning as in the hydrodynamic case and a density of water for the model and a density of .3 lb/in<sup>3</sup> ( $\approx \rho_{steel}$ ) for the sting and sector:

$$\tau_w = \sum_{i=1}^n (\rho_i V_i) r_i$$

where  $V_i$  is the strip volume. The resultant values for the most limiting case,  $\alpha_c =$

$20^\circ$ ,  $v = 30$  ft/s,  $\omega = 200$  rpm, were  $\tau_h = 14.9$  ft-lbs,  $\tau_w = 5.9$  ft lbs. Finally, the minimum required HP was found to be:

$$HP = \frac{(\tau_h + \tau_w)\omega}{550} \approx .79 \text{ HP}$$



Later testing proved two problems with this result. The first was the calculation was carried out for the preliminary sector configuration, which was more streamlined than the final design. Second, the effect of the high free stream velocity (when compared to the  $\omega r$  contribution) was neglected. The addition of the  $V$  term caused the sector to act as an inefficient foil at a varying angle of attack along its span (tunnel radius). Later attempts to model this correctly produced a very flat torque characteristic curve and also proved wrong. The effect of this error was the limitation of approximately 135 rpm for the model at  $20^\circ$ , 200 rpm, and 30 ft/s. 200 rpm could only be achieved for the model at  $20^\circ$  when the free stream velocity was reduced to approximately 10 ft/s. This problem was later fixed by placing a wing attachment on the end of the sector. The attachment was designed for a 2 to 3 degree  $\alpha$  at 200rpm and 30ft/s. The wing was a large success, providing enough lift to autorotate the model at 175 rpm (for  $V = 30$  ft/s)! With the motor assisting, the model easily achieved 200 rpm.

### 2.3.1.2 Speed Regulation

For rotary balance experiments, it is important to maintain a constant rotation rate over a cycle of data taking. To check the worst case condition, a simple calculation was done for a freely spinning system (i.e., no speed regulation). The model and sector were lumped together as an off-center weight of 26 pounds at a radius of gyration equal to 4.24 inches. The main sheave polar moment of inertia was calculated and later obtained from the manufacturer. All other polar inertia contributions were neglected on the assumption that they were small.

For this lumped system the total  $J$  was:



$$J_{total} = (J_{model} + J_{sheave}) = 4366 \text{in}^2 - \text{lbs}$$

The following relations were used to calculate the rpm variation:

$$\bar{\tau}_o = \frac{d(\bar{H}_o)}{dt} \quad \text{where} \quad \bar{H}_o = \sum_{i=1}^n m_i r_i^2 \bar{\omega} \quad , \text{ the angular momentum for this case.}$$

Substituting:

$$\bar{\tau}_o = \sum_{i=1}^n m_i r_i^2 d \frac{\bar{\omega}}{dt} = J \bar{\dot{\omega}}$$

Solving for the angular acceleration  $\dot{\omega}$ :

$$\dot{\omega} = \frac{\tau}{J} = A \sin(\omega_o t) \quad \text{where, } \omega_o \approx 20.9 \text{rad/s}$$

Finally, the angular speed variation was found from integrating this expression:

$$\omega = \int \dot{\omega} dt = -\frac{A}{\omega_o} \cos(\omega_o t) + \omega_o$$

Substituting in the numbers for 200 rpm (20.9 rad/s) and  $\tau_w = 10 \text{ ft-lbs}$ :

$$\omega = -.507 \cos(20.9t) + 20.9$$

This gave a worse case variation of  $\approx 4.8 \text{ rpm}$  over 1 revolution. The advertised speed regulation for the motor would give a max variance of  $\approx 2.2 \text{ rpm}$  over 1 cycle (1%).

To avoid all of this, the main sheave was counter weighted during the inertia and data runs.

### 2.3.1.3 System Torsional Resonance

Unknown loads on the model-sector combination could result in a resonant vibration in the system. To investigate this, the torsional resonance frequency was





calculated for varying  $J$ 's and shaft "stiffness" constants ( $K_1$ ). The system was modeled as a two disk, torsional vibratory system, shown in figure 9. The model/sector combination accounted for  $J_1$ , the main sheave,  $J_2$ .

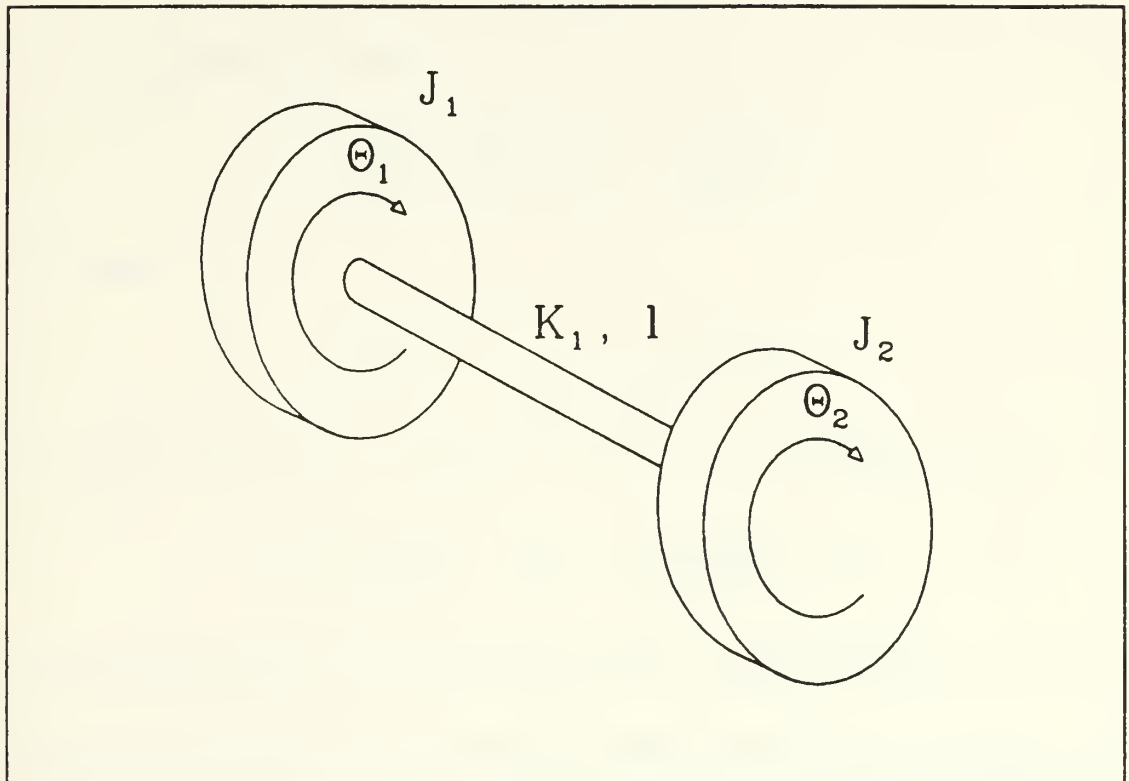


Figure 9. Torsional Vibration Model

The equation for the resonant frequency was derived starting with Lagrange's equations with no forcing function:

$$\text{Equation of motion: } \frac{d}{dt} \left( \frac{\partial L}{\partial \dot{\theta}} \right) - \left( \frac{\partial L}{\partial \theta} \right) = 0, \text{ where } L = T^* - V$$

$$T^* = \left( \frac{1}{2} \right) J_1 \dot{\theta}_1^2 + \left( \frac{1}{2} \right) J_2 \dot{\theta}_2^2 \quad (\text{Kinetic co-energy})$$

$$V = \left( \frac{1}{2} \right) K_1 (\theta_1 - \theta_2)^2 \quad (\text{Potential energy})$$



Assuming an undamped system, the angles take the harmonic form:

$$\theta_1 = A_1 e^{\pm j\omega t}$$

$$\theta_2 = A_2 e^{\pm j\omega t}$$

The resulting equation to solve is:

$$\begin{bmatrix} J_1 & 0 \\ 0 & J_2 \end{bmatrix} \begin{bmatrix} -\omega^2 A_1 \\ -\omega^2 A_2 \end{bmatrix} + \begin{bmatrix} -K_1 & K_1 \\ K_1 & -K_1 \end{bmatrix} \begin{bmatrix} A_1 \\ A_2 \end{bmatrix} = 0$$

Rearranging:

$$\begin{bmatrix} -J_1\omega^2 - K_1 & K_1 \\ K_1 & -J_2\omega^2 - K_1 \end{bmatrix} \begin{bmatrix} A_1 \\ A_2 \end{bmatrix} = \begin{bmatrix} 0 \\ 0 \end{bmatrix}$$

The characteristic equation is:  $\det[B] = 0$ . This leads to the desired relation for  $\omega$ :

$$\omega^2 = \left[ \frac{J_1 + J_2}{J_1 J_2} \right] K_1, \text{ where } K_1 = g \frac{\pi G}{32l} (d_o^4 - d_i^4)$$

$d_o$  = outer shaft diameter,  $d_i$  = inner shaft diameter,  $l$  = shaft length,  $G = 12 \times 10^6$  psi for steel, and  $g = 386 \text{ in/s}^2$ . For the final system, the torsional resonance frequency  $\approx 50 \text{ Hz}$  (3000 rpm), which is much higher than the filter cutoff frequency of 3 Hz (180 rpm) and the maximum shaft rotation rate (200 rpm).

## 2.3.2 Modifications

The MIT variable pressure water tunnel required significant modifications before the study could be undertaken. The primary modifications necessary were:

- Boring and sleeving the turning vanes to allow for the shaft installation
- Modifying the forward nacelle to accept "DU" type bushings for supporting the shaft, model, and sector in the test section



- Aligning and welding the bearing housing mount plate on the tunnel exterior
- Installing a motor and drive system for rotating the model and shaft

Special consideration was given to the rigidity of the system since unknown resonances in the model-sting-drive system would have a disastrous effect on the data. The forward nacelle is rigidly mounted to the tunnel as is the exterior bearing housing assembly. The precautions proved to be worthwhile; the apparatus showed only small amplitude vibrations up to maximum system capabilities.

### 2.3.3 System Characteristics

The basic system characteristics are:

- Model angle of attack  $0^\circ$  to  $20^\circ$  in  $2^\circ$  increments
- Rotations speed 0 to 200 RPM, both directions
- Tunnel water velocity 0 to 30 ft/sec
- Rotary speed regulation to  $\pm 1\%$  for 95% change in load
- Drive motor: GE 2 HP DC shunt wound, 1200 rpm, variable speed
- Drive system: 2-belt drive with drive ratios from 5.59:1 to 8.2:1
- 50 channel (rings) capability

Model rotation rate was derived for similitude in non-dimensional roll,  $p'$ , with full scale vessels. Using the conventions in Appendix A,  $p' = 1.37$  for 200 rpm at  $U = 30$  ft/sec. The coning angle limit of 20 degrees is based on tunnel test section dimensions.



## 2.3.4 Test Section Installation

There are three contributions to the forces and moments measured by the balance in the model (see figure 10). The first is from the inertial forces and moments of the model itself, which vary with the model attitude and rotation speed. The second is from gravity (model weight) and buoyancy, which will vary cyclically over a revolution. Finally, there is the contribution from the hydrodynamic loads. The desire to reduce or eliminate all but the desired hydrodynamic forces had a great effect on the installation design.

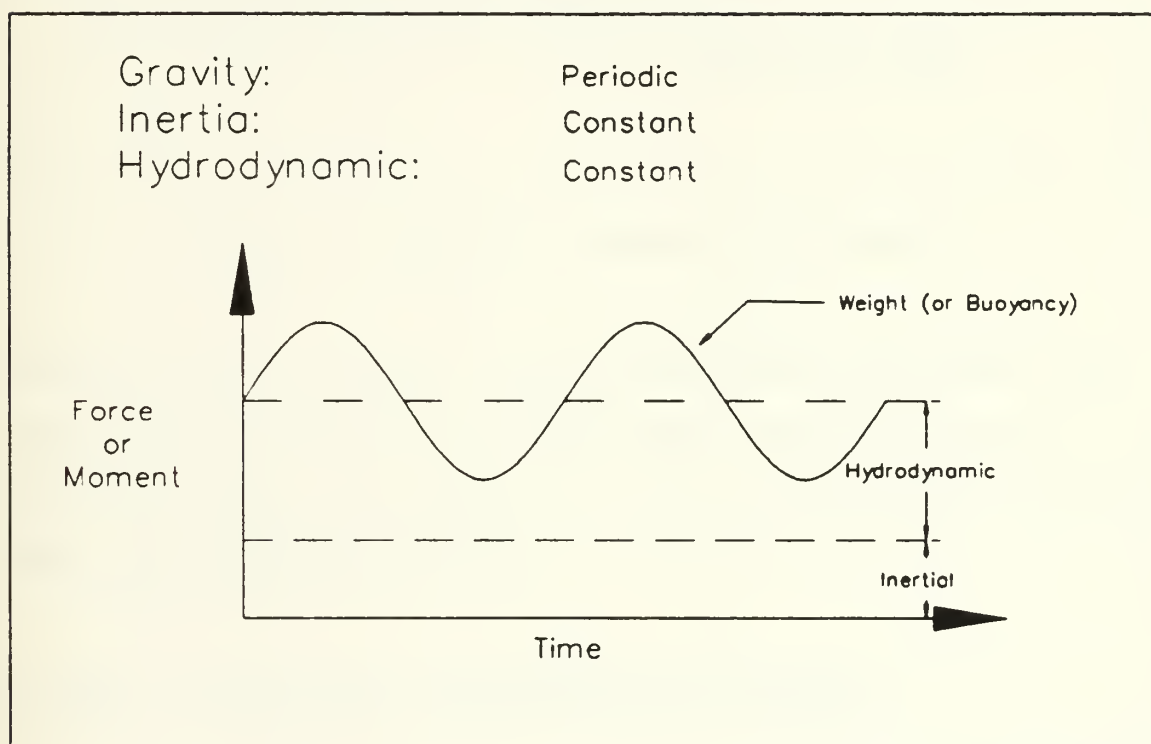


Figure 10. Forces measured by the balance for constant rotation rate

A close-up of the model in the test section is shown in figure 11. The model center of rotation was chosen such that the model center of gravity would be as close to





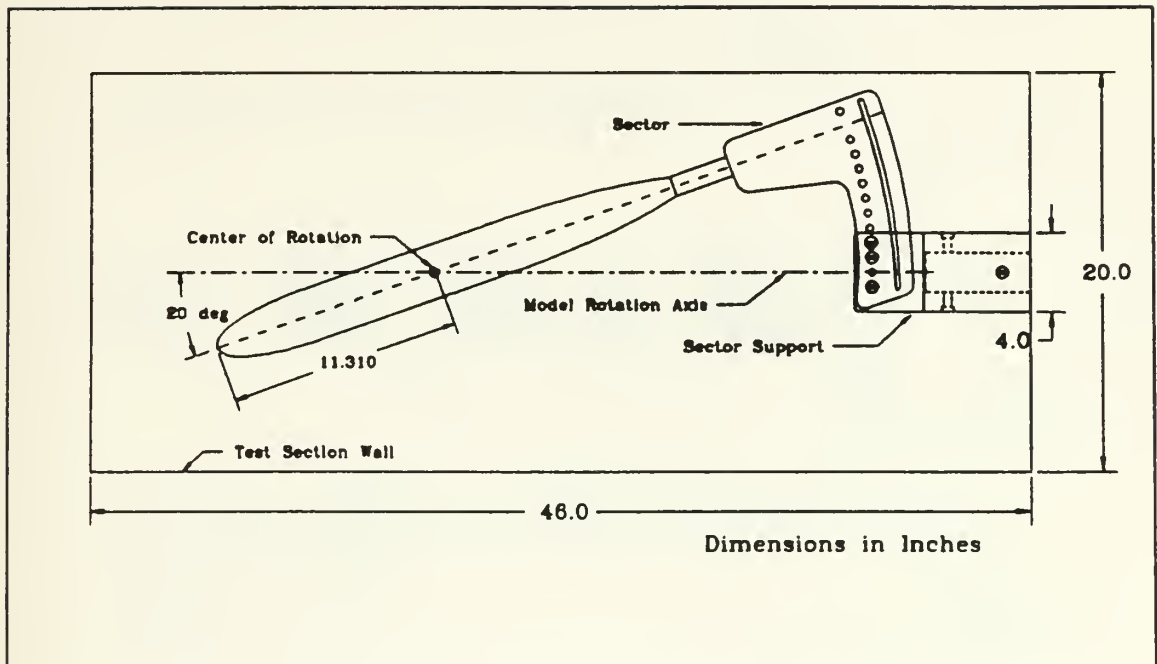


Figure 11. Coning Motion Apparatus in the Test Section

the model rotation axis as possible. This reduces the inertial force contribution. Additionally, reducing the differences in the model moments of inertia also decreases the body inertial moments (see Appendix B). As it turned out, the inertial forces were very small compared to the hydrodynamic loads.

## 2.4 Data Acquisition and Reduction System

The data were taken with the stand-alone, microcomputer-based, data acquisition and reduction system shown in figure 12. The components will be described by their functional grouping.



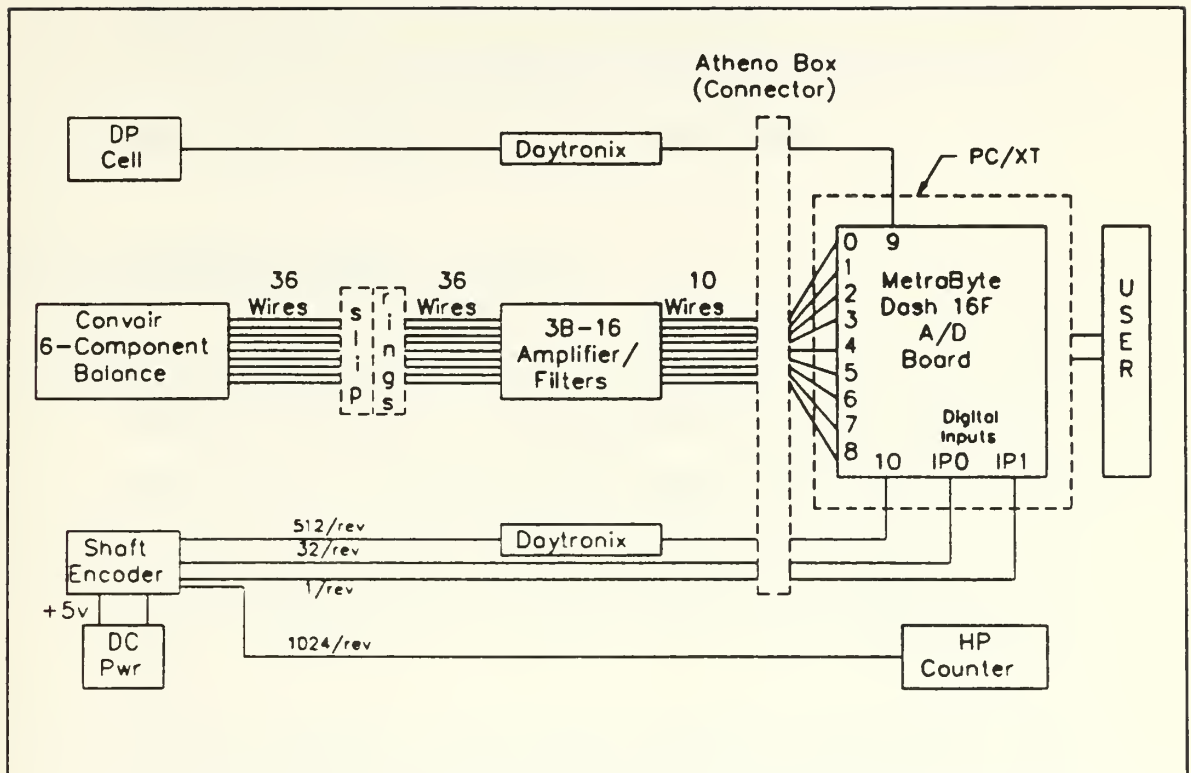


Figure 12. Data Acquisition and Reduction System

## 2.4.1 Instrument Group

The instruments consisted of the 6-component balance, tunnel differential pressure (DP) cell, and shaft encoder. Their basic functions were as follows:

- **Balance**: 9-element (strain-gauge bridge), internal balance used for measuring the forces and moments experienced by the model
- **DP Cell**: Used for measuring test section velocity
- **Shaft Encoder**: 12 bit, natural binary encoder (BEI model C-14) used for model rpm, data trigger, and shaft position for static tests. The encoder outputs a 0 to +5 volts square wave signal at frequencies from 1/revolution to



2048/revolution ( $2^{11}$ ). The 1/rev and 32/rev signals were used for shaft position, the 32/rev for triggering, the 512/rev for model rpm (computer input), and the 1024/rev for model rpm (counter input).

## 2.4.2 Amplifier/Filter Group

Signal amplification and filtering was accomplished by two sets of instruments:

- 3-B Series (Type 3B-16): A nine module block of signal conditioners and filters that filter and amplify the balance outputs to a standard  $\pm 5$  Volt analog signal. The modules had an upper cutoff frequency of 3Hz for filtering out high-frequency noise (a characteristic that caused considerable trouble later).
- Daytronix 9000 Series: Two modules were used: the strain gauge conditioner (9170) for boosting the DP output to a  $\pm 5$  Volts range, and the frequency to voltage module (9140) for converting the encoder 512/cycle output to a 0 to +5 Volt analog signal for model rpm.

## 2.4.3 Computer Group

The heart of the system was the IBM PC/XT personal computer. The PC had a MetraByte Dash 16F analog to digital (A/D) board installed for acquiring and converting the balance voltages to counts. The Dash 16F also read in outputs from the tunnel differential pressure (DP) cell and the shaft encoder. The analog portion of the board was set for a resolution of 2.44 millivolts (409.6 counts/volt). The board had a conversion time of approximately .0417 millisec./channel using direct memory access (DMA). This was a very important point which will be discussed in chapter 3.



The Dash 16F also was capable of reading in a digital signal through its digital input ports. This feature enabled the encoder to act as a trigger, using software to decipher the digital word read in from the port.

The PC/XT controlled the data taking process through software. Standard Project Athena laboratory routines were used for controlling the analog and digital sampling. The routines were incorporated into user-developed FORTRAN code. The major drawback to using the FORTRAN routines was the increased time required to obtain an analog sample. The experimentally determined sample time was approximately .052 msec/channel, an increase of .0103 msec/channel over the calculated rate.

Finally, the PC stored and processed the averaged component (DC) of the signal and on-line presented the force and moment measurements. The time-varying signal was stored on magnetic media for later off-line processing.

Not connected to the computer, but used for setting the rotation rate was the HP (Hewlett-Packard) counter shown in the figure. The counter read directly off the shaft encoder and gave an accurate counts/sec output, which was then converted to RPM.

## 2.4.4 Slip Rings

The balance signals (millivolts) were taken from the rotating model reference frame to the fixed data system frame via a 50 ring slip ring assembly. The slip ring assembly (Airflyte model DAY-491-50) used was specifically designed for strain gauge measurements. As the experiment showed, the rings were very "quiet", passing little electrical noise to the amplifier/filters.





## Chapter 3 Test Procedure and Tare Measurements

### 3.1 Balance Calibration and Check-out

The 6-component balance calibration was accomplished at Convair, prior to its installation in the model. A precise calibrating body was fit over the balance and then the assembly put in a calibration fixture. The fixture allowed for the accurate placement of loads and moments on the body, with corrections for deflection being taken into account. The calibration results were placed in a two inch thick binder containing information necessary for using the balance. The information included:

- R-cal readings for all 9 channels (shunt resistor equivalent)
- Balance constants for the different combinations of roll moment and axial force gauges
- Plots of the response of the balance vs applied load (for applied axial, normal, and side force and roll moment)

The R-cal readings are merely voltage (counts) outputs for the balance channel being tested, with and without the shunt resistor switched into the circuit. The  $\Delta$  voltage (counts) allows a second site to establish calibration ratios between the counts read on their A/D system and the equivalent readings on the Convair test bench. In this experiment, the ratio was set as:

$$\text{Ratio} = \frac{R\text{-cal}_{\text{Convair}}}{R\text{-cal}_{\text{MTT}}} \approx 2.45$$

The ratio varied by channel, however, the variance was small. The ratio calculated above shows that the Convair A/D system had approximately a factor of 2.45 better resolution than the system used in this study.



The balance constants were not used because of the simplified linear algorithm chosen for converting the balance readings to forces and moments. Several methods were available for doing this conversion, but the linear method was chosen for its simplicity and speed. Other methods available are described in References [12] and [13].

### 3.1.1 Data Reduction Model

Stevens Institute of Technology, Davidson Laboratories, developed the linear, 6<sup>th</sup> order method implemented in this study. In developing this linear model, Stevens had to fit the Convair calibration data and then compare the linear model performance against the more complex Convair algorithm.

The first step is to compute the 6x6 calibration matrix. The goal is to obtain a matrix of coefficients that accounts for the imperfections in the balance construction, which appears in the form of cross-talk, and yields the correct force vector. In other words, for a simple single, in-plane force, such as a normal force applied at the reference center, the detected force by the balance will consist of contributions from all 6 channels:

$$Z = \sum_{i=1}^6 a_i r_i$$

where  $a_i$  are the calibration coefficients and  $r_i$  are the balance readings from the six channels. For a generalized load application, the matrix equation is:

$$\overline{L} = [A]\overline{R}$$



where  $\bar{L}$  is the load vector,  $[A]$  is the desired coefficient matrix, and  $\bar{R}$  is the corresponding balance reading vector. During the calibration done at Convair, several load vectors were applied while recording the associated balance reading vectors. This resulted in the following, overdetermined system:

$$\begin{bmatrix} Z_1 & Z_n \\ M_1 & M_n \\ Y_1, \dots, Y_n \\ N_1 & N_n \\ K_1 & K_n \\ X_1 & X_n \end{bmatrix} = \begin{bmatrix} a_{11} & a_{12} & a_{13} & a_{14} & a_{15} & a_{16} \\ a_{21} & a_{22} & a_{23} & a_{24} & a_{25} & a_{26} \\ a_{31} & a_{32} & a_{33} & a_{34} & a_{35} & a_{36} \\ a_{41} & a_{42} & a_{43} & a_{44} & a_{45} & a_{46} \\ a_{51} & a_{52} & a_{53} & a_{54} & a_{55} & a_{56} \\ a_{61} & a_{62} & a_{63} & a_{64} & a_{65} & a_{66} \end{bmatrix} \begin{bmatrix} N1_1 & N1_n \\ N2_1 & N2_n \\ Y1_1, \dots, Y1_n \\ Y2_1 & Y2_n \\ R2_1 & R2_n \\ X1_1 & X1_n \end{bmatrix}$$

where the subscripts refer to the loading condition. This equation can be rewritten as:

$$[R]^T [A]^T = [L]^T$$

The solution to this system is found by utilizing a least squares approach. This is equivalent to minimizing the Euclidean norm of

$$[R]^T [A]^T - [L]^T$$

Davidson Lab has a standard program which, given a file containing the loads and results, carries out both the linear least squares fit and the matrix inversion to get the final coefficient matrix,  $[A]$  [12]. This matrix was then used to convert the balance readings obtained from the experiment into the force and moment data presented.

### 3.1.2 Balance Operation

The next logical step was to verify the correct operation of the balance. Successful completion of this portion of the experiment would give:

- A check of the data reduction method



- The balance axis convention
- A check of the data taking system
- Model weight and center of gravity

### 3.1.2.1 Weight Calibration and Axis Convention

The first experiment run was the application of known weights on the balance. Stevens Institute provided a collar attachment that fit around the stainless steel sleeve and allowed weight placement with the model set at  $\alpha_c = 0$  degrees and roll = 0 degrees. Weights were systematically placed on the collar and readings taken using the static FORTRAN code developed for these runs. Applied loads varied from .4 to 12 pounds. The resultant Z force was approximately 1.8 times the applied load. After much searching, the error was found in the coefficient matrix associated with reference to the center of rotation. The transpose of the coefficient matrix had been used, causing the Z force error. The error was corrected, allowing the next step to proceed.

The sign convention for the axis system was checked by first setting the model to 0°, 0° and taking a measurement. This measurement became the "zero" file and would be subtracted from the subsequent reading. Next, a known (in sign only, not magnitude) force or moment was applied to the model and a set of readings taken. The difference between the second reading and the zero file produced the read sign of the force (or moment). The test showed the following axis convention:

- X: positive out model bow
- Y: positive out model port side
- Z: positive down
- K: positive for model starboard side up





- M: positive for model bow down
- N: positive for model bow to port

(Bold typeface indicates non-standard sign convention.) To avoid further confusion, the axis convention above was adopted for the test readings only. The test measurements would be presented as follows:

- Dimensional forces and moments: above, non-standard convention
- Non-Dimensional forces and moments: SNAME axis convention as presented in the list of nomenclature.

### 3.1.2.2 Model Weight and CG

With the axis convention determined, the model weight and center of gravity were established. Two types of experiments were run, first, an inclining experiment, second, a simple set of roll experiments. In the first experiment, the model is set at 0° (pitch or  $\alpha_c$ ), 0° (roll), a set of zeroes taken, and then inclined 2 degrees at a time (in pitch) with readings taken at each point. The weight is found from the relation

$$X = W \sin(\alpha_c)$$

The X force is plotted against  $\sin(\alpha_c)$ . The slope of the plot is the model weight. The slope gave the model weight as  $\approx 10.3$  lbs. Though the data plotted very linearly, the maximum X force measured was  $\approx .35$  pounds. More emphasis was placed on the results of the following roll tests.

The next experiment consisted of a set of roll runs. First, the model was placed at either 0°, 0° or 0°, 90 (degrees roll angle). A set of "zeroes" were taken. Then the model was rolled 180 degrees and again sampled. The resulting readings gave the following results:



- 000, 180 Test:  $Z = 2(\text{Weight})$ ,  $X_{cg} = \frac{\Delta M}{2(W)}$ ,  $Y_{cg} = -\frac{\Delta K}{2(W)}$
- 090, 270 Test:  $Y = -2(W)$ ,  $X_{cg} = -\frac{\Delta N}{2(W)}$ ,  $Z_{cg} = \frac{\Delta K}{2(W)}$

Giving numbers:

- $W \approx 10.45$  pounds
- $X_{cg} \approx .4$  inches forward of center of rotation
- $Y_{cg} = Z_{cg} \approx 0$

As a measure of some confidence, the test data was re-reduced using the coefficient matrix referenced to the balance moment center (BMC). The results were nearly identical. Additionally, the different components of the balance gave consistent results (i.e., Y force determined  $W \approx Z$  force determined W).

### 3.1.2.3 Temperature Effects

During this check-out phase, the temperature sensitivity of the balance was discovered. Because the balance is a large mass of metal, the temperature of the balance took some fixed time to stabilize. Even the small heat generated by energizing the gauges affected the balance outputs (significantly). A quick experiment was run where, with the model in air, the balance was energized and readings taken every few minutes. The first 15 minutes produced drifts of 2.5 lbs Y, 1.1 lbs Z, 1.9 in-lbs K, and 1 in-lb M. Over the next 30 minutes, the drift fell off considerably.

To counter this "warm-up" effect, the strain gauges were left energized during the entire experiment. The temperature sensitivity caused problems in the full-up data runs later because of the tunnel water temperature rise over run time.



## 3.2 Test Procedure

### 3.2.1 Test Logic

A coning motion test produces forces and moments from multiple sources. Three components discussed in Chapter 2 are weight (or weight - buoyancy), inertia and hydrodynamic. An additional "force" is the bridge offsets or zeroes. This fourth component is a function of temperature. The only force (or moment) of interest is the hydrodynamic force. To this end, a test procedure had to be developed that accounted for each component and left the desired result. For this study, the desired result was both the time varying (or AC component) and the steady state (or DC component) hydrodynamic force. The basic test procedure was (starting with the model at the desired  $\alpha_c$ ):

#### A. Model in air

- 1) Take a set of readings at set angular positions around a 360° rotation. Measurements done every 11.25° starting at 0° and rotating in the positive (standard convention) direction (by hand) to 348.75° (32 sampling positions).  
Store the raw counts for all 9 channels (100 sample sweeps/angular position, summed to 1 point), both for each point (AC data) and the summation of all 32 points (1 revolution)/channel (DC data). **Result:** weight and offsets raw counts for that  $\alpha_c$ .
- 2) Conduct "wind-off" runs at same rotation rate ( $\omega$ ) and direction as "full-up" runs. Sample all 9 channels (1 sample sweep/angular position) and store each raw counts data point. Sum raw counts for each channel over # of revolutions (usually 10) and store for processing with DC water run results. **Result:** weight, offsets, and inertia raw counts for that  $\alpha_c$  and  $\omega$ .



- 3) Subtract DC raw counts measurements in test A.1 from the DC raw counts measurements in test A.2. Process the results for only the preferred 6 channels. **Result:** inertia force for that  $\alpha_c$  and  $\omega$ .
- 4) Repeat A.2 through A.4 for each  $\omega$ , A.1 through A.4 for each  $\alpha_c$ .

**Note:** Though not processed immediately, the weight and inertia vs angular position raw counts are stored and can be processed later for the inertial effect over a rotation cycle.

#### **B. Model in water**

- 1) After a "soak" period, usually overnight, repeat test procedure A.1, with the model in water and tunnel free stream velocity = 0. **Result:** weight - buoyancy, and offsets.
- 2) Establish tunnel test conditions (i.e., tunnel free stream velocity and model rotation rate). Conduct "full-up" run, recording 11 channels of data (9 balance, 1 DP, 1 rpm) at each angular position and storing the raw counts. Sum raw counts for each channel over # revolutions for averaged (DC) component. **Result:** weight - buoyancy, offsets, inertia, and hydrodynamic raw counts.
- 3) Subtract DC raw counts measurements in test B.1 from DC raw counts measurements in test B.2 (9 balance channels only). Process averaged data for only preferred 6 channels, DP cell, and rpm data. **Result:** inertia and hydrodynamic averaged force (over # rotation cycles).
- 4) Subtract inertia force measurements corresponding to that  $\omega$  and  $\alpha_c$  from the B.3 result. **Result:** Hydrodynamic force for those test conditions.
- 5) Repeat B.2 through B.4 for each  $\omega$ , B.1 through B.4 for each  $\alpha_c$ .





Note: Again, the time varying data are all stored as raw counts files for future processing.

The motivation behind the many decisions made in preparing this procedure is discussed in the following sections.

## 3.2.2 Code Development

At the core of the data taking was the FORTRAN software developed by the author (in conjunction with the routines developed by Glenn McKee of Stevens Institute, Davidson Labs). The form of the test procedure and its limitations dictated the form of the code. The critical issues considered were:

- Timing
- System capabilities
- Desired outputs (i.e., time varying and averaged forces)

### 3.2.2.1 Timing

The basic timing parameters considered were:

- A/D sample and conversion time for 11 channels
- Model rotation rate
- Code loop execution time
- # of divisions over a revolution
- Maximum allowed change in gravity vector over a sample sweep

The MetraByte Dash 16F specifications give an estimated A/D conversion time with DMA (Direct Memory Access) transfer of .04167 msec/conversion. For 11



channels, this works out to  $\approx .46$  msec. The experimentally determined A/D conversion and transfer time  $\approx .052$  msec/conversion giving a total  $\approx .57$  msec for 11 channels. The importance of this is seen by looking at the maximum allowed change in gravity over a sample sweep.

Using a small angle approximation for the change in rotation angle over a sample sweep, the following relation was derived:

$$\Delta G \approx \Delta\theta \approx .01\text{rad} (.57 \text{ deg})$$

for a maximum allowed change of 1%. At the maximum rotation speed of 200 rpm, this works out to .4775 msec. The data taking system used simply could not satisfy the 1% criteria (at 200 rpm). The actual  $\Delta G$  for this study was  $\approx 1.2\%$  (.68°).

The time to execute one data taking loop lead directly to the # of increments that could be sampled over 1 revolution. Use of the shaft encoder as both a trigger and a position indicator (locating the 0° position) required several logic statements in FORTRAN. The logic allowed the code to read the digital word on the D/D input ports and determine, 1) when to set 0°, and 2) when to trigger a sample sweep. Embedded in the logic loop was the Project Athena Laboratory sampling routine for reading in and storing the A/D data. By running several loop timing versions of the data taking code, the time to execute the loop was found to be  $\approx 5.2$  msec for an 11 channel sweep. Again looking at 200 rpm, the maximum number of increments in one revolution that would allow the loop to execute and return for the next trigger pulse was 32. This allowed 9.375 msec for loop execution and return. 32 data points per rotation were felt to be adequate resolution for the purposes of the experiment.

The data taking code used in this study is included in Appendix D.



### 3.2.2.2 Desired Results

During the initial code development, the thought was to work directly with the individual raw counts data points for subtracting tares and converting to forces. The averaged force values would then be computed from these results. Unfortunately, upon actual data taking, a mysterious phase shift and amplitude drop off were noticed for all rotational speeds. The offenders in this case were the 3B-16 Amplifier/Filters supplied with the balance. This should have come as no surprise, especially when the 3 Hz upper cutoff frequency was known a priori. The phase shift can be seen graphically in figure 13. Fortunately, only the time-varying or AC component was affected, passing the zero Hz or DC component unchanged.

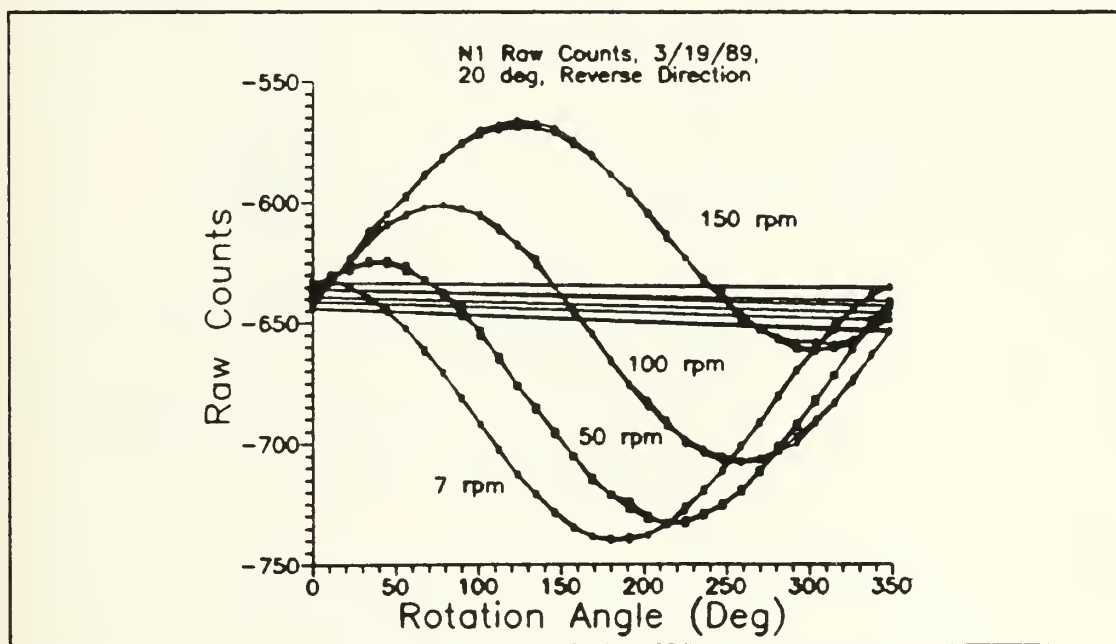


Figure 13. Phase Shift in Raw Count Data

This discovery initiated a flurry of code rewrite activity and caused a change in philosophy to working only with the averaged counts. To maintain the ability to work with the time varying data off-line, and to quantify (at least for one channel) the



amplitude reduction and phase shift, a bode plot was made. The phase shift is shown in figure 14, the amplitude plot in figure 15. The best fit line for each was recorded and stored for later use.

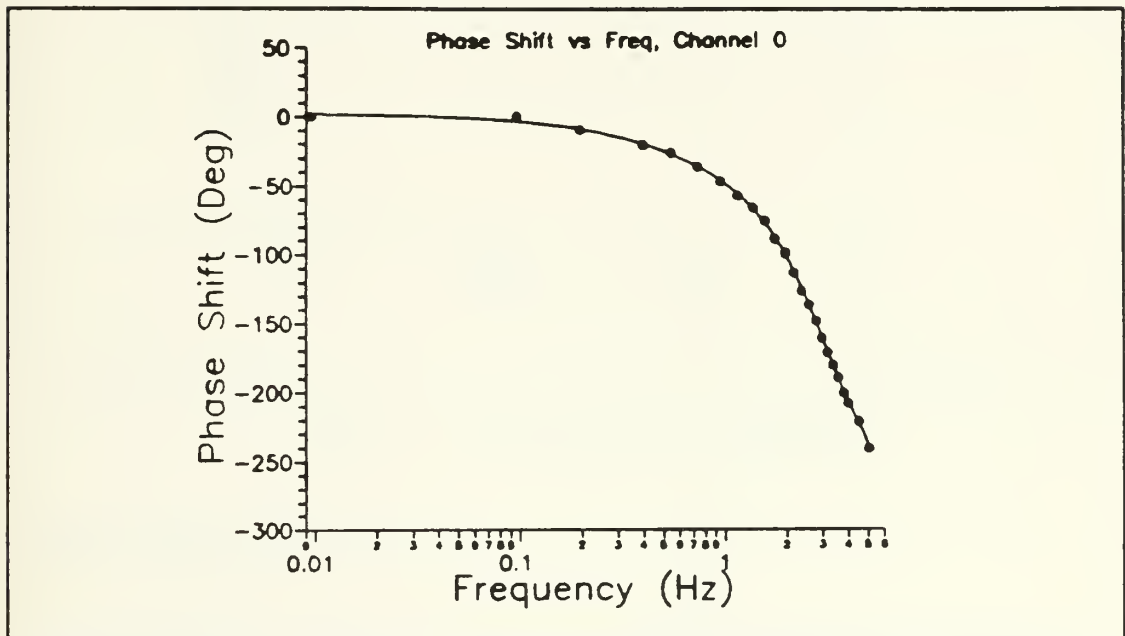


Figure 14. Phase Shift vs Frequency





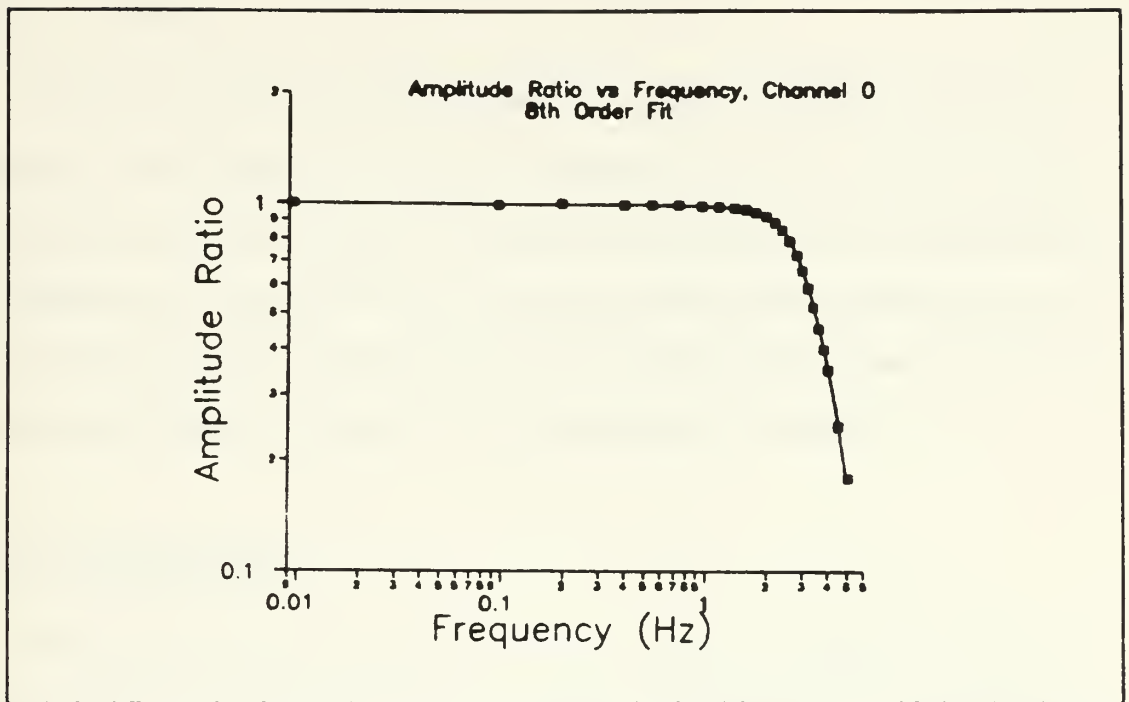


Figure 15. Amplitude Ratio vs Frequency

### 3.3 Tare Measurements

The test procedure delineated in section 3.2.1 accounts for the (W-B) and inertia effects. Though it is possible to account for these forces analytically, they were eliminated in a more straightforward manner by subtracting averaged (DC) measurements. The tare tests were run in air since, compared to water, the air acts essentially as a vacuum and doesn't influence the results. The general idea for the conduct of the tare measurements came from Reference [14].



### 3.3.1 Static

The static ( $\omega = 0$ ) tares were very simple. The model (in water) was set at the desired  $\alpha_c$ , the roll angle set to 0, and a set of readings taken. This "zero" file accounts for the (W-B) and offsets for that  $\alpha_c$ . The tunnel test conditions were set and another set of readings taken. Subtraction of the two files left the desired static hydrodynamic load. A more thorough approach would have been to repeat this at several rotational positions and average the results. Because of time constraints, this was not done.

### 3.3.2 Rotational

The inertial loads can be calculated analytically, given the model mass, moments of inertia about the principle axes, and the location of the model CG. Additionally, these values must be assumed to not vary with rotation rate. If this course is pursued, then the following relations, derived in Appendix B, result:

- For the inertia forces (in SNAME axis convention):

$$X_i = m \omega^2 x_G \sin^2 \alpha_c$$

$$Y_i = 0$$

$$Z_i = -m \omega^2 x_G \sin \alpha_c \cos \alpha_c$$

$$M_i = -\omega^2 (I_x - I_z) (\sin \alpha_c \cos \alpha_c)$$

$$K_i = N_i = 0$$

- For the weight and buoyancy forces:



$$X_{W-B} = -(W - B) \sin \alpha_c \cos \omega t$$

$$Y_{W-B} = (W - B) \sin \omega t$$

$$Z_{W-B} = (W - B) \cos \alpha_c \cos \omega t$$

$$K_W = W[y_G \cos \alpha_c \cos \omega t - z_G \sin \omega t]$$

$$M_W = -W \cos \omega t [z_G \sin \alpha_c + x_G \cos \alpha_c]$$

$$N_W = W[x_G \sin \omega t + y_G \sin \alpha_c \cos \omega t]$$

The same moment equations result for buoyancy by substituting -B for W and  $x_B, y_B, z_B$  for  $x_G, y_G, z_G$ .

There are several problems with using these relations directly. First, the model/sting combination deflects during rotation, causing the actual inertial loads to vary. Second, use of the weight and buoyancy relations would involve determining the offsets separately, rather than the more direct method of lumping them with the weight and buoyancy effects. Finally, the relations depend on accurately knowing the model mass moments of inertia, the CG, and mass. Errors in these quantities would reflect directly in the calculated forces and moments.

For this experiment, the deflection should be small due to the relatively small inertial forces at the maximum  $\alpha_c$  and  $\omega$ . As it turned out, the design of the model/sting minimized the inertia force contribution. The calculated and actual measured inertia forces for  $\alpha_c = -20^\circ$  and  $-14^\circ$  are shown in the following figures. Figures 16 and 17 are for the  $-20^\circ$  setting, figures 18 and 19 for the  $-14^\circ$  angle. The moment measurements have been corrected for sign to conform the standard convention.



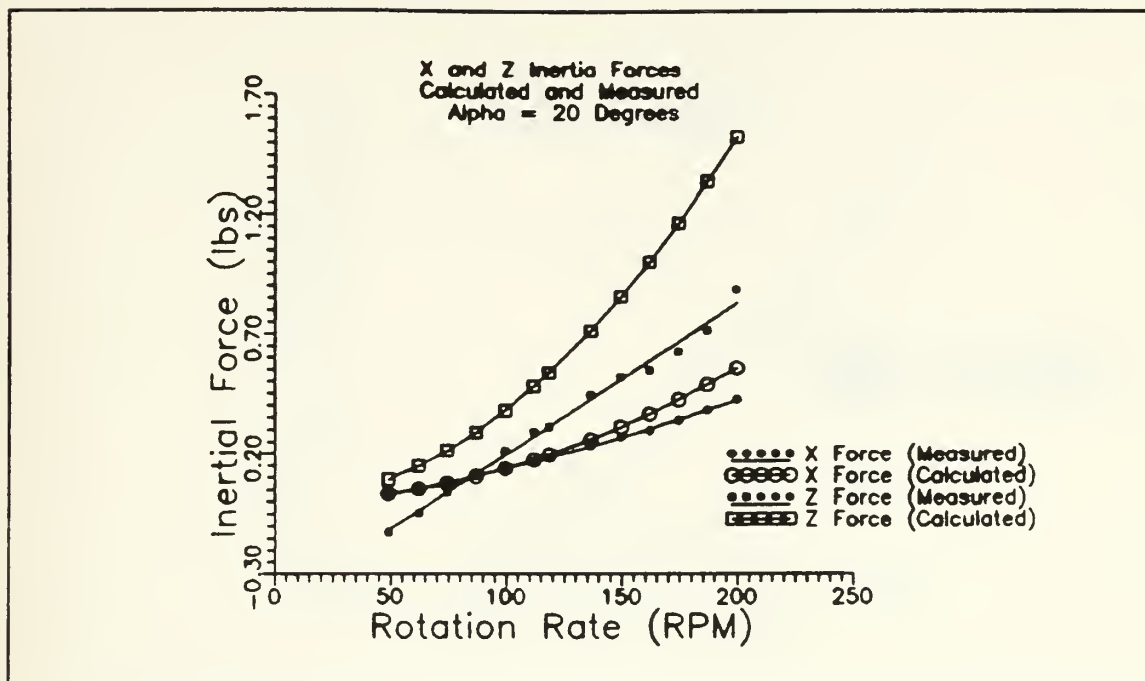


Figure 16. X and Z Inertia forces, 20°

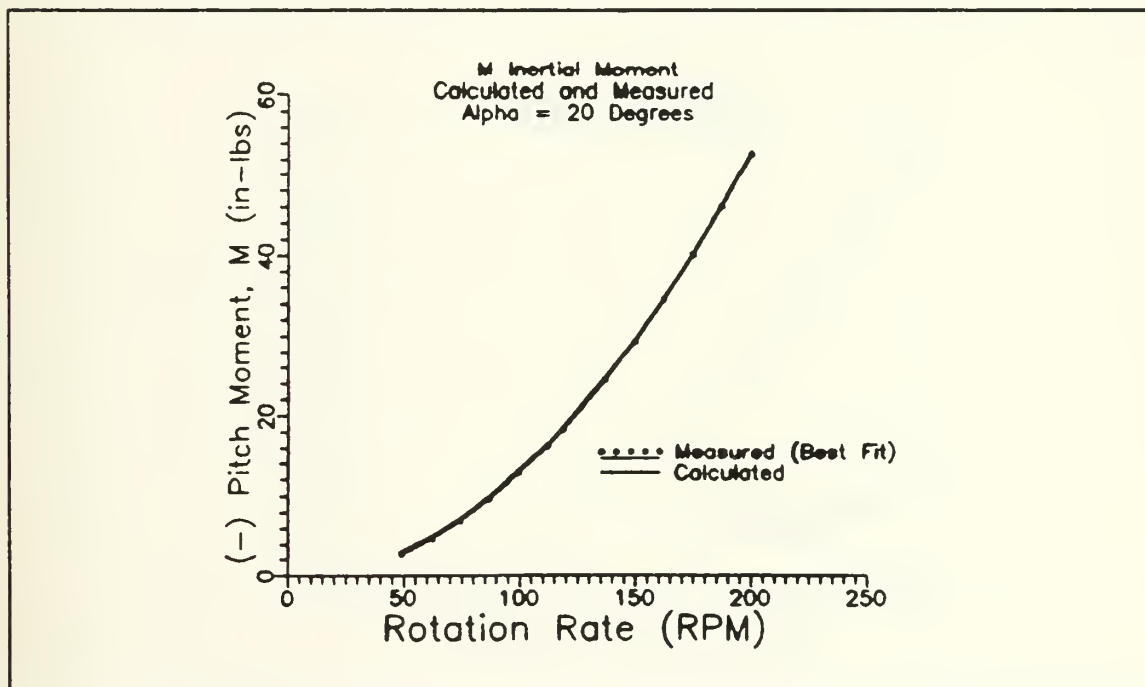


Figure 17. M Inertial Moment, 20°





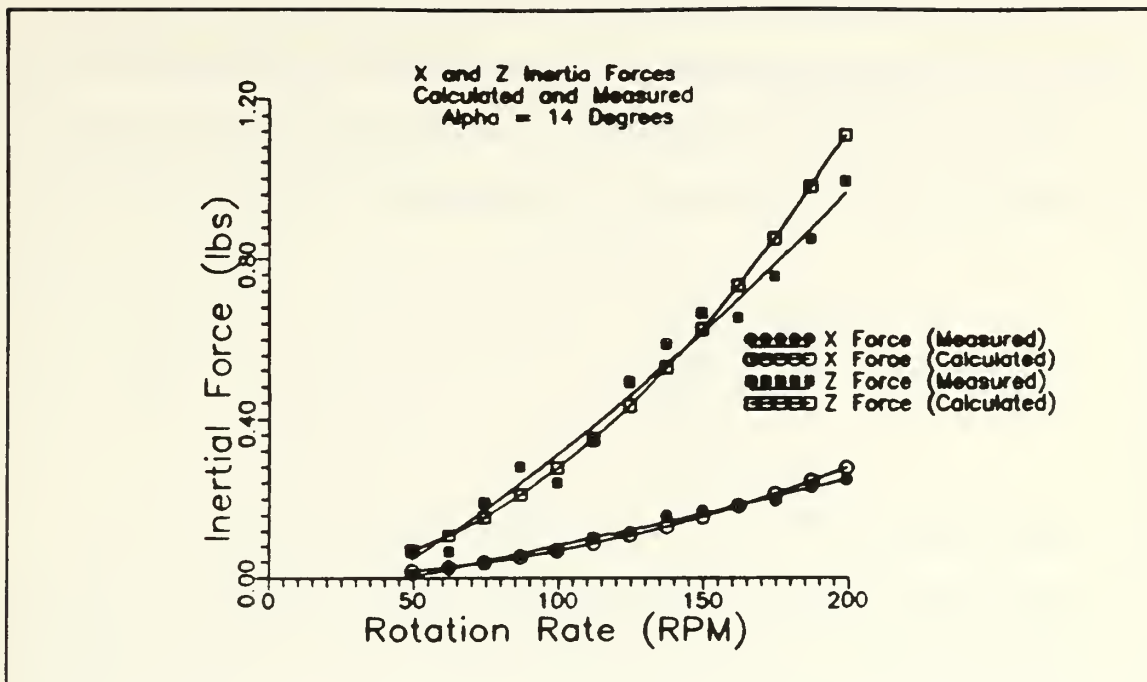


Figure 18. X and Z Inertia Forces, 14°

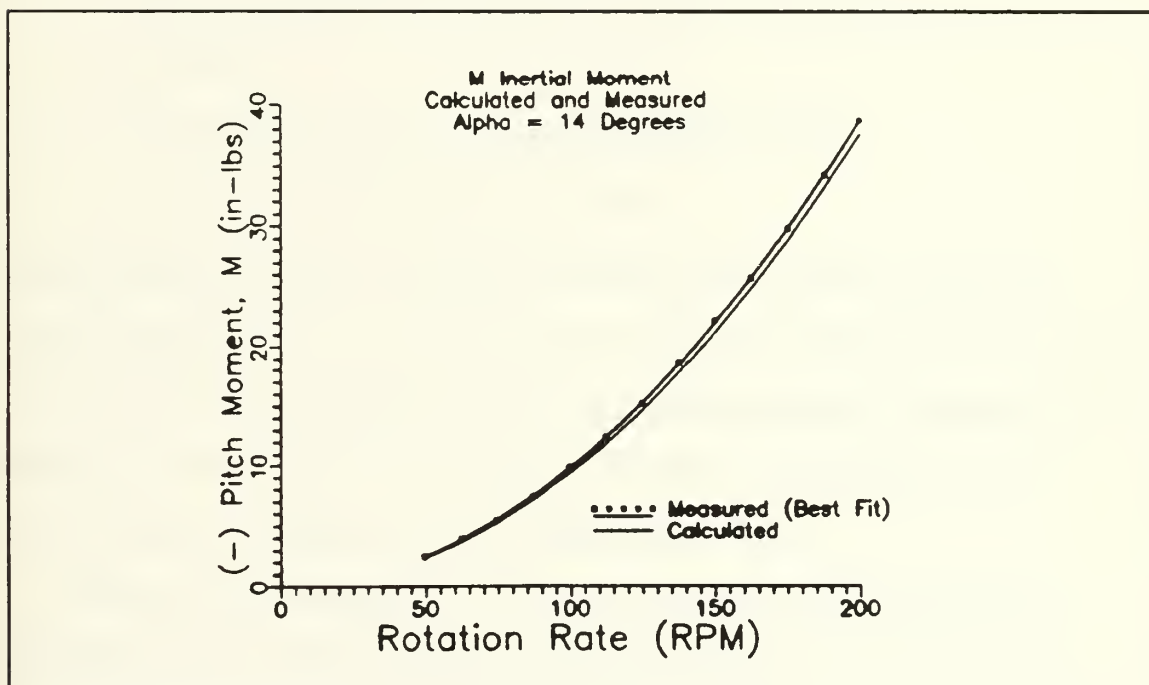


Figure 19. M Inertial Moment, 14°



Because calculation of  $I_x$  and  $I_z$  would be approximate at best, the actual data was fit with a second order curve, and the result used to empirically determine the two terms. This method worked quite well, with only a 2.9% difference between the 14° and 20° curve fit determined values. The numbers used in calculating the forces and moments were:

- $(I_x - I_z) :$  -.3706 slugs-in<sup>2</sup>
- $m:$  .3248 slugs
- $x_G:$  .40 inches

The 14° X, Z, M, and the 20° M results seem to match very well with the calculated trends. The 20° X and Z force measurements depart significantly from the calculated trends. Much scatter can be seen in the experiment results. Three factors could explain the results:

- The measured forces are very small, much less than 1% of full scale calibration load.
- The temperature effects were not well compensated for.
- $x_G$  and  $m$  are off from their actual values.

The third bullet helps explain the excellent correlation for the M plots and the poorer correlation for the force plots. Also, the moment correlation might be better because the moment values arise from subtraction of the two normal force balance outputs, possibly cancelling any errors. The Z force readings are the result of the addition of the two normal force balance readings, possibly compounding the error.

Despite the force discrepancies, the actual inertia force is small compared to the hydrodynamic force, ranging from 1.7% to 4% of the measured Z hydrodynamic force. The only significant inertia effect, M, is well predicted.



One point that has been overlooked is the deflection of the balance due to the hydrodynamic force. No attempt was made to correct for this effect, and is left as a refinement for future experiments using this apparatus.

### 3.4 Test Matrix

Before any rotational testing could be done, the test matrix had to be determined.

The matrix evolved from satisfying the goals:

- Widest possible coverage of non-dimensional spin rate,  $\omega'$ .
- Maximum hydrodynamic force.
- Minimum Reynolds effects.
- Maximum # of  $\omega$  increments in a test run (i.e., 0 - 200 rpm).
- Maximum  $\alpha_c$  coverage (i.e., 0 to 20°).
- Maximum  $p'$  and  $r'$  combination.

Because of time constraints, only three  $\alpha_c$  settings were tested; -8°, -14°, and -20°. For each  $\alpha_c$ , the tests were run in increments of 12.5 rpm, from 0 to 200 rpm (where possible), in one rotation direction, and at 25 ft/s free stream velocity. The variances on this procedure were: for -20°, do tests for 20, 25, and 30 ft/s free stream velocity to investigate Reynolds effects, for -14°, do runs in both rotation directions to get function even/odd characteristics.

The 25 ft/s base velocity was chosen as a compromise between hydrodynamic force and range of non-dimensional spin rate. This resulted in a minimum Reynolds number in the range of  $5 \times 10^6$ , well above the agreed upon lower cutoff of  $3 \times 10^6$  (for Reynolds number dependencies). The resulting  $p'$  and  $r'$  ranges were:  $p'$ : 0 - 1.93,  $r'$ : 0 - .70.



## Chapter 4 Test Results

"Full-up" test runs were conducted using the rotary rig and standard  $L/D=9.5$  model described previously. The test procedure delineated in section 3.2.1 was followed. Normal, side, and axial forces, rolling, pitching, and yawing moments were measured with the model in coning motion at coning rates up to 200 RPM. The majority of the runs were performed at 25ft/s (Reynolds Number based on model length of  $5 \times 10^6$ ). Coning angle,  $\alpha_c$ , varied from  $-8^\circ$  to  $-20^\circ$ . The measured forces are non-dimensionalized and presented as functions of the non-dimensional spin rate,  $\omega'$ . The axial force and roll moment are not presented as they were determined not to be particularly important for this experiment. All non-dimensional parameters are presented in the standard SNAME, body-fixed, axis convention [15].

Figures 20 and 21 show the non-dimensional force and moment variation with both spin rate and Reynolds number for  $\alpha_c = -20^\circ$ . Figures 22 and 23 show the non-dimensional force and moment variation with both positive and negative spin rates for  $\alpha_c = -14^\circ$ . Figures 24 and 25 present the force and moment variation for  $\alpha_c = -8^\circ$ . Finally, figures 26 and 27 show the variation of the non-dimensional side force and yawing moment, respectively, with coning angle. A tabular listing of the forces and moments is in Appendix C.





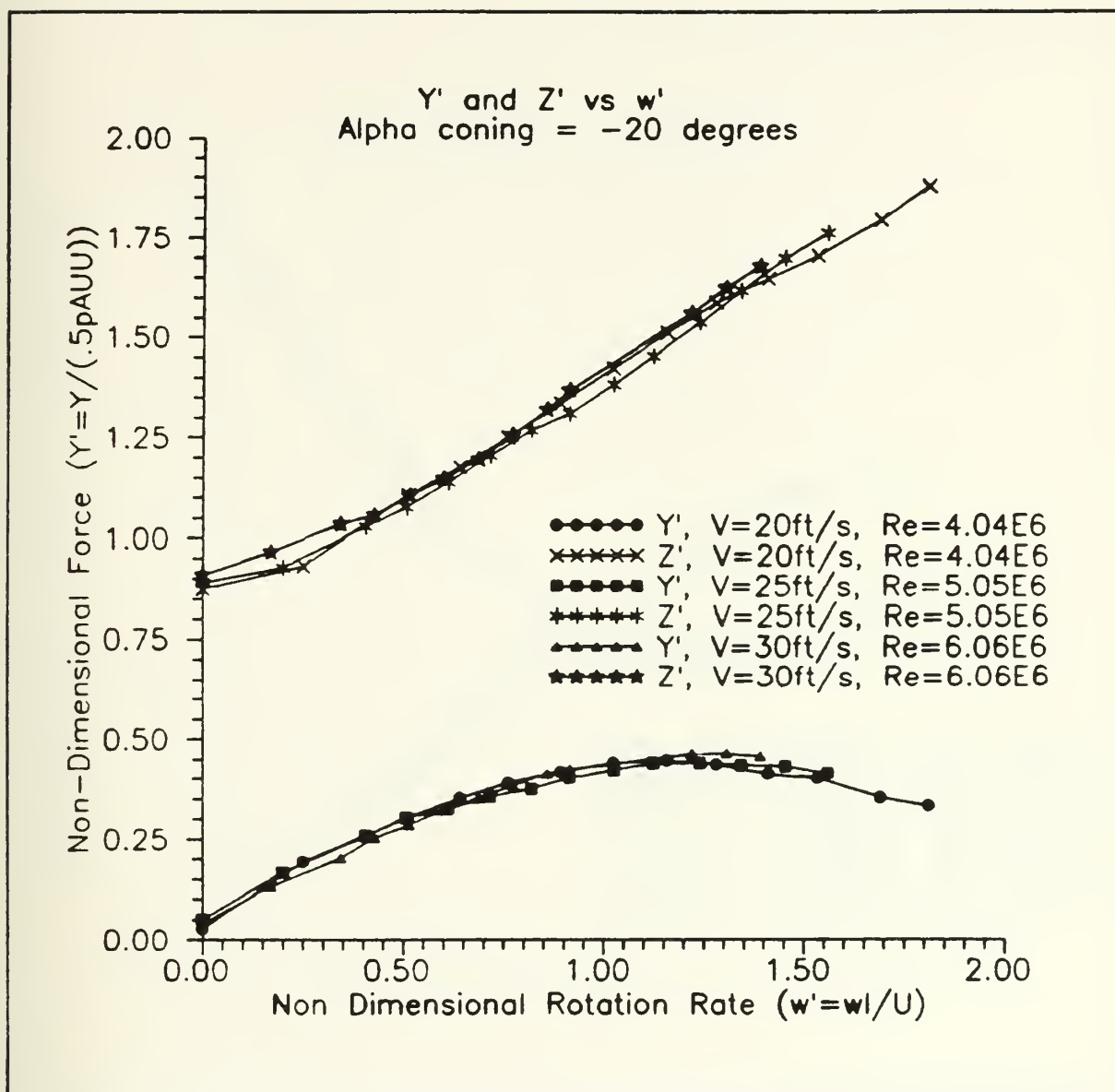


Figure 20.  $Y'$  and  $Z'$ ,  $\alpha_c = -20^\circ$



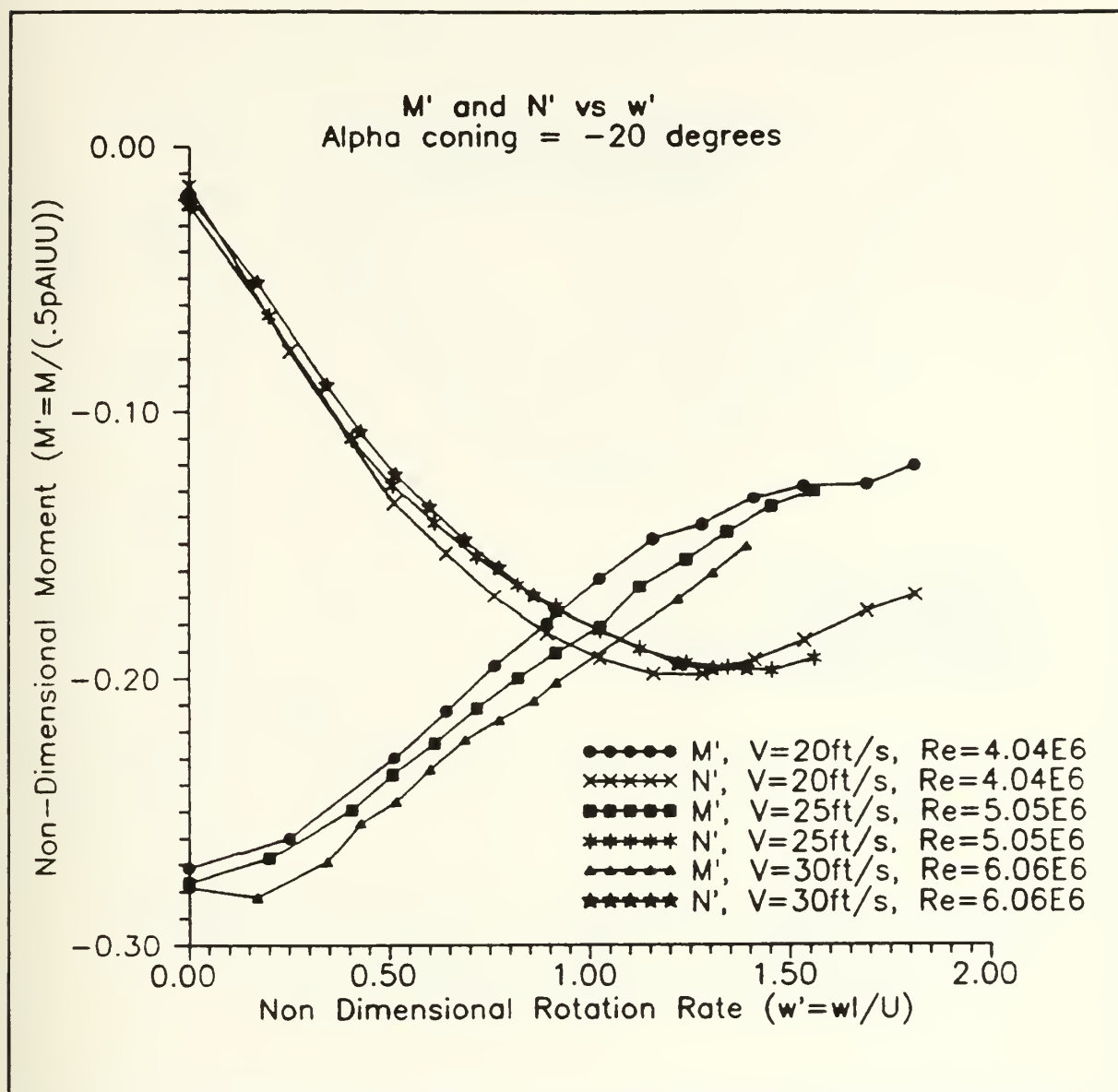


Figure 21.  $M'$  and  $N'$ ,  $\alpha_c = -20^\circ$



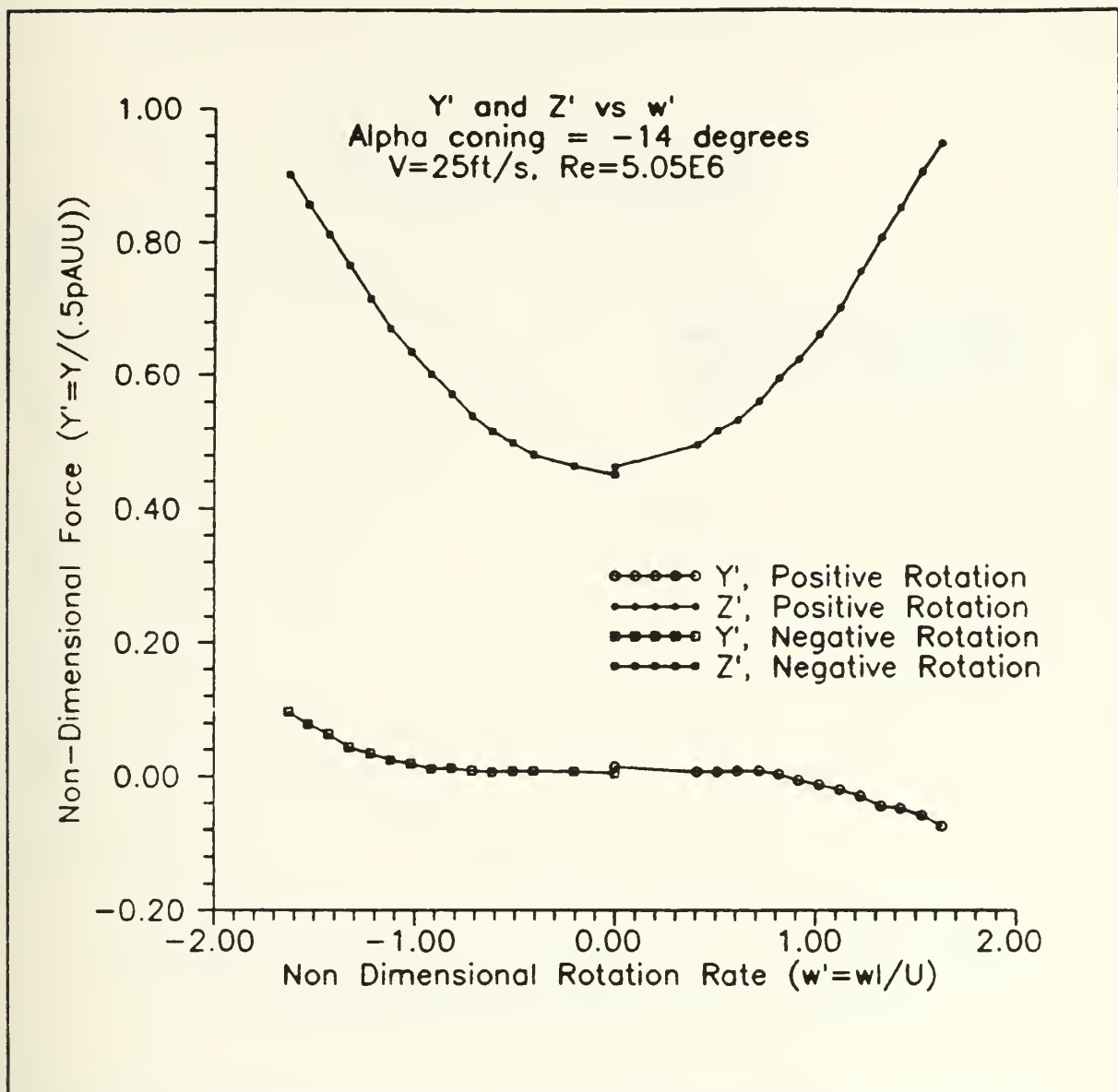


Figure 22.  $Y'$  and  $Z'$ ,  $\alpha_c = -14^\circ$



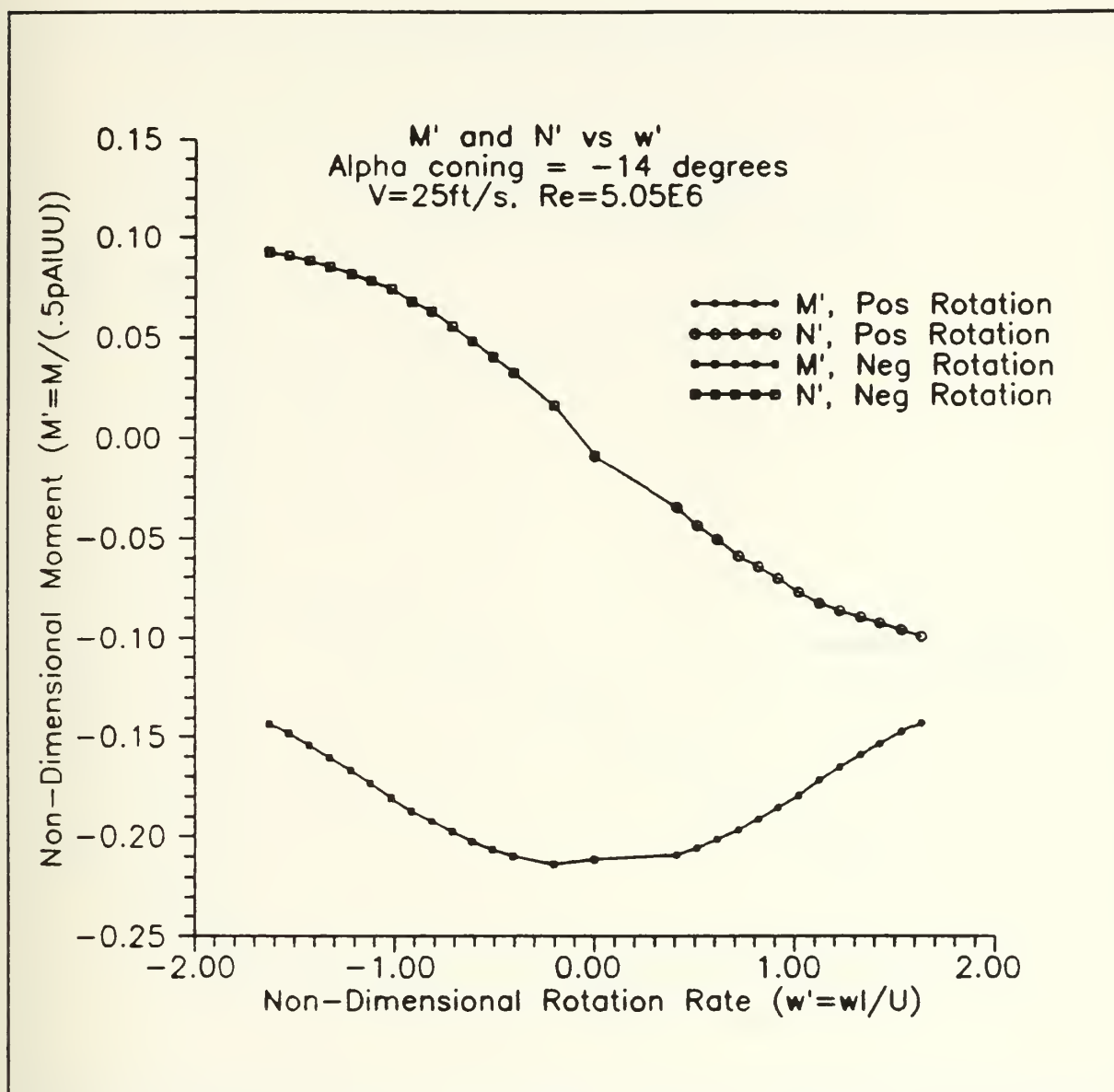


Figure 23.  $M'$  and  $N'$ ,  $\alpha_c = -14^\circ$





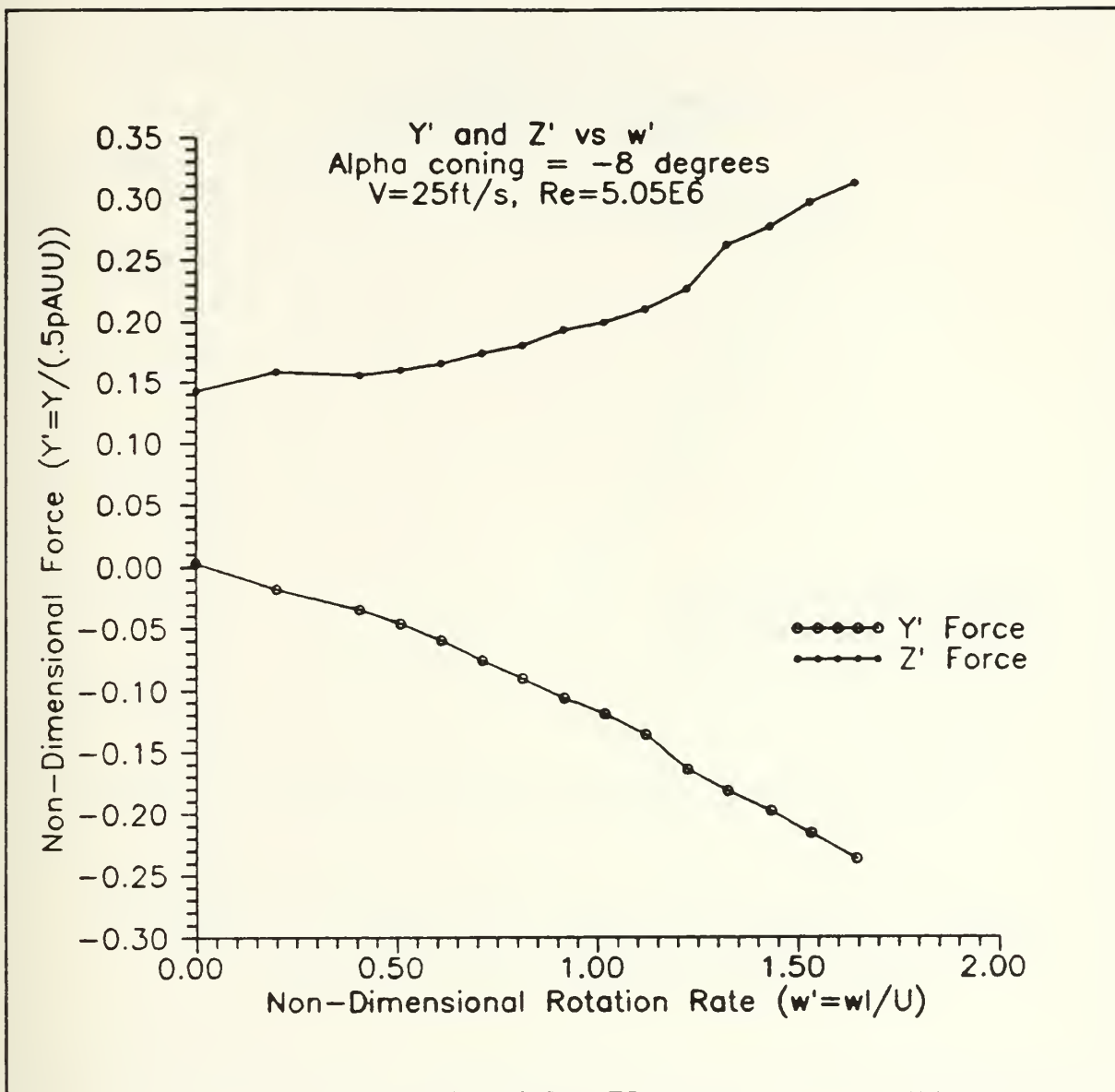


Figure 24. Y' and Z',  $\alpha_c = -8^\circ$



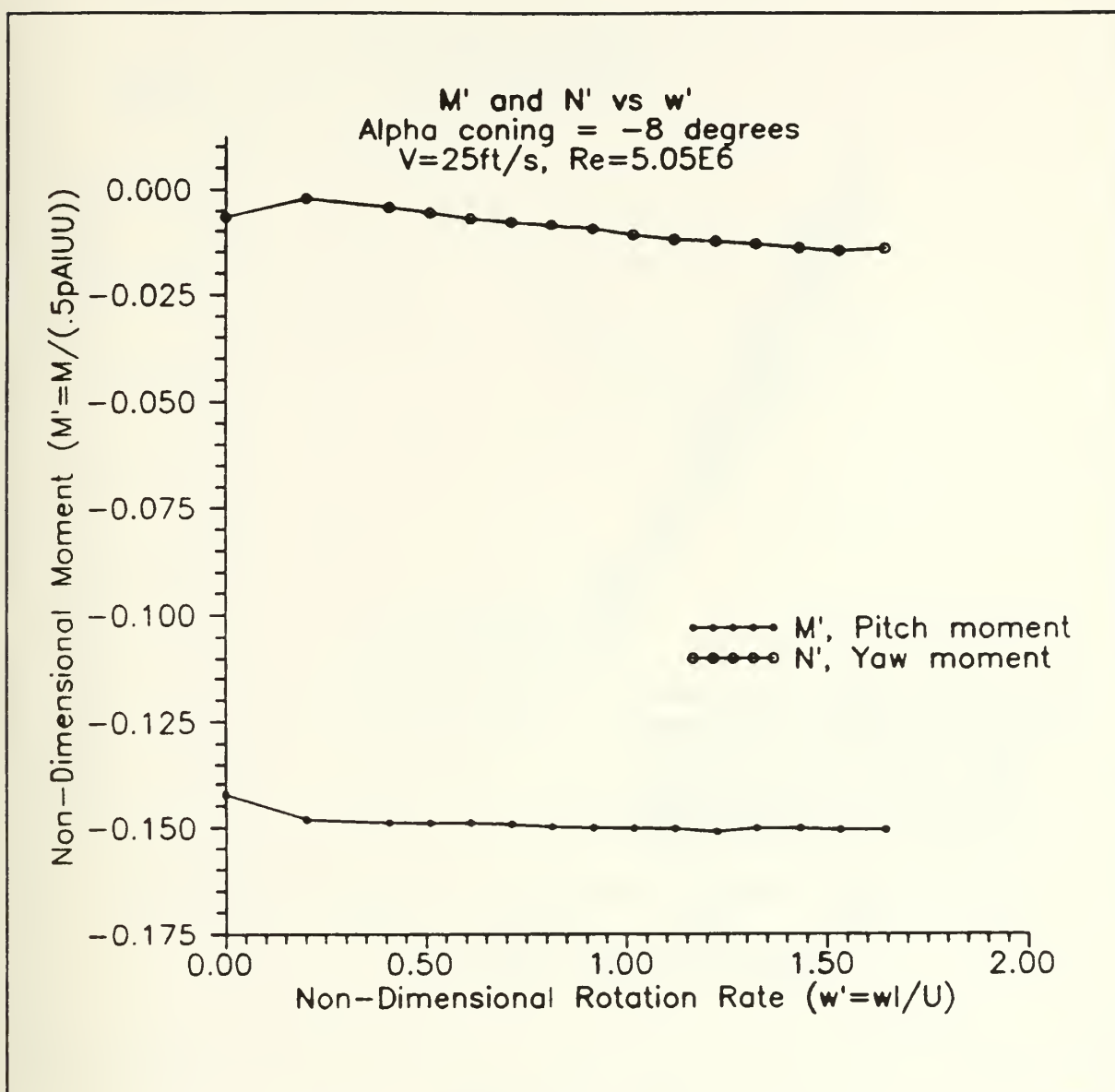


Figure 25.  $M'$  and  $N'$ ,  $\alpha_c = -8^\circ$



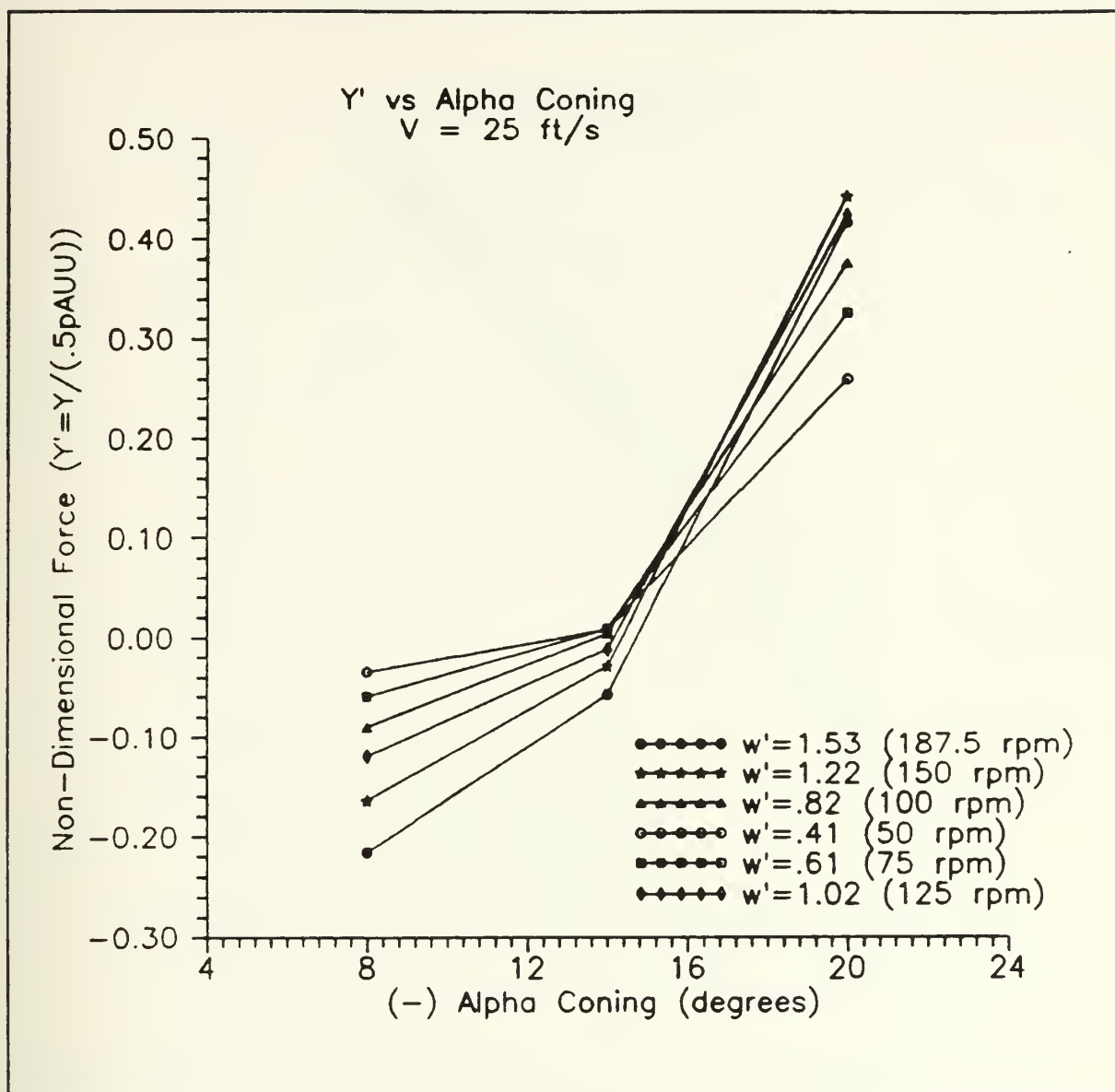


Figure 26.  $Y'$  vs  $-\alpha_c$

The 20° force data demonstrate a nearly linear dependence on coning rate for the normal force and a very non-linear dependence for the side force. Of note is the significance of the out-of-plane force ( $Y'$ ), which reaches 30% of the in-plane force. Both the pitching and



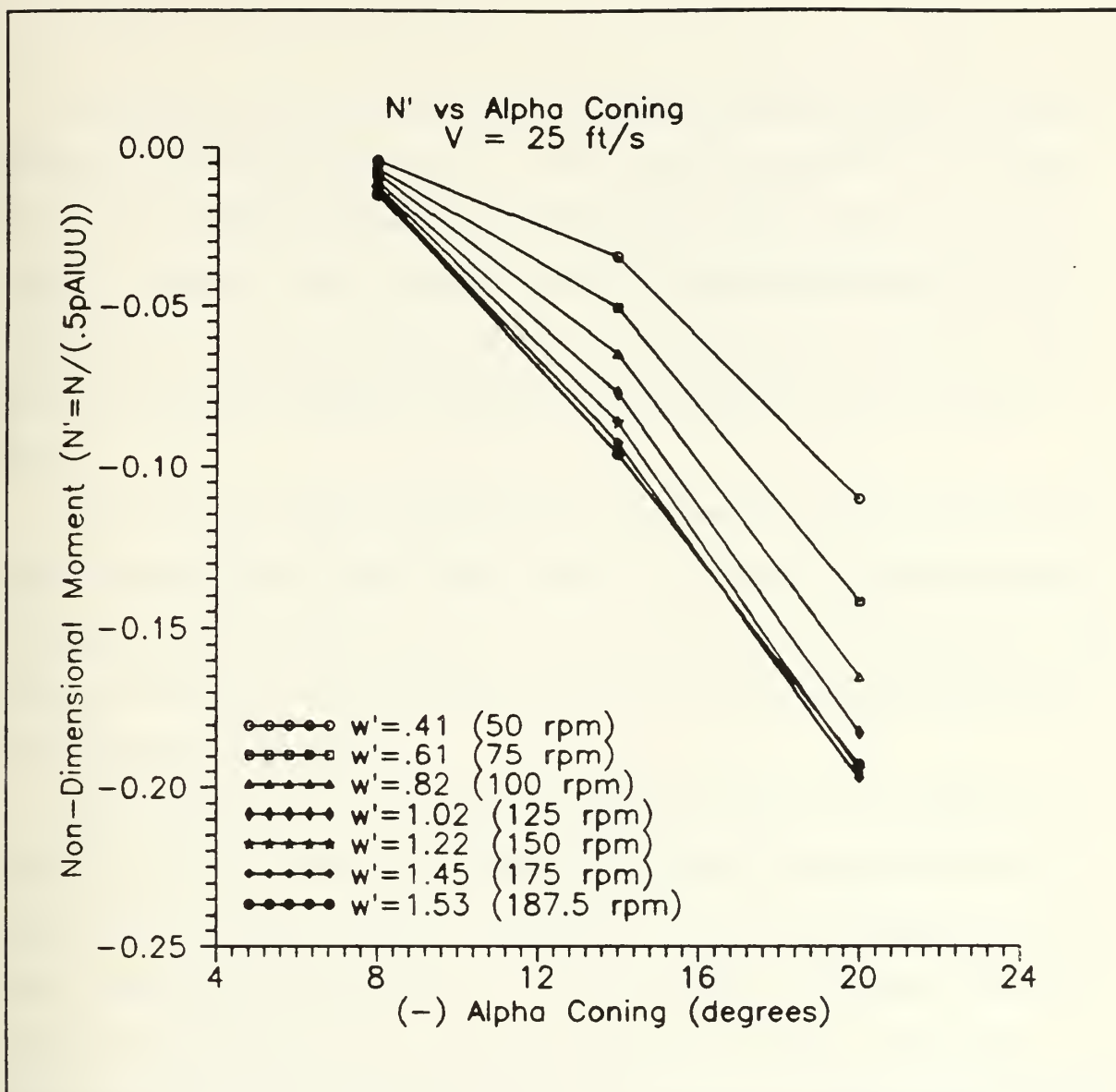


Figure 27.  $N'$  vs  $-\alpha_c$

yawing moments show a non-linear dependence on  $\omega'$ . Reynolds number effects seem negligible for the forces, and to have a slight influence on the moments. For the yawing moment, the lower Reynolds number data shows a tendency to go non-linear sooner than the 25 and 30 ft/s data. The difference in the pitching moment is not readily explained.





The normal and side forces have the even-odd characteristics anticipated. Because of symmetry, the lateral force and moment,  $Y'$  and  $N'$ , should be odd functions of the coning rate parameter, while the longitudinal force and moment,  $Z'$  and  $M'$ , should be even functions of the coning rate. The  $14^\circ$  data clearly shows the even/odd relationship for the forces and moments. The slight asymmetry in the data with respect to positive and negative spin rate could result from misalignment of the model/sting combination with the free stream velocity.

The  $8^\circ$  force data exhibited similar trends as the  $14^\circ$  and  $20^\circ$  results. The pitching and yawing moments, however, appear almost constant over the range of spin rates investigated. The slight deviations for the zero spin rate results are most likely test anomalies, and not true pictures of the trends. The  $N'$  static result should be zero, as a linear interpolation through the remaining data points suggest.

The moments and the normal force display similar trends for the  $14^\circ$  and  $20^\circ$  results. The side force shows a different character between the  $\alpha_c$  settings, especially when the  $8^\circ$  data is included. As figure 26 shows, the side force is a very non-linear function of coning angle, changing signs at approximately  $14^\circ$ . The relationship could be quadratic, but with only three data points per line, the exact form is impossible to determine. The yawing moment also shows a non-linear characteristic with coning angle, becoming nearly linear for the high spin rates. Obviously, more data points are necessary before any strong functional dependencies can be determined.



## Chapter 5 Data Analysis

The purpose of this chapter is to validate the steady-state data presented in Chapter 4.

Two main paths are pursued:

- Comparison with numerical results.
- Frequency analysis of raw balance data and encoder determined RPM data.

### 5.1 Comparison with Numerical Results

A vortex cloud numerical algorithm, developed by Nielsen Engineering and Research (NEAR), was used for producing the calculated results for comparison. A description of the computer code SUBFLO is found in reference [16]. The method basically models the body and major physical features of the flow field with singularity distributions. Mutual interactions of the body shed vorticity are considered in the prediction of the induced forces and moments [9]. The test cases shown in the following table were provided to and run by NEAR for producing the predicted forces and moments. The NEAR predictions were made for both no separation and laminar separation. Laminar separation was used to avoid the uncertainty of transition effects.

In all cases, except for the 20 ft/s, 125 rpm,  $N'$ , result, the experimentally determined force or moment fell in the range bounded by the laminar and no separation cases. Additionally, the laminar separation cases more accurately predicted the experimental result for all runs. For this study, the cross-flow Reynolds number based on diameter ranged from approximately  $1.5 \times 10^5$  to  $3 \times 10^5$ . This is on the edge of the transition region from laminar to turbulent separation, which is indicated by a rapid drop in the drag coefficient for a circular cylinder in a cross-flow. Based on this, the flow about the model should have been transitional, and is shown to be so by the test results. The actual separation point during



$V_{\infty}$ ft/s	$\omega$ rpm	$\omega'$	Case	$Z'$	$Y'$	$M'$	$N'$
30	0	0	laminar	1.339	0.0	-.247	0.0
			none	-.062	0.0	-.526	0.0
			exprmnt.	.901	.0394	-.278	-.0191
30	100	.684	laminar	1.829	.701	-.130	-.152
			none	.004	-.401	-.500	.007
			exprmnt.	1.197	.352	-.223	-.148
20	125	1.204	laminar	2.282	.869	-.089	-.131
			none	-.006	-.754	-.537	.012
			exprmnt.	1.587	.439	-.143	-.199
20	175	1.686	laminar	2.729	1.303	-.083	-.192
			none	-.016	-1.060	-.588	.015
			exprmnt.	1.878	.334	-.121	-.169

Table 5.1 Numerical and Experiment Non-Dimensional Results

the test should have been further aft than the calculated laminar separation case, leading to measured forces and moments somewhat less than the laminar predictions. That this is true lends some reassurance to the validity of the test results.



Figures 28 and 29 show the laminar separation results along with the measured forces and moments for  $\alpha_c = 20^\circ$ . The predicted normal force follows the measured trend, however, the predicted side force does not completely follow the experiment trend. The same relationship holds for the moments: the predicted in-plane moment,  $M'$ , follows the experimental data trend, where the calculated out-of-plane moment,  $N'$ , has a very different characteristic. In both figures, the last data point seems to cause the problem. Only by "filling-in" the predicted curve, however, can meaningful conclusions about the results be made.





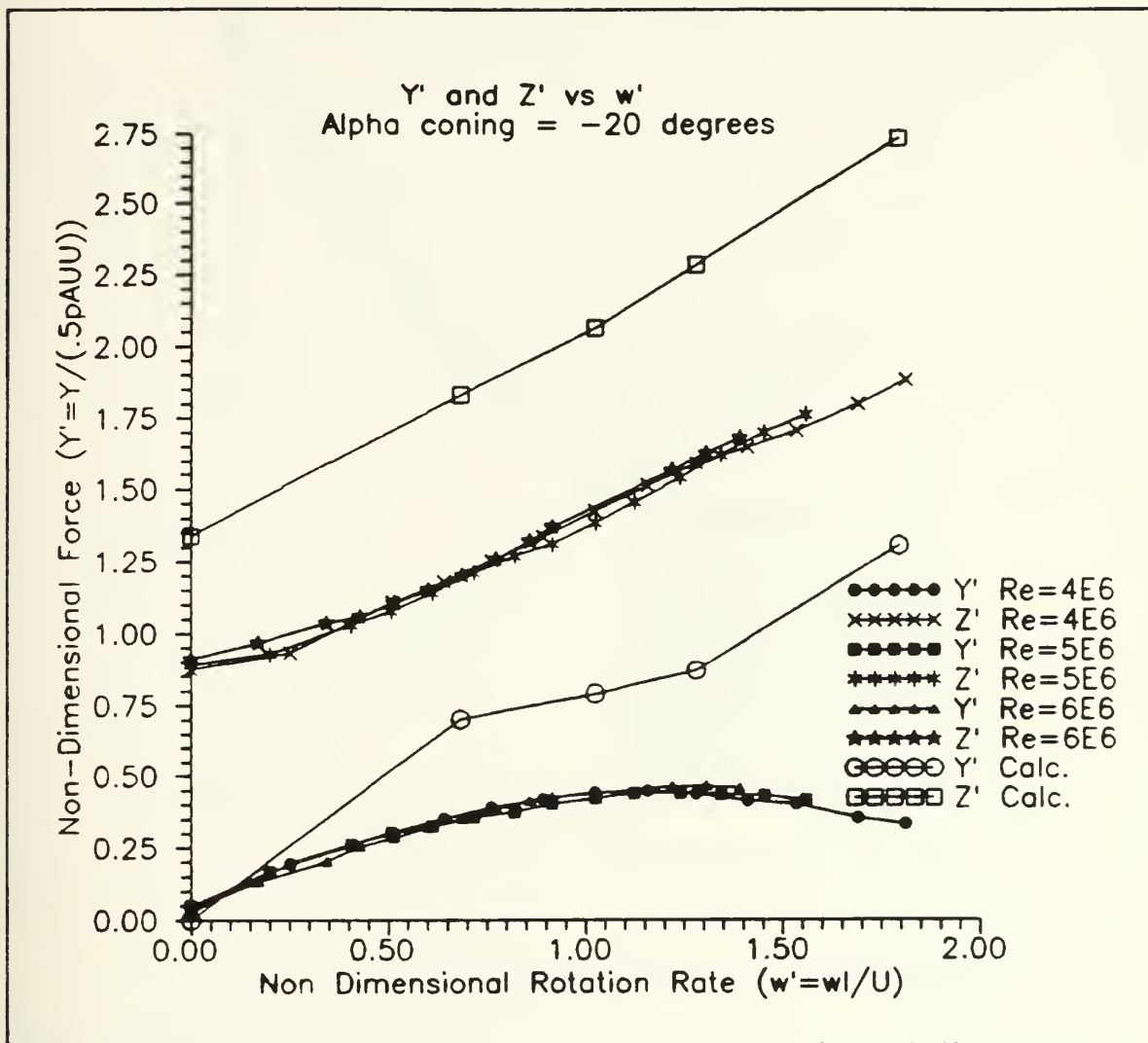


Figure 28. Predicted and Experiment Non-Dimensional Forces



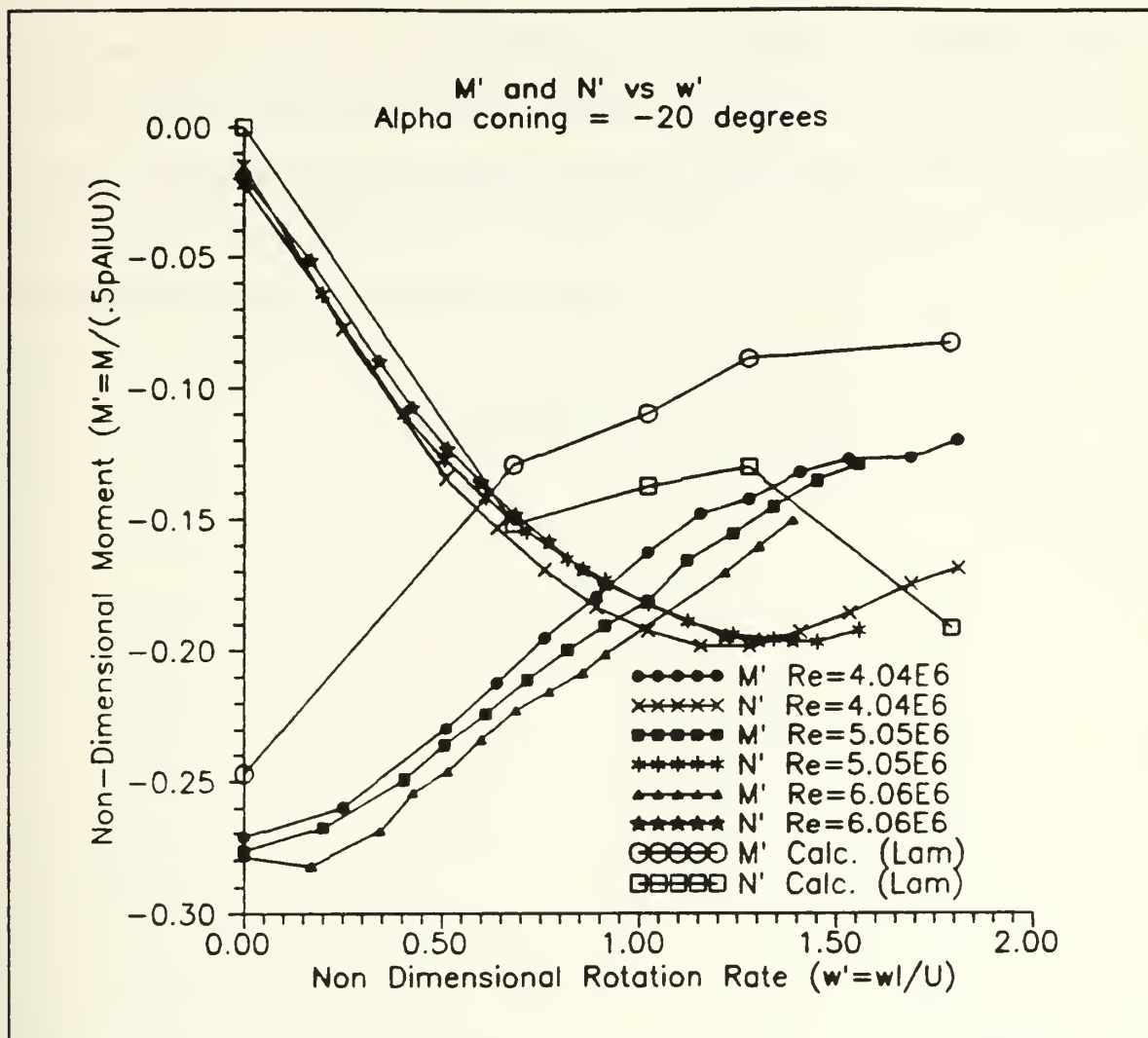


Figure 29. Predicted and Experiment Non-Dimensional Moments

## 5.2 Frequency Analysis

The quality of the steady state force measured is related to the time varying effects present during the test. To get a handle on the vibration effects, a plot of the raw counts output for the normal force bridge vs rotation angle (or time) was created. The summation of 10 revolutions worth of data is shown in figure 30. The 20°, 30 ft/s run with the wing



attachment was considered the most probable for vibration effects. To avoid any convolution of the result, the raw counts vice the processed forces were analyzed. As seen from the figure, there seems to be some scatter and possibly high frequency noise in the signal. The data points do follow the expected sinusoidal pattern, however, and when fit with a fourth order curve, produce a reasonable waveform.

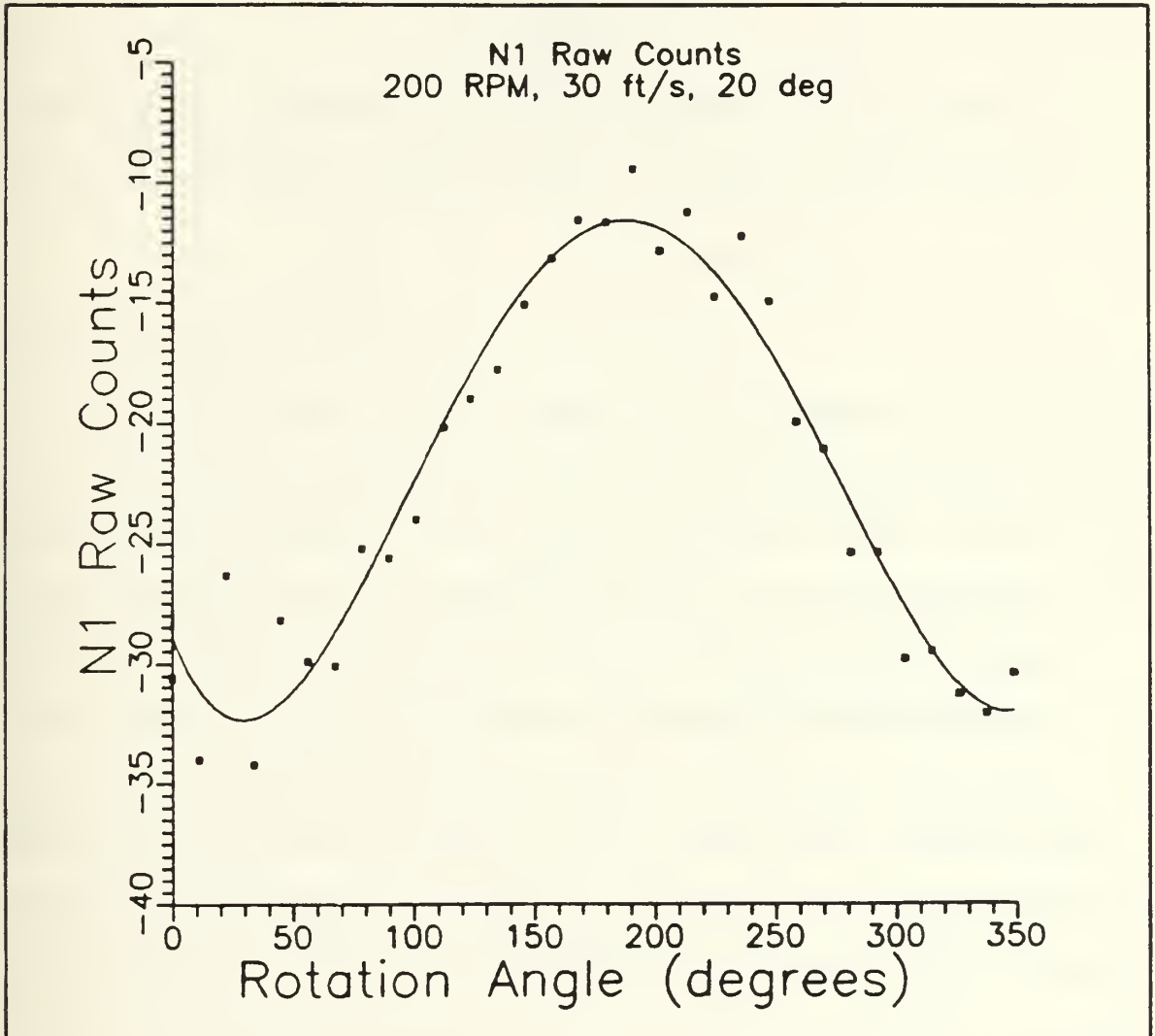


Figure 30. Summed Raw Counts Output



A fast fourier transform (FFT) algorithm [17] was programmed and used to transform the 10 revolution raw counts output for both the N1 and N2 normal force channels. The FFT quickly accomplishes the discrete fourier transform of the  $N$  real data points ( $h_k$ 's) as shown:

$$H_n = \frac{1}{N} \sum_{k=0}^{N-1} h_k e^{\frac{-2\pi i k n}{N}}$$

The FFT produced a frequency and amplitude decomposition of the data points for frequencies up to the Nyquist or folding frequency. The Nyquist frequency is defined as:

$$f_c = \frac{1}{2\Delta}, \text{ where } \Delta = \text{sample time interval.}$$

For the 200 rpm runs, the folding frequency was 53.33 Hz.

The FFT of the data used to produce figure 30 is shown in figure 31. The spike present at 3.3 Hz represents the fundamental rotation frequency (200 rpm). There are no major high frequency effects present, and only minimal lower frequency effects. This proves that the 3 Hz cutoff filters in the signal amplifiers did filter out any major high frequency noise, if any were present! For comparison, the inertia raw counts data was processed and is shown in figure 32. The figure does highlight the presence of some high and low frequency noise in the full-up data signal by comparison. The difference between the two figures could account for the scatter seen in the time varying signal. For further insight, the side force balance channels, Y1 and Y2, were also processed for the same full-up test run. The results shown in figure 33 are very similar to those for the normal force channels.





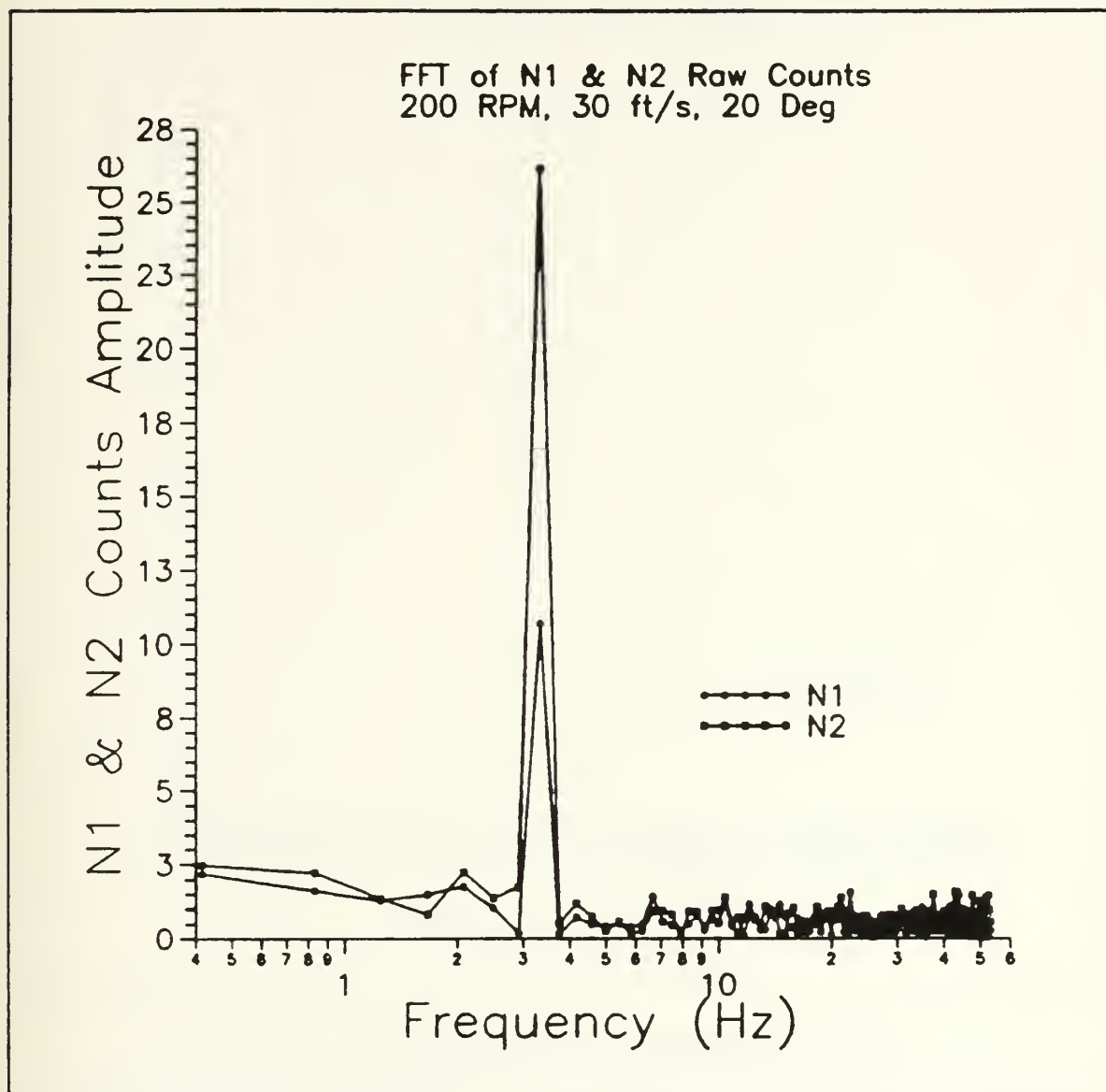


Figure 31. FFT of Normal Force Channels



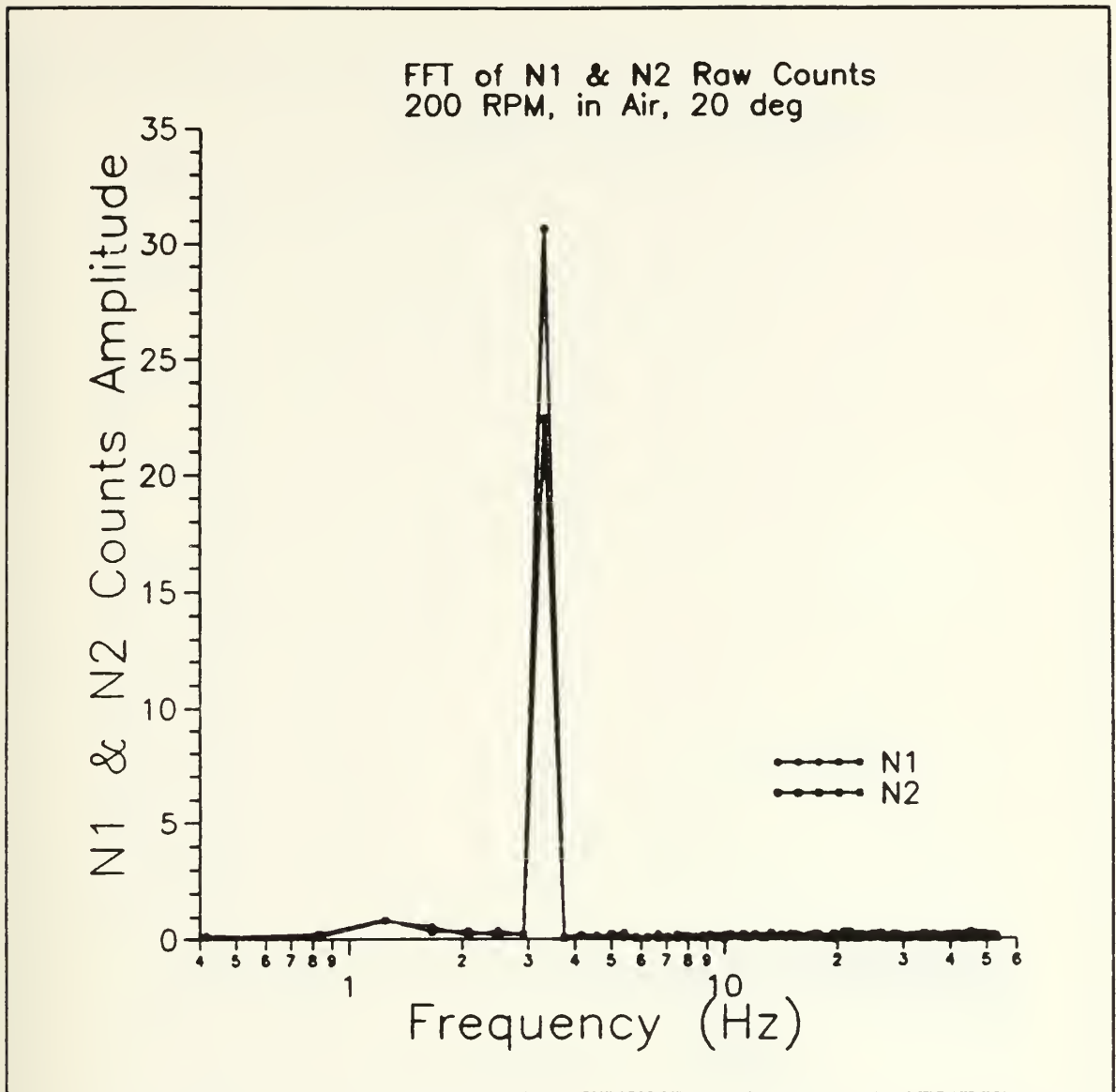


Figure 32. FFT of Normal Force Channels, Inertia Run

Because of the 3 Hz cutoff filters in the signal conditioners, no significant higher frequency effects could be seen (i.e., wall frequencies, higher harmonics, etc.). A look at the unfiltered shaft encoder output for rpm variation over a cycle however, could provide some high frequency information. Four cases were processed: 20°, 200 rpm inertia and full-up runs, and 20°, 25 rpm inertia and full-up runs. The cases covered the test spectrum for the



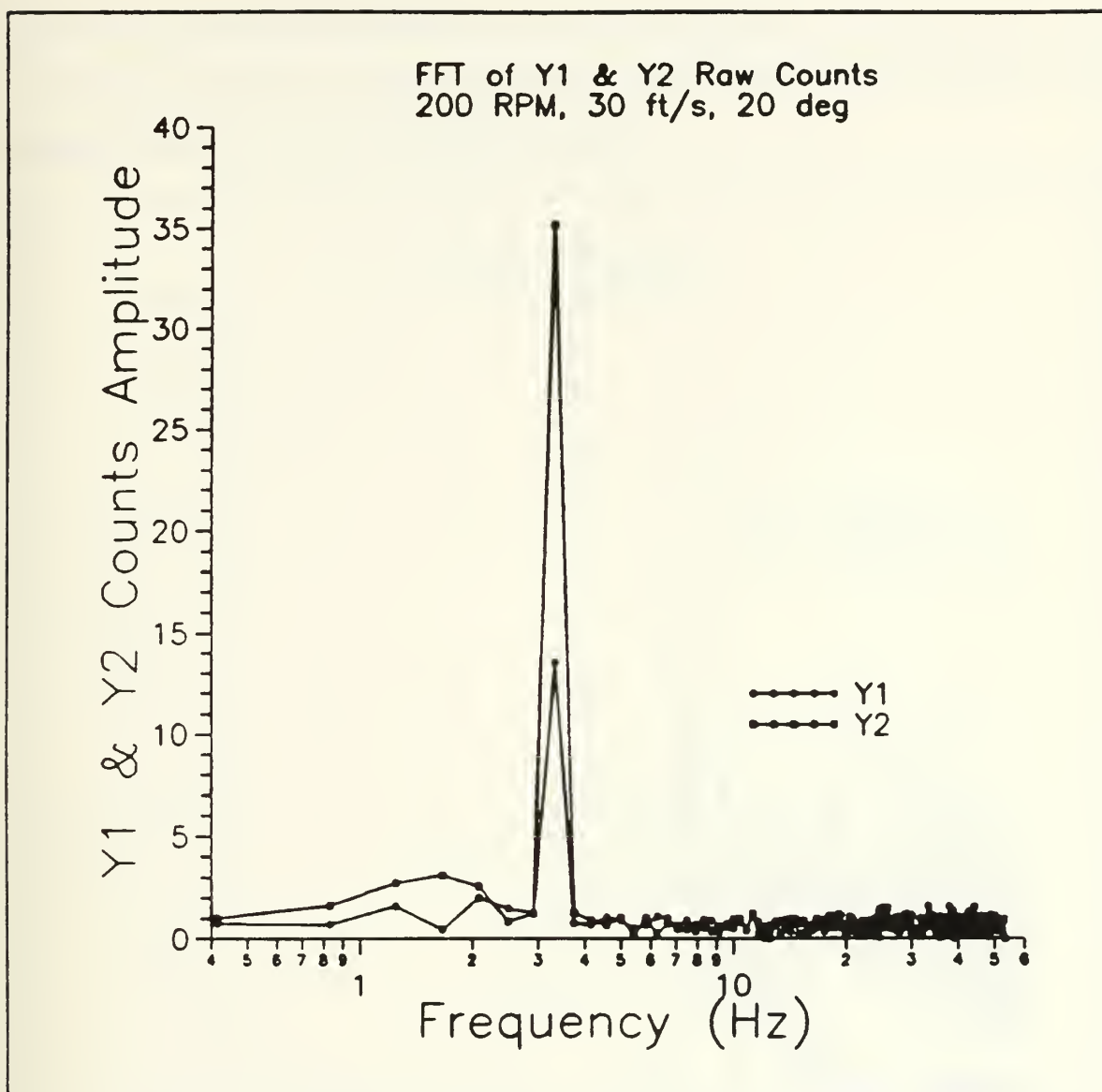


Figure 33. FFT of Side Force Channels

20' runs. The FFT results are shown in figures 34 and 35. The 200 rpm full-up run definitely shows a 2<sup>nd</sup> harmonic at 6.67 Hz. This is probably from the wing attachment passing by the support wing mounted to the forward nacelle. There are some other harmonics,



however, on the whole, the magnitudes are very small, typically tenths of rpm's. No wall frequency component ( $4 \times$  rotation frequency) was visible. Also, no 50 Hz component (the calculated torsional resonance frequency) was seen.

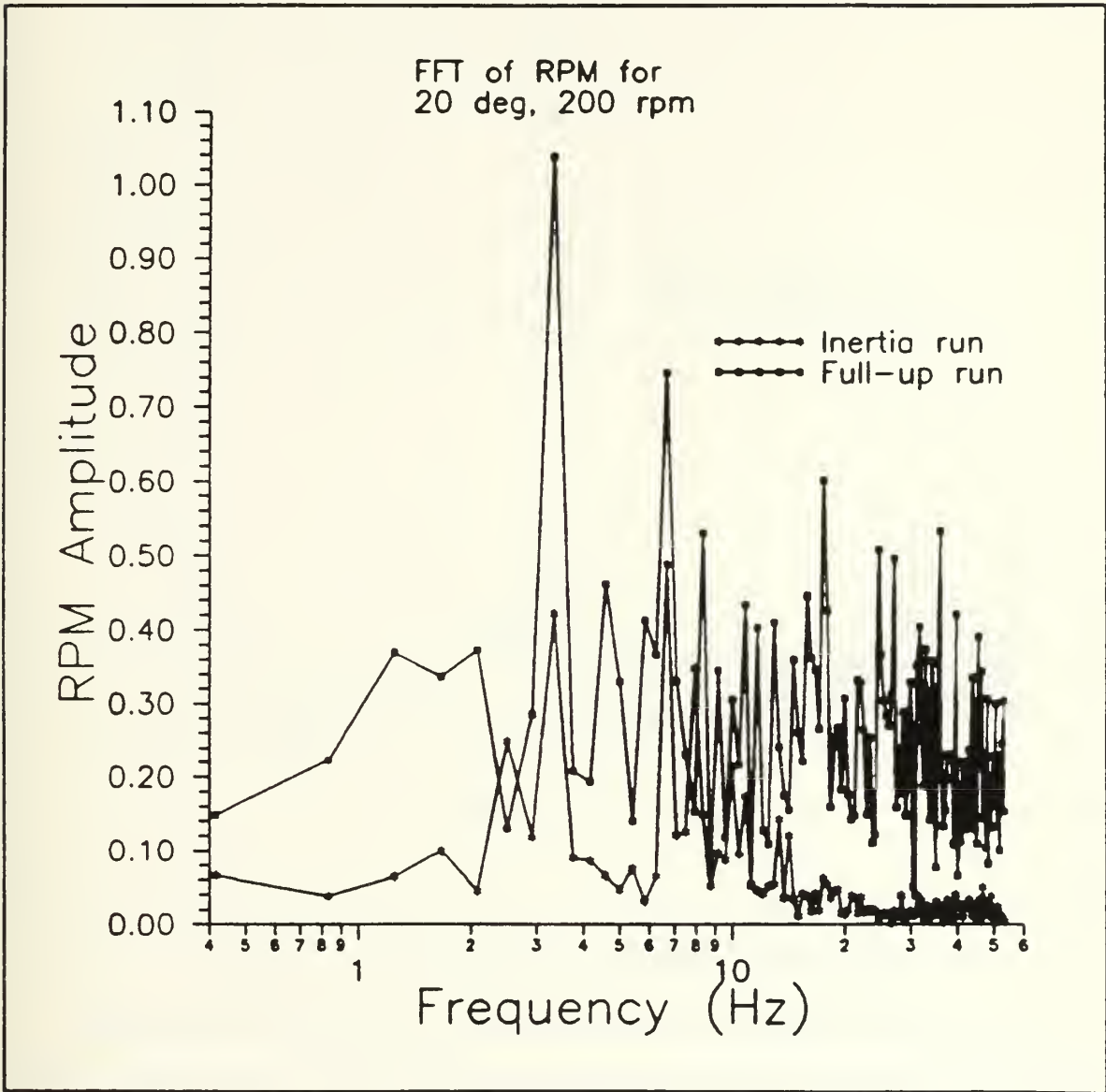


Figure 34. 200 RPM, Inertia and Full-up Run FFT Results





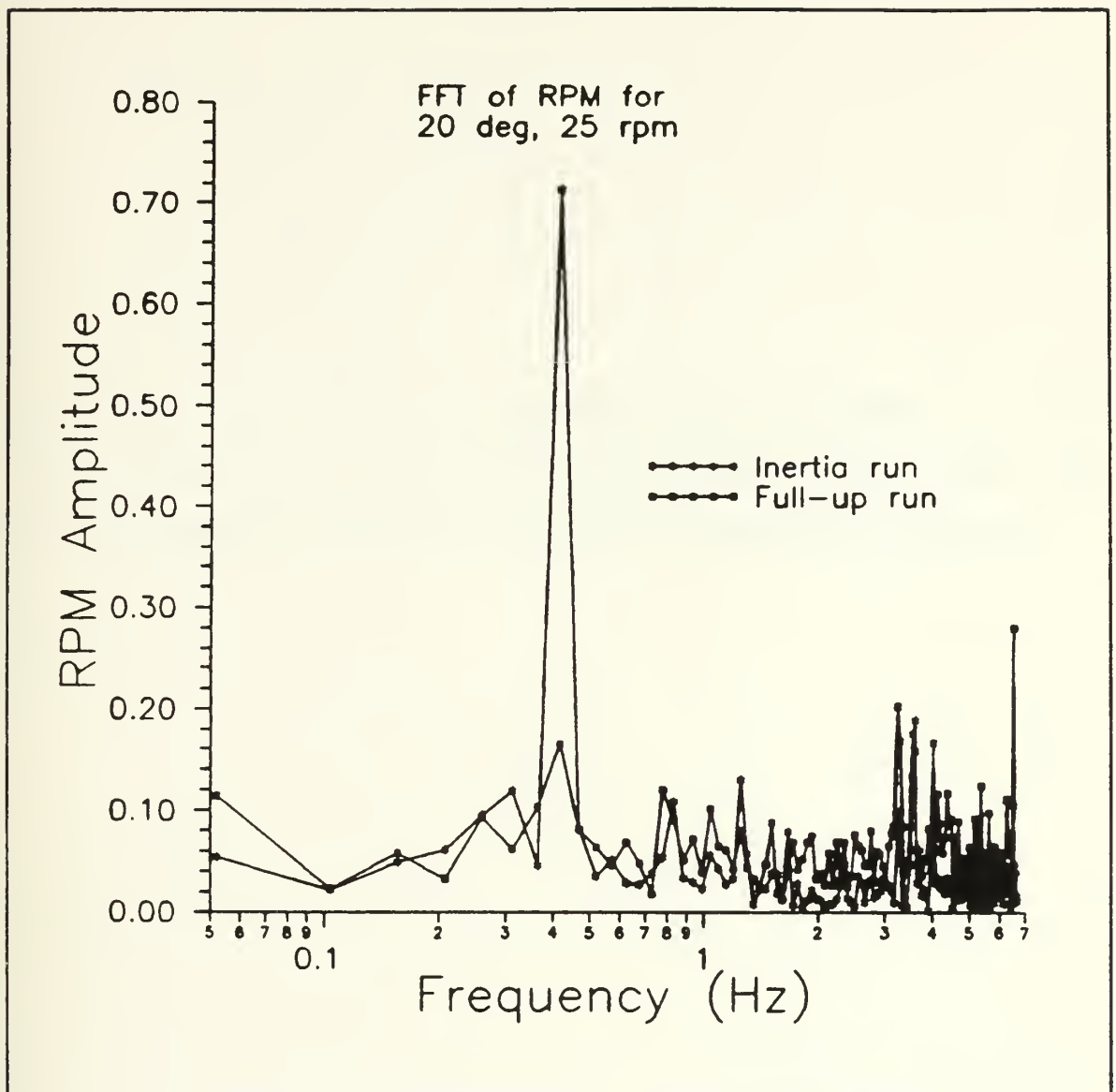


Figure 35. 25 RPM, Inertia and Full-up Run FFT Results

RPM variation over a cycle is an important factor in obtaining accurate force and moment measurements. The FFT analysis produced the variation magnitude. The fundamental rotation speed fluctuation was small for both rpm cases: 1.05 rpm for 200 rpm



(0.525%), and .18 rpm for 25 rpm (.72%) full-up runs. The 200 rpm output was much less than the calculated maximum rpm variation of 4.8 rpm. The low variance is a direct result of counter balancing the large sheave to account for the model/sting off-center weight.



## Chapter 6 Conclusions and Recommendations

### 6.1 Conclusions

As part of continuing research into the flow about slender bodies of revolution, a coning motion apparatus for hydrodynamic model testing was built and demonstrated. The resulting test apparatus represents a culmination of effort by MIT, Stevens Institute of Technology, and General Dynamics, Electric Boat Division, and Convair Division.

As the first test site for a coning motion experiment, the MIT variable pressure water tunnel required moderate modification. The modifications included installation of the model drive shaft, supports, and motor drive system. A workable data acquisition system, capable of capturing both the time varying and steady state effects, was established. The final system was capable of:

- Positive and negative rotation rates to 200 RPM.
- 0 to  $-20^\circ$  coning angle settings in  $2^\circ$  increments.
- Free stream velocities to 30 ft/s.

The demonstration tests conducted covered a limited range of spin rates and coning angle settings. Reynolds number based on model length varied from  $4.04 \times 10^6$  to  $6.06 \times 10^6$ . Cross-flow Reynolds number based on body maximum diameter extended from  $1.5 \times 10^5$  to  $3 \times 10^5$ , covering flow regimes in range of the transition from laminar to turbulent separation. The steady state forces and moments were non-dimensionalized and presented as functions of the non-dimensional spin rate. Some of the main observations are:

- Effects of Reynolds number variation are insignificant for the test range investigated.
- The out-of-plane forces and moments ( $Y'$  and  $N'$ ) are significant, reaching magnitudes of 30% of the in-plane force.



- The forces and moments are non-linear functions of the spin rate for coning angle settings  $> 14^\circ$ .
- The side force,  $Y'$ , is a possibly quadratic or higher order function of the coning angle.
- Measured test data correlates fairly well with numerical results, falling within the range of no separation to laminar separation.

Overall, the first hydrodynamic captive model test using a rotary balance apparatus was a great success and opens the door to obtaining test data for motion in a non-planar cross flow. Ultimately, this will lead to a better understanding of the physics governing the behavior of freely moving bodies in large amplitude maneuvers.

## 6.2 Recommendations

Because of the extensive literature covering the experience of aeronautic researchers with the rotary balance apparatus, many first time mistakes were avoided. However, the different nature of testing in a water versus wind tunnel brought on its own host of problems. The largest differences were the presence of buoyant forces, the thermal effects caused by immersion in water, and working in medium of roughly 1000 times greater density than air. For subsequent on testing, several recommendations can be made:

- Streamline the sector assembly to reduce both drag and cavitation caused by the sharp corners.
- Counter balance the apparatus at the model end to minimize rotational variance over a cycle. Counter balancing is essential.
- Recalibrate the balance for a standard axis system convention.





- Exchange the amplifier/filters for units with a higher cutoff frequency (if useful time varying information is desired). If this is not done, then include some separate monitoring system to check for vibration effects.
- For greater accuracy, conduct an on site calibration that accounts for local system peculiarities and determines model/sting deflection as a function of loading.
- Conduct all tests at a given  $\alpha_c$  in both rotation directions to account for flow angularity.
- Quantify the temperature sensitivity of the balance to allow for data correction later.
- Replace the 2 HP motor with a 5 HP motor. This will also minimize the RPM variance over a cycle. The current motor is undersized.



## REFERENCES

- [1] Tobak, M. and Schiff, L.B., "Aerodynamic Mathematical Modeling," AGARD Lecture Series #114, March 1981.
- [2] Coney, W.B., "Circulation Measurements on a Body of Revolution with an Attached Fin," Master's Thesis, MIT, 1985.
- [3] Kaplan, J., "Velocity Measurements on a Body of Revolution with an Attached Fin," Master's Thesis, MIT, 1986.
- [4] Reed, J., "Measurement of Forces and Moments on, and Velocity About a Body of Revolution With an Attached Fin at Angles of Attack," MIT Report 87-9, April 1987.
- [5] Shields, Lisa, "A Hydrodynamic Study of a Submerged Vehicle," MIT Report 88-3, May 1988.
- [6] Malcolm, Gerald N., "Rotary and Magnus Balances," AGARD Lecture Series #114, Dynamic Stability Parameters, March 1981.
- [7] Malcolm, Gerald N., "Impact of High-Alpha Aerodynamics on Dynamic Stability Parameters of Aircraft and Missiles," AGARD Lecture Series #114, Dynamic Stability Parameters, March 1981.
- [8] Tobak, Murray; Schiff, Lewis B. and Peterson, Victor L., "Aerodynamics of Bodies of Revolution in Coning Motion," AIAA Journal, Vol. 7, No. 1, January 1969.
- [9] Mendenhall, M. R. and Perkins, S. C., Jr., "Nonlinear Hydrodynamic Analysis of Submarine Configurations," Nielsen Engineering and Research, Inc., NEAR TR-388, June 1988.
- [10] Strumpf, A., "Equations of Motion of a Submerged Body With Varying Mass," Davidson Laboratory Report SIT-DL-60-9-771, May 1960.
- [11] Abkowitz, Martin A., Stability and Motion Control of Ocean Vehicles, The Massachusetts Institute of Technology, MIT Press, 1969.
- [12] McKee, G., "FORTRAN Codes for Multiple-Component Balance Use," Davidson Laboratory Technical Note TN-978.



- [13] Galaway, R. D., "A Comparison of Methods for Calibration and Use of Multi-Component Strain Gauge Wind Tunnel Balances," National Research Council Canada, NRC No. 18227, Aeronautical Report LR-600, Ottawa, March 1980.
- [14] Malcolm, Gerald N., "Rotary-Balance Experiments on a Modern Fighter Aircraft Configuration at High Reynolds Numbers," AIAA Paper 85-1829-CP, Snowmass, Colorado, August 1985.
- [15] "Nomenclature for Treating the Motion of a Submerged Body Through a Fluid," The Society of Naval Architects and Marine Engineers Technical and Research Bulletin No. 1-5, July 1962
- [16] Perkins, S. C., Jr. and Mendenhall, M. R., "Hydrodynamic Analysis of Submersible Vehicles Undergoing Large Unsteady Maneuvers," Vol. II - SUBFLO Program Manual, NEAR TR-341, April 1985.
- [17] Dahlquist, G., and Björck, Åke, Numerical Methods, Prentice-Hall, Englewood Cliffs, N.J., 1974.



## **Appendix A Taylor Series Expansion**





## APPENDIX A

### *Taylor Series Expansion*

## A 1 Taylor Series Expansion

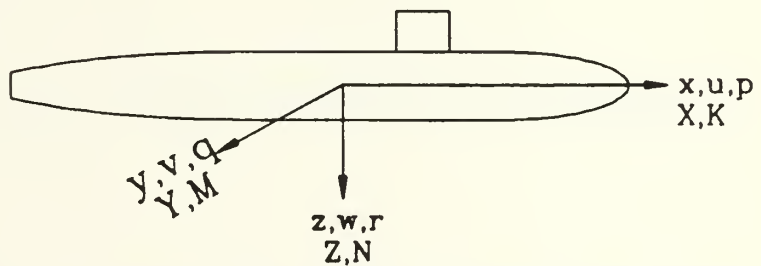
A Taylor series expansion with respect to the rectilinear and angular velocity components about a given condition is accomplished for representative forces and moments. The expansion will show the hydrodynamic derivatives that are of importance and which relate directly to this study.

### A 1.1 Conventions

The axis system, hydrodynamic forces, and the non-dimensionalizations are in accordance with reference [15]. The rectangular coordinate system in body fixed axis is as shown. The x-axis is chosen to coincide with the longitudinal axis of the body. The y-axis is in the horizontal plane and is positive to starboard.

The x-z plane is taken to be the principle plane of symmetry.

Body Fixed Axis System



The hydrodynamic force and moments,  $X$ ,  $Y$ ,  $Z$ , and  $K$ ,  $M$ ,  $N$  respectively, and the linear and angular velocity components are non-dimensionalized as follows:



## ***Taylor Series Expansion***

- Dimensionless Forces:

$$X' = \frac{X}{\frac{1}{2}\rho A U^2}$$

$$Y' = \frac{Y}{\frac{1}{2}\rho A U^2}$$

$$Z' = \frac{Z}{\frac{1}{2}\rho A U^2}$$

- Dimensionless Moments:

$$K' = \frac{K}{\frac{1}{2}\rho A l U^2}$$

$$M' = \frac{M}{\frac{1}{2}\rho A l U^2}$$

$$N' = \frac{N}{\frac{1}{2}\rho A l U^2}$$

- Dimensionless Velocities

$$u' = \frac{u}{U}$$

$$v' = \frac{v}{U}$$

$$w' = \frac{w}{U}$$

$$p' = \frac{p l}{U}$$

$$q' = \frac{q l}{U}$$

$$r' = \frac{r l}{U}$$

where:

$A$  = body frontal area

$l$  = body length

$U$  = free stream velocity

Note:

$$U^2 = u^2 + v^2 + w^2$$

$$1 = u'^2 + v'^2 + w'^2$$

$u'$ ,  $v'$ , and  $w'$  are direction cosines, not simply dimensionless  $u$ ,  $v$ , and  $w$ , because the normalizing velocity,  $U$ , varies.

## **A 1.2 Example Expansion of a Hydrodynamic Function**

Because of the tedious nature of the expansion, only the  $X$  hydrodynamic force is expanded as a representative force. The expansion is carried out about the condition of straight ahead motion at the instantaneous surge velocity,  $u(t)$ :



## ***Taylor Series Expansion***

$$u = u(t), \quad v = w = p = q = r = 0$$

or in non-dimensional form:

$$u' = 1, v' = w' = p' = q' = r' = 0$$

The X force is a function of the three linear and three angular velocities and can be written as:

$$X = X(u, v, w, p, q, r) = \frac{1}{2} \rho A U^2 X'(Re, v', w', p', q', r') \quad Re = \frac{Ul}{v}$$

Expanding about the reference point, the general form of the expansion is:

$$X'(Re, v', w', p', q', r') = \sum_{k=0}^{\infty} \frac{1}{k!} \left[ \left( v' \frac{\partial}{\partial v} + w' \frac{\partial}{\partial \delta} + p' \frac{\partial}{\partial \xi} + q' \frac{\partial}{\partial \eta} + r' \frac{\partial}{\partial \zeta} \right) \right]^k X'(Re, v, \delta, \xi, \eta, \zeta)$$

where  $v, \delta, \xi, \eta$ , and  $\zeta$  are dummy variables.

$$X'_o = X'(Re_o, 0, 0, 0, 0, 0) \quad Re_o = \frac{ul}{v}$$

Following reference [15], the standard shorthand notation is introduced:

$$X'_{,v} = \left[ \frac{\partial}{\partial v} X'(Re_o, v', 0, 0, 0, 0) \right]_{v'=0}$$

Carrying out the expansion for the zero<sup>th</sup> and first order terms:

$$X' = X'_o + \left[ \left( v' \frac{\partial}{\partial v} + w' \frac{\partial}{\partial \delta} + p' \frac{\partial}{\partial \xi} + q' \frac{\partial}{\partial \eta} + r' \frac{\partial}{\partial \zeta} \right) \right] X'(Re_o, v, \delta, \xi, \eta, \zeta) + \dots$$

$$X' = X'_o + [X'_{,v} v' + X'_{,w} w' + X'_{,p} p' + X'_{,q} q' + X'_{,r} r'] + \dots$$



## Taylor Series Expansion

Carrying out the expansion for second and some of the third order terms and employing the shorthand notation:

$$\begin{aligned}
 X' = X'_o + [k = 1 \text{ terms}] + \frac{1}{2} [X'_{vv} v'^2 + 2X'_{vn} v'w' + 2X'_{vp} v'p' + 2X'_{vq} v'q' + 2X'_{vr} v'r' \\
 + X'_{nn} w'^2 + 2X'_{np} w'p' + 2X'_{nq} w'q' + 2X'_{nr} w'r' \\
 + X'_{pp} p'^2 + 2X'_{pq} p'q' + 2X'_{pr} p'r' \\
 + X'_{qq} q'^2 + 2X'_{qr} q'r' + X'_{rr} r'^2] \\
 + \frac{1}{6} [X'_{vvv} v'^3 + 3X'_{vvn} v'^2 w' + 3X'_{vvp} v'^2 p' + 3X'_{v vq} v'^2 q' + 3X'_{vvv} v'^2 r' \\
 + 3X'_{vnn} v'w'^2 + 6X'_{vnp} v'w'p' + 6X'_{vnq} v'w'q' + \dots + X'_{rrr} r'^3] + \dots
 \end{aligned}$$

The expansion is the same for the other forces and moments:

$$X' \Rightarrow Y', Z', K', M', N'$$

The expansion becomes quite cumbersome for a complete third order and higher expansion. Fortunately, many of the terms can be eliminated on the basis of symmetry. As a result of the x-z symmetry plane;  $X', Z'$ , and  $M'$  are *even* in  $v', p', r'$  and  $Y', K'$ , and  $N'$  are *odd* in  $v', p'$ , and  $r'$ . Using this and the data presented in Tables III - VI of Reference [10], the  $X'$  and  $Y'$  force terms are reduced to:

$$\begin{aligned}
 X' = X'_o + [X'_{nn} w' + X'_{qq} q'] + \frac{1}{2} [X'_{vv} v'^2 + 2X'_{vr} v'r' \\
 + X'_{nn} w'^2 + 2X'_{nq} w'q' + X'_{pp} p'^2 + 2X'_{pr} p'r' + X'_{qq} q'^2 + X'_{rr} r'^2] \\
 + \frac{1}{6} [k = 3 \text{ terms}] + \dots
 \end{aligned}$$





## *Taylor Series Expansion*

$$\begin{aligned}
 Y' &= Y'_o + [Y'_{,v'} + Y'_{,p'} + Y'_{,r'}] \\
 &+ \frac{1}{2} [2Y'_{,vw} v' w' + 2Y'_{,vq} v' q' + 2Y'_{,wp} w' p' + 2Y'_{,wr} w' r' + 2Y'_{,pq} p' q' + 2Y'_{,qr} q' r'] \\
 &+ \frac{1}{6} [k = 3 \text{ terms}] + \dots
 \end{aligned}$$

The force and moment terms can now be put in their final dimensional form. As a representative force, the X force becomes:

$$\begin{aligned}
 X &= X'_o \left( \frac{1}{2} \rho A U^2 \right) + [X'_{,w} w' + X'_{,q} q'] \left( \frac{1}{2} \rho A U \right) \\
 &+ \frac{1}{2} [X'_{,vv} v'^2 + 2X'_{,vr} v' r' + \dots] \left( \frac{1}{2} \rho A \right) \\
 &+ \frac{1}{6} [X'_{,vvv} v'^3 + 3X'_{,vww} v'^2 w' + \dots] \left( \frac{1}{2} \left( \frac{\rho A}{U} \right) \right) + \dots
 \end{aligned}$$

The final form follows the same procedure for the other forces and moments (the dimensionalization is slightly different for the moments K, M, and N).

## **A 2 Data Analysis**

The Taylor Series expansion fits an assumed model of the form:

$$Y' = \sum_j b_j f_j(v', w', p', q', r') + \epsilon$$

where:

$Y'$  = measured hydrodynamic forces

$b_j$  = coefficients

$f_j$  = "fitting" functions

$\epsilon$  = truncation error



## *Taylor Series Expansion*

The fitting functions are the controlled variables during the experiment (i.e., the resulting linear and angular velocities and their combinations for a given rotation rate, coning angle, and tunnel velocity). The measured hydrodynamic forces and moments are the dependent variables resulting from the test runs. The basic matrix equation to solve is:

$$\{Y\} = [X] \{b\} \quad (1)$$

where:

$\{Y\}$  = measured hydrodynamic force vector (1 x m)

$[X]$  = fitting functions (n x m)

$\{b\}$  = least squares fit coefficients (1 x n)

m = # data runs

n = # fitting functions

$\{Y\}$  and  $[X]$  are known from the experiment. The basic equation is unsolvable as is; therefore, a least squares approach is adopted. The method is to find the vector  $\{b\}$  that minimizes the sum of squares of the error. This is equivalent to minimizing the equation:

$$([X] \{b\} - \{Y\})^T ([X] \{b\} - \{Y\})$$

The minimization is found by multiplying both sides of equation (1) by  $[X]^T$  and then solving for  $\{b\}$  :

$$[X]^T [X] \{b\} = [X]^T \{Y\}$$

$$\{b\} = ([X]^T [X])^{-1} [X]^T \{Y\} \quad (2)$$



## *Taylor Series Expansion*

Once the coefficient vector  $\{b\}$  is known, it can be directly related to the corresponding hydrodynamic coefficients through a multiplicative constant. For example:

$$X' = X'_o + b_1 w' + b_2 q' + b_3 v'^2 + \dots$$

$$b_1 = X'_w$$

$$b_2 = X'_q$$

$$b_3 = \left(\frac{1}{2}\right) X'_{vv}$$



## **Appendix B Inertia, Gravity and Buoyancy Forces**





## B 1 Inertial Forces

The forces and moments experienced by the body-fixed balance due to the rotary motion of the apparatus are calculated as functions of the model moments of inertia ( $I_{xx}$ ,  $I_{yy}$ ,  $I_{zz}$ ), the rotation rate ( $\omega$ ), and the coning angle ( $\alpha_c$ ). The approach will be completely general, and later adapted to this particular study.

The axis convention is as follows:

- Fixed (in space) axis system:  $x_o, y_o, z_o$ .
- Body fixed axis system:  $x, y, z$ .

The coning angle,  $\alpha_c$ , is defined as the angle between the  $x$  and  $x_o$  axes. The  $x$ -axis is colinear with the centerline of the model, the  $x_o$ -axis is colinear with the centerline of the test section. The rotation rate vector,  $\vec{\omega}$ , is also colinear with the tunnel centerline. The nomenclature and axis system used here is consistent with the list of nomenclature.

The equations of motion can be derived from a dynamic analysis. Using the basic Newtonian force/moment relationships:

$$\vec{F}_G = \frac{d}{dt}(\overline{\text{Momentum}}) = \frac{d}{dt}(m \vec{U}_G) \quad (1)$$

$$\vec{M}_G = \frac{d}{dt}(\overline{\text{Angular Momentum}}) = \frac{d}{dt}(\vec{H}_G) \quad (2)$$

where :

$m$  = model mass

$\vec{U}_G$  = velocity of model CG

$\vec{H}_G$  = angular momentum of model at CG



For a reference point not at the CG, equations (1) and (2) can be rewritten as:

$$\begin{aligned}\overline{F_c} &= m \frac{d}{dt} (\overline{U_c} + \overline{\Omega_c} \times \overline{R_G}) \\ \overline{M_c} &= \overline{M_G} + \overline{R_G} \times \left\{ \frac{d}{dt} (m \overline{U_G}) \right\}\end{aligned}$$

where :

$$\overline{U_c} = u\hat{u}_x + v\hat{u}_y + w\hat{u}_z = \text{Velocity of reference point in space.}$$

$$\overline{\Omega_c} = p\hat{u}_x + q\hat{u}_y + r\hat{u}_z = \text{Angular velocity of body about the reference point.}$$

$$\overline{R_G} = x_G\hat{u}_x + y_G\hat{u}_y + z_G\hat{u}_z = \text{Vector distance of CG from reference point.}$$

Carrying out the differentiation and vector multiplication and setting the acceleration terms = 0, the force and moment components reduce to:

$$X = m[qw - rv - x_G(q^2 + r^2) + y_G(pq) + z_G(pr)]$$

$$Y = m[ru - pw - y_G(r^2 + p^2) + z_G(qr) + x_G(qp)]$$

$$Z = m[pv - qu - z_G(p^2 + q^2) + x_G(rp) + y_G(rq)]$$

$$\begin{aligned}K &= (I_z - I_y)qr + m[y_G(pv - qu) - z_G(ru - pw) \\ &\quad + x_Gy_G(pr) - x_Gz_G(pq) + y_Gz_G(r^2 - q^2)]\end{aligned}$$

$$\begin{aligned}M &= (I_x - I_z)rp + m[z_G(qw - rv) - x_G(pv - qu) \\ &\quad + y_Gz_G(qp) - y_Gx_G(qr) + x_Gz_G(p^2 - r^2)]\end{aligned}$$

$$\begin{aligned}N &= (I_y - I_x)pq + m[x_G(ru - pw) - y_G(qw - rv) \\ &\quad + z_Gx_G(rq) - z_Gy_G(rp) + y_Gx_G(q^2 - p^2)]\end{aligned}$$

where  $x_G, y_G, z_G$  are the component distances of the model CG from the reference point.



For the formulation to be useful, the body-fixed velocities had to be defined with respect to the known variables,  $\omega$  and  $\alpha_c$ . A transformation matrix was derived that resolved the rotation rate ( $\omega$ ), which was defined in the  $x_o, y_o, z_o$  coordinate system, into the body-fixed  $x, y, z$  system. The derived result (for no roll angle,  $\phi = 0$ ) is as shown:

$$\begin{bmatrix} x \\ y \\ z \end{bmatrix} = \begin{bmatrix} \cos \alpha_c & \sin \alpha_c \sin \omega t & -\sin \alpha_c \cos \omega t \\ 0 & \cos \omega t & \sin \omega t \\ \sin \alpha_c & -\cos \alpha_c \sin \omega t & \cos \alpha_c \cos \omega t \end{bmatrix} \begin{bmatrix} x_o \\ y_o \\ z_o \end{bmatrix}$$

Given that the rotation vector is  $\bar{\omega} = \omega \hat{u}_{x_o}$ , the relevant transformation is:

$$p = (\cos \alpha_c) \omega$$

$$q = 0$$

$$r = (\sin \alpha_c) \omega$$

Because the reference point is fixed,  $u = v = w = 0$ . Substituting into the force and moment equations:

$$X_i = m \omega^2 [-x_G (\sin^2 \alpha_c) + z_G (\cos \alpha_c \sin \alpha_c)]$$

$$Y_i = -m \omega^2 y_G$$

$$Z_i = m \omega^2 [-z_G (\cos^2 \alpha_c) + x_G (\sin \alpha_c \cos \alpha_c)]$$

$$K_i = m \omega^2 y_G \sin \alpha_c [x_G \cos \alpha_c + z_G \sin \alpha_c]$$

$$M_i = \omega^2 [(I_x - I_z) (\sin \alpha_c \cos \alpha_c) + m x_G z_G (\cos^2 \alpha_c - \sin^2 \alpha_c)]$$

$$N_i = -m \omega^2 y_G \cos \alpha_c [z_G \sin \alpha_c + x_G \cos \alpha_c]$$

The  $i$  subscript refers to inertia forces.

For the model used in the experiment,  $y_G = z_G = 0$  and  $x_G = .40$  inches. Because of the symmetry of the model about the  $x$ - $z$  and  $x$ - $y$  planes (both geometric and inertial):

- $I_{xy} = I_{yz} = I_{zx} = 0$



- $I_{yy} = I_{zz}$

By inserting these relations into the inertial force and moment equations, the final form results:

$$X_i = -m\omega^2 x_G \sin^2 \alpha_c$$

$$Y_i = 0$$

$$Z_i = m\omega^2 x_G \sin \alpha_c \cos \alpha_c$$

$$M_i = \omega^2 (I_x - I_z) (\sin \alpha_c \cos \alpha_c)$$

$$K_i = N_i = 0$$

The forces and moments above are actually the **reaction** forces and moments. To be consistent with the inertial forces and moments measured by the balance, the negative of the relations should be used for comparison. Therefore, the negative of the relations were used to predict the inertia forces experienced by the balance, and then compared with experiment results.

## B 2 Gravitational and Buoyancy Forces

Having derived the transformation matrix in the previous section, the calculation of gravitational and buoyancy forces (and moments) is straight forward. The gravity and buoyancy vectors are:  $\vec{G} = W \hat{u}_{z_o}$  and  $\vec{B} = -B \hat{u}_{z_o}$ . The forces follow directly:

$$X_{W-B} = -(W - B) \sin \alpha_c \cos \omega$$

$$Y_{W-B} = (W - B) \sin \omega$$

$$Z_{W-B} = (W - B) \cos \alpha_c \cos \omega$$





For the moments, a simple moment balance at the reference point results in the relations for weight and buoyancy:

$$K_w = W[y_G \cos \alpha_c \cos \omega - z_G \sin \omega]$$

$$M_w = -W \cos \omega [z_G \sin \alpha_c + x_G \cos \alpha_c]$$

$$N_w = W[x_G \sin \omega + y_G \sin \alpha_c \cos \omega]$$

The same equations result for buoyancy by substituting  $-B$  for  $W$  and  $x_B, y_B, z_B$  for  $x_G, y_G, z_G$ .



## **Appendix C Test Data**

The following pages contain the steady state inertia and test run data for the plots presented in Chapters 3 and 4.



## C 1 Inertia Data

$$\alpha_c = -20^\circ$$

Measured Forces & Moments

SNAME Axis Convention  
Calculated Forces & Moments

$\omega$	X	Z	M	X	Z	M
RPM	lbs	lbs	in-lbs	lbs	lbs	in-lbs
49.25	0.0288	-0.1236	2.8651	0.0337	0.0926	-3.2139
62.31	0.0546	-0.0462	4.8078	0.0539	0.1481	-5.1444
74.57	0.0790	0.0408	7.0166	0.0772	0.2122	-7.3679
87.12	0.1096	0.1140	9.6901	0.1054	0.2896	-10.0566
99.76	0.1367	0.2128	12.8832	0.1382	0.3797	-13.1865
112.09	0.1678	0.2913	16.3004	0.1745	0.4794	-16.6475
118.71	0.1826	0.3119	18.3621	0.1957	0.5377	-18.6720
136.78	0.2346	0.4435	24.5037	0.2598	0.7139	-24.7891
149.81	0.2714	0.5189	29.4050	0.3117	0.8564	-29.7370
162.15	0.2982	0.5495	34.6056	0.3652	1.0033	-34.8377
174.79	0.3388	0.6281	40.2188	0.4243	1.1658	-40.4808
187.23	0.3816	0.7160	46.1558	0.4869	1.3376	-46.4480
200.04	0.4249	0.8854	52.7484	0.5558	1.5269	-53.0212



$$\alpha_c = -14^\circ$$

Measured Forces & Moments

SNAME Axis Convention  
Calculated Forces & Moments

$\omega$	X	Z	M	X	Z	M
RPM	lbs	lbs	in-lbs	lbs	lbs	in-lbs
49.57	0.0090	0.0724	2.4397	0.0171	0.0685	-2.3100
62.33	0.0218	0.0672	3.9159	0.0270	0.1083	-3.6523
74.50	0.0402	0.1913	5.4709	0.0386	0.1547	-5.2178
87.01	0.0586	0.2811	7.4337	0.0526	0.2110	-7.1173
99.63	0.0662	0.2408	9.7965	0.0690	0.2766	-9.3316
112.13	0.1038	0.3423	12.4130	0.0874	0.3504	-11.8200
124.64	0.1180	0.4912	15.1671	0.1079	0.4330	-14.6046
137.40	0.1588	0.5891	18.5433	0.1312	0.5261	-17.7479
149.75	0.1711	0.6659	22.0771	0.1558	0.6250	-21.0818
162.26	0.1867	0.6543	25.5793	0.1829	0.7338	-24.7512
174.85	0.1955	0.7555	29.6556	0.2124	0.8520	-28.7412
187.39	0.2285	0.8517	34.0778	0.2440	0.9786	-33.0116
199.41	0.2475	0.9916	38.5838	0.2763	1.1082	-37.3825





## C 2 Water Test Data

$$\alpha_c = -20^\circ, V = 20 \text{ ft/s}$$

Dimensional Forces and Moments:

$\omega$	V	X	Y	Z	K	M	N
RPM	ft/s	lbs	lbs	lbs	in-lbs	in-lbs	in-lbs
0.00	20.00	1.7807	-0.4127	13.3950	-0.0499	97.7634	5.4022
24.73	20.14	1.8050	-3.0184	14.4783	-0.0893	94.9171	28.2857
49.88	19.94	1.7565	-4.6306	16.8702	0.7687	82.3410	48.3047
62.60	20.00	1.6496	-5.4057	18.0369	0.7171	76.5490	55.3021
74.96	20.16	1.6015	-6.0838	19.4667	0.6990	71.5372	62.0918
87.28	20.04	1.4227	-6.4383	20.5436	0.8320	65.0586	66.3317
99.91	20.00	1.3748	-6.7695	21.8154	0.8238	58.7498	69.3997
112.86	19.98	1.3545	-6.8481	23.1153	0.8295	53.3163	71.3852
124.97	20.00	1.3613	-6.7248	24.3194	0.8603	51.5026	71.6046
137.57	19.99	1.3772	-6.3449	25.2051	0.8519	47.9207	69.5812
149.93	20.03	1.4644	-6.1989	26.1849	0.0097	46.3321	67.3002
162.33	19.68	1.0483	-5.2636	26.6441	-0.3071	44.5136	61.1284
174.93	19.80	1.1375	-5.0225	28.2116	-0.2395	42.5456	59.8012



$$\alpha_c = -20^\circ, V = 20 \text{ ft/s}$$

Non-Dimensional Force and Moments (SNAME Axis Convention)

$\omega'$	$X'$	$Y'$	$Z'$	$K'$	$M'$	$N'$
0.0000	0.11617	0.02692	0.87384	0.00014	-0.27139	-0.01500
0.2518	0.11612	0.19418	0.93142	0.00024	-0.25984	-0.07743
0.5130	0.11528	0.30390	1.10718	-0.00215	-0.22996	-0.13490
0.6419	0.10761	0.35265	1.17666	-0.00199	-0.21250	-0.15352
0.7625	0.10282	0.39061	1.24986	-0.00191	-0.19545	-0.16964
0.8932	0.09244	0.41834	1.33484	-0.00230	-0.17988	-0.18340
1.0245	0.08969	0.44162	1.42315	-0.00229	-0.16309	-0.19265
1.1584	0.08854	0.44764	1.51097	-0.00231	-0.14830	-0.19856
1.2814	0.08881	0.43870	1.58650	-0.00239	-0.14297	-0.19877
1.4113	0.08993	0.41433	1.64593	-0.00237	-0.13316	-0.19335
1.5351	0.09525	0.40318	1.70309	-0.00003	-0.12823	-0.18627
1.6916	0.07063	0.35463	1.79514	0.00088	-0.12762	-0.17526
1.8118	0.07571	0.33430	1.87778	0.00068	-0.12050	-0.16938



$$\alpha_c = -20^\circ, V = 25 \text{ ft/s}$$

Dimensional Forces and Moments:

$\omega$	V	X	Y	Z	K	M	N
RPM	ft/s	lbs	lbs	lbs	in-lbs	in-lbs	in-lbs
0.00	25.00	2.8352	-1.1874	21.3436	-0.1478	155.7889	12.6462
24.61	25.16	2.9638	-4.0519	22.5019	-0.1640	152.6435	36.6306
49.60	24.99	2.8429	-6.1961	24.6022	0.2214	140.2328	62.0913
62.00	24.99	2.7436	-7.2647	25.7674	0.2760	132.8883	71.9413
74.96	25.08	2.7272	-7.8359	27.4710	0.6629	127.0355	80.4999
87.57	25.02	2.5884	-8.5436	28.9508	0.9469	119.1681	87.2302
100.07	25.01	2.5976	-8.9943	30.3857	1.0378	112.7317	93.1821
112.01	25.09	2.4454	-9.7209	31.6042	0.2466	108.1354	98.4144
124.96	24.99	2.3587	-10.1292	33.0844	0.2946	101.9607	102.7088
137.11	25.00	2.3444	-10.5471	34.8084	0.4102	93.5887	106.4660
150.54	24.88	1.8940	-10.4834	36.4530	-0.2555	86.9464	108.3579
162.47	24.80	1.8399	-10.2761	38.1074	-0.3561	80.7528	108.6325
175.72	24.79	1.7725	-10.2041	39.9737	-0.1667	75.4170	109.1923
188.13	24.74	1.8304	-9.7537	41.2867	-0.1466	71.8783	106.3098



$$\alpha_c = -20^\circ, V = 25 \text{ ft/s}$$

Non-Dimensional Force and Moments (SNAME Axis Convention)

$\omega'$	$X'$	$Y'$	$Z'$	$K'$	$M'$	$N'$
0.0000	0.11837	0.04958	0.89112	0.00026	-0.27678	-0.02247
0.2006	0.12217	0.16703	0.92757	0.00029	-0.26776	-0.06425
0.4070	0.11879	0.25890	1.02799	-0.00039	-0.24934	-0.11040
0.5088	0.11464	0.30355	1.07668	-0.00049	-0.23628	-0.12792
0.6129	0.11314	0.32507	1.13964	-0.00117	-0.22426	-0.14211
0.7178	0.10790	0.35614	1.20680	-0.00168	-0.21138	-0.15473
0.8206	0.10837	0.37522	1.26762	-0.00184	-0.20012	-0.16542
0.9155	0.10137	0.40295	1.31006	-0.00043	-0.19074	-0.17360
1.0255	0.09856	0.42324	1.38242	-0.00052	-0.18129	-0.18262
1.1247	0.09788	0.44035	1.45329	-0.00073	-0.16627	-0.18915
1.2408	0.07984	0.44193	1.53667	0.00046	-0.15597	-0.19438
1.3435	0.07806	0.43599	1.61679	0.00064	-0.14579	-0.19613
1.4537	0.07526	0.43328	1.69734	0.00030	-0.13627	-0.19730
1.5595	0.07804	0.41583	1.76019	0.00027	-0.13040	-0.19287





$$\alpha_c = -20^\circ, V = 30 \text{ ft/s}$$

Dimensional Forces and Moments:

$\omega$	V	X	Y	Z	K	M	N
RPM	ft/s	lbs	lbs	lbs	in-lbs	in-lbs	in-lbs
0.00	30.00	4.3006	-1.3594	31.3776	-0.1053	225.6850	15.5032
24.92	29.90	4.4342	-4.4899	33.1005	-0.1902	227.2220	41.6996
50.21	29.85	4.5976	-6.9112	35.3535	0.0677	215.9177	72.3032
62.27	29.80	4.3944	-8.6193	35.9759	-0.0549	203.3624	86.2138
75.06	29.84	4.3591	-9.7270	37.7076	-0.0179	197.5555	99.1324
87.40	29.81	4.2430	-10.9743	39.0950	0.0850	187.5376	109.2362
99.99	29.77	4.1492	-11.9608	40.6420	0.0809	177.9788	118.4719
112.48	29.82	4.1958	-13.0763	42.8066	0.0665	172.7654	127.1844
124.86	29.79	4.1469	-14.0665	44.8761	-0.0910	166.8419	135.3630
133.16	29.80	4.0082	-14.4679	46.5603	-0.1000	161.3638	139.8783
175.38	29.48	3.2557	-15.4335	51.9799	-0.1183	133.8079	152.6120
188.06	29.52	3.1270	-15.5296	54.2381	-0.3068	126.2722	154.3934
200.24	29.51	2.9708	-15.3121	56.0134	-0.4757	118.3547	154.2632



$$\alpha_c = -20^\circ, V = 30 \text{ ft/s}$$

Non-Dimensional Force and Moments (SNAME Axis Convention)

$\omega'$	$X'$	$Y'$	$Z'$	$K'$	$M'$	$N'$
0.0000	0.12469	0.03941	0.90976	0.00013	-0.27845	-0.01913
0.1709	0.12943	0.13105	0.96614	0.00024	-0.28222	-0.05179
0.3450	0.13465	0.20240	1.03536	-0.00008	-0.26908	-0.09011
0.4285	0.12913	0.25327	1.05713	0.00007	-0.25428	-0.10780
0.5159	0.12775	0.28506	1.10504	0.00002	-0.24636	-0.12362
0.6013	0.12459	0.32226	1.14801	-0.00011	-0.23434	-0.13650
0.6888	0.12217	0.35217	1.19665	-0.00010	-0.22299	-0.14844
0.7735	0.12313	0.38372	1.25616	-0.00008	-0.21574	-0.15882
0.8595	0.12194	0.41361	1.31954	0.00011	-0.20876	-0.16937
0.9164	0.11778	0.42513	1.36814	0.00013	-0.20177	-0.17490
1.2200	0.09775	0.46340	1.56073	0.00015	-0.17097	-0.19499
1.3065	0.09364	0.46502	1.62413	0.00039	-0.16090	-0.19673
1.3915	0.08902	0.45882	1.67843	0.00061	-0.15091	-0.19670



$\alpha_c = -14^\circ$ ,  $V = 25$  ft/s, Positive Rotation

Dimensional Forces and Moments:

$\omega$	V	X	Y	Z	K	M	N
RPM	ft/s	lbs	lbs	lbs	in-lbs	in-lbs	in-lbs
0.00	25.00	2.3593	-0.3637	11.0793	-0.2315	118.9746	5.2151
50.13	25.15	2.1468	-0.1873	12.0240	-0.4143	119.1945	19.8490
62.54	25.12	2.2187	-0.1900	12.4948	-0.2749	116.9479	24.7597
74.89	25.16	2.2069	-0.2131	12.9181	-0.3648	115.0202	28.9395
87.43	24.99	2.1640	-0.2153	13.4082	-0.3277	110.8816	33.2202
99.90	25.07	2.1321	-0.0992	14.2999	-0.3418	108.3303	36.7816
112.39	25.18	2.1140	0.1228	15.1658	-0.1307	105.8834	40.3816
124.94	25.15	2.1198	0.2798	16.0281	-0.3430	102.3409	44.0197
137.38	25.11	2.0655	0.4543	16.9207	-0.1895	97.5814	47.0065
149.79	25.08	2.1170	0.6891	18.1925	-0.3328	93.7642	48.9417
162.24	25.04	2.0804	1.0546	19.3723	-0.1990	89.9766	50.6473
174.85	25.17	2.0583	1.1420	20.6688	-0.1912	87.8205	52.8804
187.30	25.06	2.1453	1.3929	21.8235	-0.2175	83.5978	54.3327
199.88	25.13	2.1710	1.7954	22.9710	-0.2591	81.2250	56.5706



$\alpha_c = -14^\circ$ ,  $V = 25$  ft/s, Positive Rotation

Non-Dimensional Force and Moments (SNAME Axis Convention)

$\omega'$	$X'$	$Y'$	$Z'$	$K'$	$M'$	$N'$
0.0000	0.09850	0.01518	0.46257	0.00041	-0.21138	-0.00927
0.4088	0.08857	0.00773	0.49605	0.00073	-0.20925	-0.03485
0.5106	0.09175	0.00786	0.51670	0.00048	-0.20579	-0.04357
0.6104	0.09097	0.00878	0.53251	0.00064	-0.20176	-0.05076
0.7175	0.09042	0.00900	0.56026	0.00058	-0.19715	-0.05907
0.8172	0.08852	0.00412	0.59371	0.00060	-0.19139	-0.06498
0.9153	0.08700	-0.00505	0.62417	0.00023	-0.18544	-0.07072
1.0188	0.08745	-0.01154	0.66123	0.00060	-0.17966	-0.07728
1.1220	0.08548	-0.01880	0.70028	0.00033	-0.17185	-0.08278
1.2248	0.08782	-0.02859	0.75472	0.00059	-0.16552	-0.08640
1.3287	0.08658	-0.04389	0.80623	0.00035	-0.15935	-0.08970
1.4246	0.08478	-0.04704	0.85133	0.00034	-0.15393	-0.09268
1.5328	0.08914	-0.05788	0.90680	0.00038	-0.14781	-0.09607
1.6311	0.08971	-0.07419	0.94917	0.00046	-0.14282	-0.09947





$\alpha_c = -14^\circ$ ,  $V = 25$  ft/s, Negative Rotation

Dimensional Forces and Moments:

$\omega$	V	X	Y	Z	K	M	N
RPM	ft/s	lbs	lbs	lbs	in-lbs	in-lbs	in-lbs
0.00	25.00	2.3311	-0.1258	10.7966	-0.2803	119.0579	4.9293
25.01	25.12	2.2146	-0.1924	11.2166	-0.3202	121.5729	-9.1623
49.99	25.20	2.1628	-0.2097	11.7338	-0.5221	119.9938	-18.6229
62.57	25.18	2.1256	-0.2045	12.1380	-0.5368	117.8443	-23.1318
75.20	25.17	2.0386	-0.1631	12.5462	-0.5930	115.6808	-27.4298
87.42	25.15	2.0036	-0.2240	13.0628	-0.3885	112.6635	-31.5581
99.89	25.15	1.9862	-0.3090	13.8510	-0.5131	109.5740	-35.7383
112.36	25.18	1.9899	-0.2888	14.5891	-0.3202	106.8952	-38.6488
124.76	25.19	1.9411	-0.4733	15.4395	-0.5789	103.2240	-42.3514
137.53	25.20	1.8981	-0.6121	16.3070	-0.4262	99.1405	-44.6834
149.81	25.22	2.0000	-0.8555	17.4064	-0.6541	95.6590	-46.6318
162.54	25.16	1.8789	-1.0731	18.5559	-0.6544	91.4785	-48.4517
174.83	25.13	1.8371	-1.5472	19.6166	-0.5844	87.8058	-50.0444
187.59	25.17	1.8424	-1.9110	20.7705	-0.6725	84.6128	-51.6031
199.45	25.16	1.7601	-2.3692	21.8756	-0.7228	81.5450	-52.6280



$\alpha_c = -14^\circ$ ,  $V = 25$  ft/s, Negative Rotation

Non-Dimensional Force and Moments (SNAME Axis Convention)

$\omega'$	$X'$	$Y'$	$Z'$	$K'$	$M'$	$N'$
0.0000	0.09733	0.00525	0.45077	0.00050	-0.21152	-0.00876
0.2042	0.09158	0.00796	0.46384	0.00056	-0.21393	0.01612
0.4068	0.08887	0.00862	0.48215	0.00091	-0.20982	0.03256
0.5096	0.08748	0.00842	0.49956	0.00094	-0.20638	0.04051
0.6127	0.08397	0.00672	0.51677	0.00104	-0.20276	0.04808
0.7128	0.08266	0.00924	0.53890	0.00068	-0.19778	0.05540
0.8145	0.08194	0.01275	0.57142	0.00090	-0.19236	0.06274
0.9151	0.08190	0.01189	0.60043	0.00056	-0.18721	0.06769
1.0157	0.07983	0.01946	0.63493	0.00101	-0.18064	0.07411
1.1192	0.07799	0.02515	0.67007	0.00075	-0.17335	0.07813
1.2182	0.08205	0.03510	0.71411	0.00114	-0.16700	0.08141
1.3248	0.07745	0.04424	0.76491	0.00115	-0.16046	0.08499
1.4267	0.07591	0.06393	0.81056	0.00103	-0.15439	0.08799
1.5284	0.07589	0.07871	0.85552	0.00118	-0.14830	0.09045
1.6257	0.07255	0.09766	0.90175	0.00127	-0.14304	0.09232



$$\alpha_c = -8^\circ, V = 25 \text{ ft/s}$$

Dimensional Forces and Moments:

$\omega$	V	X	Y	Z	K	M	N
RPM	ft/s	lbs	lbs	lbs	in-lbs	in-lbs	in-lbs
0.00	25.00	1.9863	-0.0767	3.4095	-0.3790	80.1419	3.6989
24.80	25.16	2.1618	0.4343	3.8312	-0.3979	84.4368	1.3001
49.98	25.09	2.0907	0.8401	3.7424	-0.4012	84.3726	2.4721
62.65	25.14	2.0675	1.1172	3.8602	-0.4904	84.7644	3.2220
75.00	25.12	2.0189	1.4423	3.9817	-0.4864	84.6001	3.9571
87.52	25.11	2.0707	1.8278	4.1736	-0.5542	84.7622	4.4011
99.94	25.16	2.0728	2.1869	4.3494	-0.6486	85.4094	4.8563
112.54	25.13	2.0469	2.5681	4.6541	-0.6813	85.3669	5.3994
124.89	25.13	2.0621	2.8901	4.7967	-0.6348	85.4009	6.2727
137.47	25.14	2.0869	3.2998	5.0631	-0.6216	85.5469	6.9445
149.97	25.10	2.0590	3.9614	5.4368	-0.4451	85.6515	7.2211
162.17	25.10	2.1892	4.3835	6.2989	-0.5452	85.2166	7.5703
174.81	25.01	2.2065	4.7426	6.6110	-0.4609	84.6084	8.0544
187.18	25.04	2.2980	5.1863	7.0959	-0.5585	84.9933	8.4963
199.92	24.91	2.2402	5.6277	7.3972	-0.5405	84.1505	8.1367



$$\alpha_c = -8^\circ, V = 25 \text{ ft/s}$$

Non-Dimensional Force and Moments (SNAME Axis Convention)

$\omega'$	$X'$	$Y'$	$Z'$	$K'$	$M'$	$N'$
0.0000	0.08293	0.00320	0.14235	0.00067	-0.14238	-0.00657
0.2021	0.08911	-0.01790	0.15793	0.00070	-0.14811	-0.00228
0.4085	0.08666	-0.03482	0.15513	0.00071	-0.14883	-0.00436
0.5111	0.08536	-0.04613	0.15938	0.00086	-0.14892	-0.00566
0.6123	0.08349	-0.05964	0.16466	0.00086	-0.14887	-0.00696
0.7148	0.08570	-0.07565	0.17273	0.00098	-0.14928	-0.00775
0.8146	0.08544	-0.09015	0.17929	0.00114	-0.14982	-0.00852
0.9184	0.08458	-0.10611	0.19231	0.00120	-0.15010	-0.00949
1.0192	0.08521	-0.11942	0.19820	0.00112	-0.15016	-0.01103
1.1214	0.08616	-0.13624	0.20904	0.00109	-0.15030	-0.01220
1.2253	0.08528	-0.16408	0.22519	0.00078	-0.15096	-0.01273
1.3250	0.09067	-0.18156	0.26090	0.00096	-0.15020	-0.01334
1.4334	0.09205	-0.19785	0.27580	0.00082	-0.15020	-0.01430
1.5330	0.09564	-0.21584	0.29532	0.00099	-0.15052	-0.01505
1.6459	0.09421	-0.23666	0.31108	0.00097	-0.15059	-0.01456





## **Appendix D FORTRAN Routines**

The following pages contain the FORTRAN routines used for obtaining the data presented in the study. Also included is the FFT algorithm used for the data analysis.



\$DEBUG  
program DC

```
c -----PROGRAM DC.FOR-----
c
c ---- Version: 1.2
c
c ---- Date: 03 April 1989
c
c ---- Purpose: Main driver program that links with the following
c               programs: Davlab, Common, DCDave and Calibr.For.
c               This program is to obtain readings from the balance,
c               store them (ac and dc), and convert the steady state
c               components to forces and moments.
c               Program for ROTATING measurements, DC forces
c               and moments.
c
c ---- Programmer: Dave Johnson and Glenn Mckee
c
c ---- Language: Microsoft Fortran 4.1
c
c ---- Variables:
c       fdata(i): Raw MIT counts array filled with counts
c                  from all a/d channels. ("full" data)
c
c       pdata(i): Raw MIT counts array with 6 preferred
c                  channels of a/d channels. Array values
c                  are later corrected for zeros and convair
c                  /MIT counts. This array is then mult.
c                  by a(i,j) for the balance loads.
c                  ("preferred" data)
c
c       loads(i): Array with balance loads. loads(i) comes
c                  from the matrix multiplication of pdata(i)
c                  and a(i,j).
c
c       zerot(i): Row array with averaged counts for all
c                  a/d channels. This array is read by the
c                  subroutine "filter" to convert to the
c                  preferred 6 channels and put into zeros(i).
c
c       a(i,j): Coefficient matrix [B] . From {L} = [B]{R}
c
c ---- Files:
c       name: Raw MIT counts file with data from all
c             a/d channels
c
c       Ratio: file of Convair R-cal/MIT R-cal readings for the
c             6 preferred channels.
c
c       M2X1T.DAT: Balance coefficients for Roll bridge 2 and
c                  Axial bridge 1, referenced to C of Rot.
c
c *** Data Conventions Used in This Code ***
```



```

c
c      Index      Readings()      Loads()
c      1          Normal Force 1      Normal Force at center
c      2          Normal Force 2      Pitch Moment at center
c      3          Side Force 1        Side Force at center
c      4          Side Force 2        Yaw Moment at center
c      5          Selected Roll Bridge Roll Moment at center
c      6          Selected Axial Bridge Axial Force at center

```

```

c      ( The zeros() and ratios() vectors use the same conventions as
c      the pdata() )
c
c -----

```

```

real pdata(6), loads(6), zeros(6), ratios(6), fdata(9)
real zerot(9), dpc, rpmc, dp, rpma, iloads(6)
character*3 tcase, zcase
character*11 zname, lname, mname, iname, calibr
character*80 id, header, head1, headc
character ans

```

```

common /dpcell/ rho, zero, full, tt
common /rpm/ rvz, rvcal
common /revsect/ nrev, nsect

```

```

c ----- open files
open (unit=10, file = 'ratio' , status = 'old' )

write (*,*)
write (*,*) '          *** PROGRAM DC.FOR *** '
write (*,*)

```

```

cdb --- Debug commands for reading in Convair test case. This is to
cdb      check the data reduction algorithm .....
cdb      goto 52

```

```

write (*,*) ' Note: Zeros for this program are stored in the '
write (*,*) '       file zname. The program zero should be '
write (*,*) '       run first to get the proper DAILY zeros. '
write (*,*)
write (*, ' (A\)' ) ' Input the zero (counts) file name: '
read (*,1) zname
write (*,*)

```

```

c ----- Read in zeros from file zname
open (unit = 2, file = zname , status = 'old')
read (2, ' (a80)' ) header
read (2, ' (a80)' ) id
read (unit=2, fmt = 2, err = 51) zcase, (zerot(i) , i = 1,9)
write (*,*)
write (*,*) ' Zeroes read in successfully! '
write (*,*)
c -----Debug command
write (*,*) zerot(1),zerot(9)

```



```

      goto 52
51      write (*,*)
      write (*,*) ' Error in reading zero file '
      goto 100
52      continue

c ----- Read in ratios from file of preferred channels (file "RATIO")
      read (unit = 10, fmt = 6, err = 55) (ratios(i) , i=1,6)
      write (*,*)
      write (*,*) ' Ratios read in successfully'
c -----Debug command
      write (*,*) ratios(1),ratios(6)
      goto 56
55      write (*,*) ' Error in reading in ratios'
      goto 100
56      continue

cdb --- Debug for reading in Convair test case ....
cdb      goto 57

c ----- Call filter subroutine for producing zeros(i)
      call filtz (zerot,zeros)

57      continue

c      ... assign a vacant FORTRAN unit number ...
      lunit = 3
c      ... use the CONVAIR preferred set of coefficients (R2X1) ...
      item = 4
      call intcoef( lunit, item )
      Write (*,*) ' Coefficient Data has been read '

c      ... these are the A/D readings without applied external forces ...
      call setzero( zeros )

c      ... these are the ratios of the current signals divided by the ...
c      ... original signal levels at calibration ...
      call setrcal( ratios )

cdb --- Debug for reading in Convair test case .....
cdb      goto 58

c ----- Offer option of either taking data or processing a previous
c      run's data .....
70      write (*,*)
      write (*,*) ' Do you wish to take new data or process'
      write (*, ' (a\)' ) ' old data ? (N/O): '
      read (*, fmt=9) ans
      if (ans .eq. 'n') then

c ----- Calibrate or read from an old calibration file?
      write (*,*)
      write (*, ' (a\)' ) ' Calibrate? (y/n):'
      read (*,9) ans

```





```

    if (ans .eq. 'n') then
        write (*,*)
        write (*,' (a\\)' ) ' Input old calibration file:'
        read (*,1) calibr
        open(unit=5, file=calibr,status='old')
        read (5,' (a80)') headc
        read (5,' (a80)') id
        read (5,15) rho,zero,full,tt,rvz,rvcal
        close (unit=5)
        goto 80
    endif

c ----- Call calibration routines .....
    call dpcal
    call rpmcal

c ----- write result of recent calibration to file Calibr....
    write (*,*)
    write (*,' (a\\)' ) ' Input new calibration file:'
    read (*,1) calibr
    write(*,*) ' Type in new calibration file header:'
    read (*,' (a80)') headc
    open (unit=5,file=calibr)
    write (5,' (a80)') headc
    write (5,17)
    write (5,15) rho,zero, full,tt,rvz,rvcal
    close(unit=5)

80      write (*,*)
c -----      write (*,' (a\\)' ) ' Input # of revolutions, nrev:'
c -----      read (*,3) nrev
c -----      write (*,*)
               write (*,' (a\\)' ) ' Type in tcase (3 max): '
               read (*,' (a3)') tcase
               nsect = 32
               nrev = 10

c ----- Go to data taking subroutine
               Call takedata (fdata,dpc,rpmc,tcase,header)
               write (*,*) ' takedata finished! '
               write (*,*)

c ----- debug command
cdb      pause
          goto 62
        endif

cdb --- Debug for reading in Convair test case or for inputing
c      previous run file ....
58      continue
        write (*,*)
        write (*,' (A\\)' ) ' Input PREVIOUS (DC) raw counts file: '
        read (*,1) mame
        write (*,*)

```



```

open (unit=9, file = rname, status = 'old')
read(9,' (a80)') header
read(9,' (a80)') id
read (unit=9,fmt=18,err=61) tcase,(fdata(i), i=1,9),dpc,rpmc
write (*,*) ' Previous counts .....'
write (*,*) fdata(1), rpmc

c ----- Read in old calibration file.....
write (*,*)
write (*,' (a\')') ' Input old calibration file:'
read (*,1) calibr
open(unit=5, file=calibr,status='old')
read (5,' (a80)') header
read (5,' (a80)') id
read (5,15) rho,zero,full,tt,rvz,rvcal
close (unit=5)

cdb      do 60 j = 1,6
cdb      zeros(j)=0.0
cdb60    continue
        goto 62

61      write (*,*) ' Error in reading Previous counts....'
        goto 100
62      continue

c ***** Data Reduction Portion *****

c ----- Call filter subroutine to reduce the readings to the preferred
c      6 channels (i.e. read in data to pdata(i))
        call filter(fdata, pdata)

        write (*,*) ' filter done '
c ----- debug command
cdb      pause

        write (*,*)
        write (*,*) ' Now Processing Data!!! '
        write (*,*)

c      ... adjust the values by removing the zeros and compensating ....
c      ... for the ratio of the signal level ...
        call doadjus( pdata )

        call doload( pdata, loads, ierr )
        if( ierr .ne. 0 ) then
            write(6,12) tcase
        endif
20      continue

c ----- Convert dpc and rpmc counts to velocity and rpm...
        call rpmvel(dpc,rpmc,dp,rpma)

c ----- Write loads to screen

```



```

write (*,*)
write (*,*) ' Loads for this run... '
write (*,*)
write (*,10)
write (*,7) tcase, (loads(i) , i=1,6),dp,rpma

c ---- Ask if INERTIA run or HYDRO run. This determines whether or not
c the inertial forces are subtracted out from the above loads.....
75  write (*,*)
    write (*,' (a\)' ) ' Is this an inertial or hydro run? (i/h):'
    read (*,9) ans
    if (ans .eq. 'h') then
        write (*,*)
        write (*,' (a\)' ) ' Input Inertial FORCE & MOMENT file:'
        read (*,' (a11)' ) iname
        open (unit=6, err=75,file=iname,status='old')
        read(6,' (a80)' ) head1
        read(6,' (a80)' ) id
        read (6,16) tcase,(iloads(i), i=1,6)
        close(unit=6)

c ----- Do Load subtraction .....
        do 85 i=1,6
            loads(i)=loads(i)-iloads(i)
85      continue
    endif

c ----- Write loads to file lname.....
    write (*,' (A\)' ) ' Input the load output file name: '
    read (*,1) lname
    write (*,*)

    open(unit=7, file = lname, status = 'new' )
c ----- write (*,*) ' Input header for load file . . . . '
c ----- read (*,' (a80)' ) header
    write (7,' (a80)' ) header
    write (7,10)
    write(7,7) tcase, (loads(i), i=1,6),dp,rpma

c ---- Write loads to screen again.....
    write (*,*)
    write (*,*) ' Final loads for this run... '
    write (*,*)
    write (*,10)
    write (*,7) tcase, (loads(i) , i=1,6),dp,rpma

    write (*,*)
90  write (*,' (A\)' ) ' Would you like another test run? (y/n) : '
    read (*,fmt =9, err = 90) ans
    m=m+1
    if (ans .EQ. 'y') goto 70

c ----- Format Statements .....
1   format(A11)

```



```

2    format (A3, 9F7.1)
3    format (i2)
6    format (6F8.4)
7    format (A3, 6F9.4, 2f9.2)
9    format (A1)
10   format('TC', 4X, 'Z', 8X, 'M', 8X, 'Y', 8X, 'N', 8X, 'K',
+      8X, 'X', 8X, 'VEL', 6X, 'RPM')
12   format(' Convergence problem on point ', A10)
15   format (6f9.5)
16   format(a3, 6f9.4)
17   format (3X, 'Rho', 6X, 'Zero', 5X, 'Full', 6X, 'Tt', 6X, 'Rvz',
+      6X, 'Rvcal')
18   format (a3, 11F7.1)

```

c ----- Close all remaining open files .....

```

close(unit = 10)
close(unit = 7)
close(unit = 1)
close(unit = 2)

```

```

100   continue
      end

```





## \$DEBUG

```
c ----- PROGRAM DCDAVE.FOR -----
c
c ---- Version: 1.2
c
c ---- Note: Full Revolution Version , Therefore nrev=10 max!
c
c ---- Date: 29 March 1989
c
c ---- Purpose : To provide the collection of subroutines necessary
c                  for rotating data taking and DC processing. This
c                  program is for linking with the main driver program
c                  DC.FOR.
c
c ---- Programmer: Dave Johnson
c
c ---- Language: Microsoft Fortran 4.1
c
c ---- Subroutines:
c          TAKEDATA: Primary rotary data collection sub-
c                   routine
c
c          FILTER: Reduces readings to the preferred 6
c                   channels for later processing
c
c          FILTZ:   Reduces zero readings to 6 preferred
c                   chanelns for later processing
c
c          RPMVEL:  Converts dp and rpm counts to actual
c                   tunnel velocity and model rpm
c *****
c
c          SUBROUTINE TAKEDATA(fdata,dpc,rpmc,tcase,header)
c
c ----- SUBROUTINE TAKEDATA-----
c
c ---- Arrays:  fdata(i,j): Averaged (over nsamp) raw MIT counts
c                  for all 9 a/d channels of balance data.
c
c          iarray(i):   Row array filled by EACH mcbatod call
c
c          tarray(i,j): Temporary array with rows of iarray
c                  and columns of nrev*nsect samples
c
c          bigarray(i,j): Summed counts array that is divided
c                  by nsamp and written to tares(i,j)
c
c          dpc(i): Raw MIT counts read from dpcell
c
c          rpmc(i): Raw MIT counts read from daytronix chan C
c
c ---- Files:      RCxxxx.xxx: Raw data file in MIT counts.
c
```



```

c -----
c ----- Dimensions set for max of 32 sectors/rev x 10 revs = 96 data pts
c       and max of 11 channels sampled at 3 samples/channel .....
integer*2 iarray(33), tarray(320,33), nval, n, m, nsamp
integer*2 nchan, echan, k
real rfdata(320,9), bigarray(320,11), frpmc(320), fdpc(320)
real rpmc,dpc,rpma,dp,sum1(32,11),fdata(9)
character*11 mame,rsum,tsum
character*80 header
character*3 tcase

common /revsect/ nrev, nsect

nchan = 11
echan = 10

c ----- Setclock set for 1kHz
call mbopen
call setclock(.001,1)

c ----- Input data counts filename and # of samples to be taken at
c       each data point .....
write (*,*)
write (*,*) ' Format for Raw Cts File is RCxxxxxx.xxx '
write (*,*) ' where xxxxx.xxx is tst case, V, alpha, rpm '
write (*,*)
write (*, ' (A\ ) ') ' Input Raw Counts Output Filename : '
read (*, 5) mame
open (unit = 1, file = mame)

write (*,*)
c ----- write (*,*) ' Before entering # of samples per data point, '
c ----- write (*,*) ' remember that for any high speed data taking, '
c ----- write (*,*) ' nsamp should not be > 1. '
c ----- write (*,*)
c ----- write (*, ' (A\ ) ') ' Input # of samples for each data point: '
c ----- read (*, 6) nsamp
nsamp = 1

write (*,*)
pause 'Press any key to start data taking ..... '

c ----- The following logic is based on inputs to the digital input
c       ports #0 and #1 being 32(J) and 1/rev(K) pulses respectively.
c       The elaborate if-then statements ensure that the data taking
c       actually starts at 0 degrees and counts for nrev revolutions.

c ----- Initialize counters .....
n = 0
m = 0
k = 0
call dina(nval)

```



```

c ----- If the following expression is true, then K is low....
100     if (nval .le. 1) goto 200
        call dina(nval)
        goto 100

c ----- If the following expression is true, then K is high and thus
c       the model is at 0 degrees. Now start counting 32 times for 1
c       revolution and then start taking data on 33rd count.....
200     call dina(nval)
250     if (nval .ge. 2) goto 290
        call dina(nval)
        goto 250

c ----- Start counting 32 times off J trigger
290     call dina(nval)
300     if ((mod(nval,2)) .EQ. 1) goto 400
        call dina(nval)
        goto 300
400     n = n + 1
        if (n .EQ. 32) goto 500

c ----- Look for J low ....
450     if ((mod(nval,2)) .EQ. 0) goto 290
        call dina(nval)
        goto 450

c ----- Look for J low before taking data ....
500     if ((mod(nval,2)) .EQ. 0) goto 600
        call dina(nval)
        goto 500

c ----- Look for J high to trigger data taking. This ensures start at
c       0 degrees....
600     call dina(nval)
650     if ((mod(nval,2)) .EQ. 1) goto 700
        call dina(nval)
        goto 650

c ----- Now at 0 degrees, begin taking data .....
700     call mcbatod (0,echan,1,nsamp, iarray)
        m = m+1

c ----- Throw temporary data into tarray to prevent overwrite of data ....
        do 750 i=1, (nsamp*nchan)
            tarray (m,i) = iarray (i)
750     continue

c ----- Exit condition; exit loop after nrev revs of data taking (10 max)
        if (m .EQ. (nrev*nsect)) goto 755

c ----- Look for J low, if J is low, go up to top of loop and look for
c       J high again. This prevents multiple triggers off the same
c       pulse, especially important for slow rpm runs .....
751     if ((mod(nval,2)) .EQ. 0) goto 600

```



```

call dina(nval)
goto 751

c ----- Done taking data, now put into proper arrays and store in file....
write (*,*)
write (*,*) ' Done taking data .....'
write (*,*)

c ----- Fill array bigarray(i,j) with zeroes ....
755   do 760 i = 1, (nrev*nsect)
      do 760 j = 1, (nchan)
        bigarray(i,j) = 0.0
760   continue

c ----- Place sum of nsamp number of data points in each storage bin ....
765   do 780 i = 1, (nrev*nsect)
      do 780 j = 1, (nchan)
        bigarray(i,j) = bigarray(i,j) + tarray(i, (j+(nchan*k)))
780   continue

      k = k+1
      if (k .EQ. nsamp) goto 781
      goto 765
781   continue

c ----- Next, divide the samples by nsamp and put in arrays rfddata(i,j),
c         fdpc(i) and frpmc(i)
      do 791 i = 1, (nrev*nsect)
        do 790 j = 1, 9
          rfddata(i,j) = bigarray(i,j)/nsamp
790        continue
          fdpc(i) = (bigarray(i,10))/nsamp
          frpmc(i) = (bigarray(i,11))/nsamp
791        continue

c ----- Finally. put data values into the data file mame .....
write (*,*)
write (*,*) ' Type in file Header .....'
read (*, '(a80)') header
write (1, '(a80)') header
write (1,14)
do 795 i = 1, (nrev*nsect)
  write (1,15) (rfddata(i,j), j = 1,9), fdpc(i), frpmc(i)
795  continue

c ----- DATA HANDLING -----

c ----- Sum up nrev points into 1 rev of data and put into file ...
c   Fill sum1, fdata, dpc, and rpmc with zeros ....
do 82 i = 1, 11
  do 82 j = 1, nsect
    sum1(j,i) = 0.0
82  continue

```





```

      do 81 i = 1,9
        fdata(i)=0.0
81      continue
      dpc = 0.0
      rpmc = 0.0

c ----- First do balance counts ....
      k = 0
83      do 85 i = 1, 9
        do 85 j = 1, nsect
          sum1(j,i) = sum1(j,i) + rfdata(j+(nsect*k),i)
85      continue
        k = k + 1
        if (k .eq. nrev) goto 86
        goto 83
86      continue

c ----- Now do dp and rpm measurements .....
      k = 0

89      continue
      do 90 j = 1,nsect
        sum1(j,10) = sum1(j,10) + fdpc(j+(nsect*k))
        sum1(j,11) = sum1(j,11) + frpmc(j+(nsect*k))
90      continue
        k = k + 1
        if (k .eq. nrev) goto 91
        go to 89

c ----- Divide by nrev for averaged values over 1 revolution ...
91      do 110 i=1, 11
        do 110 j = 1, nsect
          sum1(j,i) = sum1(j,i)/nrev
110      continue

c ----- Now sum up over remaining revolution for averaged counts .....
      do 95 i = 1, 9
        do 95 j = 1, nsect
          fdata(i) = fdata(i) + sum1(j,i)
95      continue

c ----- Again, do dp and rpm ....
      do 105 j = 1 , nsect
        dpc = dpc + sum1(j,10)
        rpmc = rpmc + sum1(j,11)
105      continue

c ----- Divide by nsect .....
      do 120 i=1,9
        fdata(i) = fdata(i)/nsect
120      continue

      dpc = dpc/nsect
      rpmc=rpmc/nsect

```



```

c ----- Write sum1 and fdata, dpc, rpmc, to files ...
      write (*,*)
      write (*, '(A\\)') ' Input summed (over 1 rev) file: '
      read(*,1) rsum
      write (*,*)
      write (*, '(A\\)') ' Input TOTAL summed counts output file: '
      read (*,1) tsum
      open (unit = 15, file = rsum, status = 'new')
      open (unit = 16, file = tsum, status = 'new')
      write (15,' (a80)') header
      write (16,' (a80)') header
      write (15,14)
      write (16,10)
      write (16,7) tcase,(fdata(i), i = 1,9),dpc,rpmc
      do 130 j = 1,nsect
         write(15,15) (sum1(j,i), i = 1,11)
130      continue

```

```

c ----- FORMAT statements .....
1      format (a11)
5      format (a11)
6      format (I2)
7      format (a3,11f7.1)
10     format('TC',4x,'N1',5x,'N2',5x,'Y1',5x,'Y2',5x,'R1',
+           5x,'R2',5x,'X1',5x,'X2',5x,'X3',5x,'DP',4x,'RPM')
14     format(3x,'N1',5x,'N2',5x,'Y1',5x,'Y2',5x,'R1',
+           5x,'R2',5x,'X1',5x,'X2',5x,'X3',5x,'DP',5x,'RPM')
15     format (11F7.1)

1000    continue
        close (unit = 1)
        return
        end

```

c \*\*\*\*\*

```

      subroutine filtz(zerot,zeros)

```

```

c ----- SUBROUTINE FILTZ -----
      real zerot(9), zeros(6)

      do 30 i= 1,4
         zeros(i) = zerot(i)
30      continue
         zeros(5) = zerot(6)
         zeros(6) = zerot(7)

      return
      end

```

c \*\*\*\*\*

```

      subroutine filter(fdata, pdata)

```



```

c ----- SUBROUTINE FILTER -----
c
c ---- Date: 16 Feb 1989
c
c ---- Purpose: Filter subroutine to take all channels of data and read
c               in the 6 preferred channels for processing by Maintst.
c
c ---- Variables :
c
c               fdata(i): array with all channels of data (11)
c               pdata(i): array with 6 preferred channels of
c                       balance data.
c
c -----
c       real pdata(6),fdata(9)
c ---- debug command
cdb     write (*,*) ' Have reached subroutine filter '
cdb     pause

c ---- Do test reading conversion
c       do 10 i=1,4
c           pdata(i) = fdata(i)
10      continue

c ---- debug command
cdb     write (*,*) ' First 4 points read in successfully '

c       pdata(5) = fdata(6)
c       pdata(6) = fdata(7)

c       return
c       end

c *****

c       subroutine rpmvel (dpc, rpmc, dp, rpma)

c -----SUBROUTINE RPMVEL -----
c
c ---- Purpose: To convert dpcell and rpm readings to actual
c               velocities and rpm's.
c
c -----

c       real dpc, rpmc, dp, rpma
c       common /dpcell/ rho,zero,full,tt
c       common /rpm/ rvz,rvcal

c ---- Convert dp counts to voltages and convert to ft/sec
c       using 409.6 counts/volt and Lisa's function dpspeed .....

c       dpc = (dpc)/409.6
c       dp = dpspeed(dpc)

```



```
c ----- Convert rpm counts to rpm's  
    rpmc = (rpmc)/409.6  
    rpma = (revs(rpmc))*60/512  
  
return  
end
```





c -----Program DAVLAB.FOR-----

subroutine doload( pdata, loads, ierr )

c -----Subroutine doload-----

real pdata(6), loads(6)  
integer ierr

c \*\*\* The subroutine takes the readings corrected for zeros and \*\*\*  
c and scaling, and then converts them to equivalent loads  
c using a linear 6th order fit determined by the Davidson  
c Laboratory MCB program.  
c \*\*\*\*\*

common /convair/ a(6,6)

c ... there is no possible error in this case ...  
ierr = 0

c ... do the matrix multiplication ...  
do 20 i = 1, 6  
loads(i) = 0.0  
do 10 j = 1, 6  
loads(i) = loads(i) + a(j,i)\*pdata(j)  
10 continue  
20 continue

c ... done, so return ...  
return  
end

C -----Subroutine intcoef-----

subroutine intcoef( runit, item )  
integer runit, item

c \*\*\* Subroutine to obtain the necessary information from a file \*\*\*  
c and to store it for later use of the conversion routines.

c RUNIT: An available FORTRAN unit number for reading the  
c data file

c ITEM: The set of coefficients selected for use in the  
c conversion routine.

ITEM #	Selection	
	Roll Bridge	Axial Bridge
1	1	1
2	1	2
3	1	3
4	2	1
5	2	2
6	2	3

c \*\*\*\*\*



```

character*80 id
character*9 name(6)
common /convair/ a(6,6)

data name/ 'M1X1T.DAT', 'M1X2T.DAT', 'M1X3T.DAT',
1          'M2X1T.DAT', 'M2X2T.DAT', 'M2X3T.DAT'/

c      *** attempt to open the data file ***
open( unit=runit, file = name(item), status = 'old', err= 70 )

c      *** insure that zero is the default value ***
do 10 i = 1, 6
    do 10 j= 1, 6
        a(i,j) = 0.0
10      continue

c      *** read the contents of the file ***
read(runit,15) id
15      format(a80)
do 20 i = 1, 6
    read(runit,*,end=25,err=25) ( a(i,j), j=1, 6 )
20      continue
goto 30
25      print *, '  ERROR - Trouble reading Coefficient Data'
return
30      continue
cdb      write(6,40) id

c ---  debug commands
c      open (unit = 6, file = 'loadcoef', status = 'new' )
c 40      format(1x,a80)
c      do 60 i = 1, 6
c          write(6,50) i, (a(i,j), j=1,6)
c 50          format(1x,i4,6f12.6)
c 60          continue
c ----      debug command
c      close (unit = 6)
close( runit )
return
70      write(6,80) name(item)
80      format(5x,'ERROR - Data file ',a9,' can not be read'/
1          5x,'      All coefficients are zero'//)

end

```



c -----Program COMMON.FOR-----

c -----Subroutine doadjus-----

```
subroutine doadjus( pdata )  
real pdata(6)
```

```
c    *** This subroutine takes the current readings, corrects for the ***  
c    readings for zero applied load, and then scales the result  
c    back to the levels at which the calibration was done. The  
c    returned values should be the bits that would be read at  
c    CONVAIR calibration bench.
```

c \*\*\*\*\*

```
common /convar1/ zero(6), rcal(6)
```

```
do 10 i = 1, 6
```

```
c    ... remove the zero first ...
```

```
    pdata(i) = pdata(i) - zero(i)
```

```
    pdata(i) = pdata(i)*rcal(i)
```

```
10    continue
```

```
    return
```

```
end
```

c -----Subroutine setzero-----

```
subroutine setzero( zeros )  
real zeros(6)
```

```
c    *** This subroutine takes zero applied load readings and stores ***
```

```
c    *** them for later use ***
```

```
common /convar1/ zero(6), rcal(6)
```

```
do 10 i = 1, 6
```

```
    zero(i) = zeros(i)
```

```
10    continue
```

```
    return
```

```
end
```

c -----Subroutine setrcal -----

```
subroutine setrcal( ratios )  
real ratios(6)
```

```
c    *** This subroutine takes calibration signal ratios and stores ***
```

```
c    *** them for later use ***
```

```
common /convar1/ zero(6), rcal(6)
```

```
do 10 i = 1, 6
```

```
    rcal(i) = ratios(i)
```



10        continue

return  
end





\$DEBUG

c -----Program CALIBR.FOR-----

c ----- This program contains the calibration subroutines for calibrating  
c the dpcell and rpm channel.

### SUBROUTINE DPCAL

c  
c Calibrates the differential pressure cell.  
c Stores the calibrations "zero", and "full"  
c in the common block called "dpcell".  
c

c  
c After calling DPCAL once in your program,  
c a special function exists in the MHL library  
c that you can use to convert voltages from  
c the Daytronics channel C to velocity. It  
c is called "dpspeed", and has one calling  
c parameter, "voltage".  
c

c  
c Example:

c call dpcal  
c .  
c .  
c .  
c <do an A/D conversion on channel 2 (Daytronics C)>  
c freestream=dpspeed(voltage)  
c .  
c . etc  
c

c You do not have to include the common block in your  
c main program to make these routines work  
c

c Lisa Shields  
c June 12, 1987

common /dpcell/ rho,zero,full, tt  
integer\*2 channel,ig,ival  
character ans, line\*70

write(\*,\*)  
write(\*,\*) ' Welcome to Dpcal!'  
10 write(\*,\*)  
write(\*,'(A)\') ' Please input water temp (deg f): '  
read(\*,\*,err=10) tt  
rho=1.9574-0.00028\*tt  
  
100 FORMAT(5x,a70)  
write(\*,\*)  
99 write(\*,\*)



```

line='The dpcell should be connected to the Daytronic channel c'
write(*,100) line
write(*,*)
line='The span and balance should be set such that the digital'
write(*,100) line
line='display reads from -820 (zero flow) to +600 (with '
write(*,100) line
line='the "-cal" button depressed.) '
write(*,100) line
write(*,*)
write(*,*)
write(*,*)
write(*,101)
101   format(5x,'Please hit return after checking this ',\ )
      read(*,104) ans
      write(*,*)
      line='Sampling zero flow voltage for 5 seconds and averaging'
      write(*,100) line

      call mbopen
      call setclock(0.01,0)
      zero=0.0
      channel=9
      ig=1
      do 110, i=1,500
      call atodtk(channel,ig,ival)
110   zero=zero + ival
      zero=zero/500.0/409.6

      write(*,*)
      line='Sampling finished.'
      write(*,100) line
      write(*,*)
      write(*,*)
      line='Now please press the "-cal" button and hold it down'
      write(*,100) line
      write(*,111)
111   format(5x,'for 5 seconds. Hit return when ready',
^      ' to do this.',\ )
      read(*,104) ans
      write(*,*)
      write(*,*)
      line='Sampling simulated full scale speed and averaging'
      write(*,100) line

      call setclock(0.01,0)
      full=0
      do 120 i=1,500
      call atodtk(channel,ig,ival)
120   full=full + ival
      full=full/500.0/409.6

      write(*,*)
      line='Sampling finished.'

```



```

write(*,100) line
write(*,*)
write(*,*)
write(*,102)      zero, full
102  FORMAT(5x,'Zero voltage: ',F6.3,' Full scale voltage: ',F6.3)
write(*,*)
write(*, '(A\') '  Accept these? (y/n): '
read(*,104) ans
if(.not.((ans .eq. 'y') .or. (ans .eq. 'Y')))) goto 99
write(*,*)
RETURN
104  format(a)
END

```

c -----Subroutine RPMCAL-----

```

Subroutine rpmcal
common /rpm/ rvz, rvcal
integer*2 channel
character ans*1

```

c This subroutine is used to calibrate the Daytronics  
c channel B, used to record propeller rpm data

```

write(*,*)
write(*,*)
5  write(*,10)
10  format(10x,'Welcome to the RPM (Channel B)',
^   ' calibration routine.')
15  write(*,*)
write(*,*)
write(*,20)
20  format(15x,'A: Set Zero to read 000')
write(*,30)
30  format(15x,'B: Push cal button, adjust span to 1500')
write(*,*)
write(*,*)
pause ' With propeller stopped, take time to do this now!'

write(*,*)
write(*,*)
write(*,40)
40  format(1x,'Hit any key while holding down channel B',
^   ' cal button for 5 seconds:')
read(*,41) ans
41  format(a)

channel=10
rvcal=average(.05,channel)

write(*,*)

```



```

write(*,*)
write(*,50)
50   format(1x,' Please release cal button, and hit any',
^     ' key to take rpm zero: ')
     read(*,41) ans

rvz=average(0.05,channel)

write(*,*)
write (*,55) rvz,rvcal
55   format (2x,'Rvz = ',f7.4,5x,'Rvcal = ',f7.4)
write (*,*)
write(*,' (a\)' ) ' Do you wish to recalibrate? (y/n): '
read(*,41) ans
if (ans .ne. 'n') goto 5
return
end

```





```

c ----- Program DCZero.For -----
c
c -----Version: 1.1
c
c -----Date: 29 March 89
c
c -----Pupose: To take static balance readings at different points around
c             the circle and store them for later use as a zero reference
c             file. The data taken here represents the weight ( or W-B
c             if done in water) effect AND the offsets of the balance.
c
c -----Programmer: Dave Johnson
c
c -----Language : Microsoft Fortran 4.1
c
c -----Variables:
c             iarray: row array in DMA filled by each MCBATOD
c                   call.
c
c             zerot: array with averaged counts for all
c                   channels. This array will be read by
c                   the subroutine filter to convert to the
c                   preferred 6 channels and put into zeros(i).
c
c -----
c
integer*2 iarray(1000),bchan,echan,nsamp,nchan,n,nsect
real zerot(32,9), angle, sum(9)
character*11 fname, dname
character*3 tcase
character*80 header
character*1 ans
nsect = 32
bchan = 0
echan = 8

write (*,*)
write (*,*) ' ***** Welcome to DCZero! ***** '
write (*,*)

c ----- Input zero filename
write (*,*)
1  write (*, ' (A\ ) ') ' Type in name of zeroes file (11 char max): '
read (*, ' (A11) ', err = 1) fname
open (unit = 1, file = fname)
write (*,*)
write (*,*) ' Type-in file header ..... (80 char max):'
read (*, ' (a80)') header
write (1, ' (a80)') header
write (1,2)

c ----- fill zerot(j,i) with zeros
do 50 j=1,nsect
do 50 i=1,nchan

```



```

        zerot(j,i) = 0.0
50    continue
    angle = 0.0

c ----- Input Test case number
    write (*,*)
    write (*,' (A\)' ) ' Type in test case (3 char. max): '
    read (*,' (A3)' ) tcase

c -----Setclock set for 100Hz

    call mbopen
    call setclock(.01,1)

    write (*,*)
    write (*,' (A\)' ) ' Input Number of samples (e.g. 100): '
    read (*,6) nsamp

    write (*,*)
20    pause ' Press enter to start taking of zeroes '

c ----- Take Zeroes! -----

    call mcbatod (bchan,echan,1,nsamp,iarray)

c ----- calculate number of channels sampled
    nchan= (echan - bchan) + 1
    k=0
    n=n+1

c ----- read in data to zerot(n,i)
55    do 60 i=1, nchan
        zerot(n,i) = zerot(n,i) + iarray(i+(nchan*k))
60    continue

    k=k + 1
    if (k .EQ. nsamp) goto 71
    goto 55
71    continue

c ----- Next, divide the values in zerot(n,i) to get averaged values
    do 80 i=1,nchan
        zerot(n,i) = (zerot(n,i))/nsamp
80    continue

c ----- write zerot(n,i) to file fname and to screen.....
    write (1,7) angle, (zerot(n,i) , i=1,nchan)
    write (*,*)
    write (*,2)
    write (*,7) angle, (zerot(n,i), i=1,nchan)
    write (*,*)

    angle = angle + 11.25

```



```

c ----- Check to see if another run is next ....
    if (n .eq. 32 ) then
        write (*,*)
        write (*,*) ' N = 32 !, One full revolution has been done'
        write (*,*)
    endif
    write(*, '(a\')) ' Another run? (y/n):'
    read (*, '(a1)') ans
    if (ans .eq. 'y') then
        goto 20
    endif
    close (unit=1)

c ----- Next sum up all points/chan and put in dc 'zero' file ....
    do 90 i=1,9
        sum(i)=0.0
90    continue

    do 96 i=1,9
        do 95 j=1,nsect
            sum(i)=sum(i) + zerot(j,i)
95        continue
        sum(i)=(sum(i))/nsect
96    continue

c ----- Write to file ...
    write (*,*)
    write (*, '(a\')) ' Type dc counts output file name: '
    read (*, '(a11)') dcname
    open (unit=2,file=dcname,status='new')
    write (*,*) ' Input header for summed file .....'
    read (*, '(a80)') header
    write (2, '(a80)') header
    write (2,3)
    write (2,4) tcase, (sum(i), i=1,9)
    close (unit=2)

c ----- FORMAT statements
2    format ('Angle',3x,'N1',5X,'N2',5X,'Y1',5X,'Y2',5X,'R1',
+          5X,'R2',5X,'X1',5X,'X2',5X,'X3')
3    format ('tcase',1x,'N1',5X,'N2',5X,'Y1',5X,'Y2',5X,'R1',
+          5X,'R2',5X,'X1',5X,'X2',5X,'X3')
4    format (a3,9f7.1)
6    format (I4)
7    format (f6.2,9F7.1)

end

```



\$DEBUG

```
c -----Program FFT-----
c
c ---- Version: 1.3
c
c ---- Date: 27 April 89
c
c ---- Programmer: Dave Johnson
c
c ---- Language: Microsoft Fortran 4.1
c
c ---- Purpose: To perform a fast fourier transform on coning
c               motion test data.
c
c ---- Subroutines:
c
c               FAST: Performs the FFT and outputs the Fk's
c
c -----
```

```
complex x(320)
integer npow,ndim,nreal,nread
real one, xreal,mag(320),freq(160),delta,rpm
character*11 fname, outname,gname
```

```
one = -1.0
ndim = 320
```

```
c ---- Input NPOW, the power of 2 that equals the # of data points ..
```

```
write(*,*)
write(*, '(a\)' ) ' Input power, n, such that 2^n = # data pts: '
read(*, 5) npow
nread = 2**npow
write(*,*)
write(*, '(a\)' ) ' Input the RPM data was taken at: '
read(*, 6) rpm
delta = 60/(32*rpm)
write(*,*) delta
```

```
c ---- Input Data file name .....
```

```
write(*,*)
write(*, '(a\)' ) ' Input name of data file: '
read(*, '(a11)' ) fname
```

```
c ---- Read in data from file fname .....
```

```
open (unit=1,err=20,file=fname,status='old')
do 15 i=1,nread
  read (1,*,end=25) xreal
  x(i)=cmplx(xreal,0)
```

```
15 continue
```

```
goto 30
```

```
20 write(*,*) ' Error in opening file'
go to 100
```





```

25  write (*,*) ' Error in reading file'
    goto 100
30  continue

c ---- Call FFT subroutine....
    call FAST(x,ndim,npow,one)

c ---- Write FFT data to output file ....
    write(*,*)
    write(*,' (a\)' ) ' Input FFT output file name: '
    read (*,' (a11)' ) outname
    open (unit=2,file=outname,status='new')
    write(2,10) outname
    write(2,9)
    do 40 i=1,nread
        mag(i)=cabs(x(i))
        write(2,12) x(i),mag(i)
40  continue

c ---- Create data file for Grapher plot .....
    write (*,*)
    write (*,' (a\)' ) ' Input Grapher Data file name: '
    read (*,' (a11)' ) gname
    open (unit=3,file=gname,status='new')
    write (3,13) 0.,mag(1)
    do 50 i=2, (nread/2)
        freq(i)=(i-1)/(nread*delta)
        write (3,13) freq(i),(2*(mag(i)))
50  continue
    write (3,13) (freq(nread/2)+freq(2)), mag(nread/2 + 1)

c ---- Format statements ....
5  format(i3)
6  format(f5.0)
9  format(6x,'Real',9x,'Imag.',14x,'Magnitude')
10 format(2x,' FFT Output File:',A11)
12 format(2x,f12.3,4x,f10.3, 9x, f12.3)
13 format(2x,f6.3,5x,f12.3)

    close(unit=1)
    close(unit=2)
    close(unit=3)

100 continue
end

```



c This is the fft routine. I'll give you the meaning of 'ONE'  
c later...

SUBROUTINE FAST(X,NDIM,NPOW,ONE)

C  
C IMPLEMENT THE FAST FOURIER TRANSFORM  
C

IMPLICIT REAL(A-H,O-Z),INTEGER(I-N)  
COMPLEX T,U,W,X(NDIM)  
DATA PI/3.1415926535897932384/  
N1=2\*\*NPOW  
N2=N1/2  
N3=N1-1  
J= 1  
DO 300 I=1,N3  
IF(I.GE.J) GO TO 100  
T= X(J)  
X(J)=X(I)  
X(I)=T  
100 K=N2  
200 IF(K.GE.J) GO TO 300  
J=J-K  
K=K/2  
GO TO 200  
300 J=J+K  
DO 500 L=1,NPOW  
LE1=2\*\*L  
LE2=LE1/2  
ANG=PI/LE2  
U=CMPLX(1.,0.)  
W=CMPLX(COS(ANG),ONE\*SIN(ANG))  
DO 500 J=1,LE2  
DO 400 I=J,N1,LE1  
IP=I+LE2  
T= X(IP)\*U  
X(IP)=X(I)-T  
400 X(I)= X(I)+T  
500 U=U\*W  
IF(ONE.EQ.1.)RETURN  
SCL= 1./REAL(N1)  
DO 600 I=1,N1  
600 X(I)=X(I)\*SCL  
RETURN  
END







Thesis

J5746

Johnson

c.1

A coning motion  
apparatus for hydro-  
dynamic model testing  
in a non-planar cross-  
flow.

Thesis

J5746

Johnson

c.1

A coning motion  
apparatus for hydro-  
dynamic model testing  
in a non-planar cross-  
flow.





A coning motion apparatus for hydrodynam



3 2768 000 82209 2

DUDLEY KNOX LIBRARY